THESIS FOR THE DEGREE OF DOCTOR OF PHILOSOPHY

CARBONACEOUS AEROSOL IN EUROPE

OUT OF THE WOODS AND INTO THE BLUE?

Jan Robert Bergström

UNIVERSITY OF GOTHENBURG

FACULTY OF SCIENCE

DEPARTMENT OF CHEMISTRY AND MOLECULAR BIOLOGY
UNIVERSITY OF GOTHENBURG
GOTHENBURG, SWEDEN 2015

Carbonaceous Aerosol in Europe

out of the woods and into the blue?

ISBN 978-91-628-9505-1 (PDF)
ISBN 978-91-628-9506-8 (Print)
Available online at: http://hdl.handle.net/2077/40004

Department of Chemistry and Molecular Biology
University of Gothenburg
SE-412 96 Göteborg, Sweden

Printed by Ineko AB
Göteborg, Sweden 2015

Abstract

Particulate matter (PM) in the atmosphere influences weather and climate and may have important health impacts. Regional scale chemical transport modelling aims to describe the composition of particulate matter, to track different sources, estimate their relative importance, and to give realistic predictions of responses to changes in emissions and atmospheric conditions. The focus of this thesis is the modelling of an important constituent of PM — carbon containing PM.

The EMEP MSC-W chemical transport model is used for European policy making regarding air pollution, to provide scientific support to the convention on long-range transboundary air pollution (CLRTAP). The organic aerosol (OA) treatment in the EMEP model has been extended to include more realistic primary OA emissions, and new schemes for the formation of secondary OA, based on the volatility basis set method.

Long-term model simulations of OA and elemental carbon (EC) over Europe have been performed for the period 2002–2010. The model results were compared to observations, including source-apportionment data. Total organic carbon concentrations matched measured concentrations for summer periods, but problems were found during winter, with poor agreement between modelled and measured organic carbon, and tracers of wood-burning. To tackle these problems a new inventory for emissions of OA and EC from residential wood combustion (RWC) was developed. Total European OA emissions from RWC are almost 3 times larger in the new inventory than in the old one. According to the new inventory, about 60% of the primary OA emissions in Europe are due to RWC. EC emissions are to a larger extent due to fossil fuel combustion; RWC emissions contribute about 1/5 of the total anthropogenic fine particle EC-emissions in Europe.

The model results indicate that many sources contribute to OA in Europe. During summer, fossil fuel combustion, biomass burning and biogenic secondary OA all contribute considerably. RWC is the dominant OA source during winter, contributing more than 50% to the model OA. According to the model results, non-fossil sources contribute more to regional scale OA than fossil fuel, except in the Po Valley during summer. EC comes mainly from fossil fuel during the warm seasons, but EC from RWC is important during winter.

Modelling is useful to investigate potential impacts of newly discovered sources of organic aerosol. Biotic stress-induced emissions (SIE) were investigated in this thesis. The fractions of stressed trees in European forests were estimated, based on observed tree damage. Emission estimates for sesquiterpenes, methyl salicylate and unsaturated C_{17}-compounds, and the SOA yield from the oxidation of these SIE, were based on plant chamber experiments. The model results suggest that SIE may contribute substantially to SOA in Europe. During some periods, SIE may contribute more to OA than the non-stressed biogenic emissions of volatile organic compounds. Thus, further research on SIE is warranted.

Keywords: organic aerosol, elemental carbon, chemical transport modelling, residential wood combustion, biotic stress induced emissions, source apportionment, EMEP MSC-W model

List of publications

This thesis is based mainly on the work presented in the following papers. In the text the papers will be referred to by their Roman numerals.

I. **Modelling of organic aerosols over Europe (2002–2007) using a volatility basis set (VBS) framework: application of different assumptions regarding the formation of secondary organic aerosol**
R. Bergström, H. A. C. Denier van der Gon, A. S. H. Prévôt, K. E. Yttri, and D. Simpson
Atmospheric Chemistry and Physics, 12 (2012) 8499–8527, doi:10.5194/acp-12-8499-2012.

II. **Source apportionment of carbonaceous aerosol in southern Sweden**
J. Genberg, M. Hyder, K. Stenström, R. Bergström, D. Simpson, E. O. Fors, J. Å. Jönsson, and E. Swietlicki
Atmospheric Chemistry and Physics, 11 (2011) 11387–11400, doi:10.5194/acp-11-11387-2011.

III. **Biotic stress: a significant contributor to organic aerosol in Europe?**
R. Bergström, M. Hallquist, D. Simpson, J. Wildt, and T. F. Mentel
Atmospheric Chemistry and Physics, 14 (2014) 13643–13660, doi:10.5194/acp-14-13643-2014.

IV. **Light-absorbing carbon in Europe – measurement and modelling, with a focus on residential wood combustion emissions**
J. Genberg, H. A. C. Denier van der Gon, D. Simpson, E. Swietlicki, H. Areskoug, D. Beddows, D. Ceburnis, M. Fiebig, H. C. Hansson, R. M. Harrison, S. G. Jennings, S. Saarikoski, G. Spindler, A. J. H. Visschedijk, A. Wiedensohler, K. E. Yttri, and R. Bergström
Atmospheric Chemistry and Physics, 13 (2013) 8719–8738, doi:10.5194/acp-13-8719-2013.

V. **Particulate emissions from residential wood combustion in Europe – revised estimates and an evaluation**
H. A. C. Denier van der Gon, R. Bergström, C. Fountoukis, C. Johansson, S. N. Pandis, D. Simpson, and A. J. H. Visschedijk
Atmospheric Chemistry and Physics, 15 (2015) 6503–6519, doi:10.5194/acp-15-6503-2015.

List of abbreviations

ASOA	anthropogenic secondary organic aerosol
AVOC	anthropogenic volatile organic compound
BC	black carbon
BSOA	biogenic secondary organic aerosol
BVOC	biogenic volatile organic compound
C^*	effective saturation concentration
CCN	cloud condensation nuclei
CLRTAP	convention on long-range transboundary air pollution
EC	elemental carbon
EC_1	EC in PM_1
$EC_{2.5}$	EC in $PM_{2.5}$
EC_{10}	EC in PM_{10}
EMEP	European Monitoring and Evaluation Programme
IVOC	intermediate volatility organic compound
JPAC	Jülich Plant Atmosphere Chamber
LVOC	low volatility organic compound
MAC	mass absorption cross section
MeSA	methyl salicylate
MSC-W	The Meteorological Synthesizing Centre-West
MT	monoterpenes
OA	organic aerosol
OC	organic carbon
$OC_{2.5}$	OC in $PM_{2.5}$
OM	organic matter
$OM_{2.5}$	OM in $PM_{2.5}$
PM	particulate matter
PM_1	particulate matter with diameter less than 1 µm
$PM_{2.5}$	particulate matter with diameter less than 2.5 µm
PM_{10}	particulate matter with diameter less than 10 µm
POA	primary organic aerosol
RWC	residential wood combustion
S/IVOC	semi- and/or intermediate volatility organic compounds
SIE	stress-induced emissions
SOA	secondary organic aerosol
SQT	sesquiterpenes
SVOC	semi-volatile organic compound
TC	total carbon
TOA	thermal optical analysis
VBS	volatility basis set
VOC	volatile organic compound
VOC-SOA	SOA formed from oxidation of VOCs

Table of Contents

1 Introduction

1.1 Particles in the atmosphere

Particulate matter (PM) in the atmosphere has been a widely studied subject for many years (for recent reviews, see [1], [2]). Interest has largely been for two reasons – the importance of PM for weather and climate (e.g. impacts on clouds, precipitation and radiation) [3] and the potential impacts on human health [4]. PM also has important impacts on visibility [5] and some particle components may contribute to acidification and eutrophication of ecosystems (e.g. [6]).

Particles in the atmosphere come in a wide range of sizes, from nanometer-sized clusters up to about 100 μm diameter dust particles. In general the largest particles fall rapidly to the ground and in the present work only particles with diameters less than 10 μm (PM_{10}) have been included; these often remain long enough in the atmosphere to be subject to long-range transport. A lot of air quality regulations have focused on PM_{10} (since these particles have been considered to have the potential to penetrate past the larynx when inhaled [7]) but more recent EU legislation [4], [8] has also included limit concentrations on particles smaller than 2.5 μm ($PM_{2.5}$) These "fine particles" are able to penetrate deeper into the lungs to a higher degree than coarser PM.

The focus of this thesis is the modelling of an important constituent of PM in the atmosphere — particulate carbonaceous matter — i.e. carbon containing PM.

At many locations a large fraction of both PM_{10} and $PM_{2.5}$ consists of carbon-containing particles (carbonaceous aerosol particles); e.g. 10–40% (mean 30%) of the total concentration of PM_{10} at rural and natural background sites in Europe consisted of carbonaceous material, during a one-year measurement campaign 2002–2003 [9]; another overview [10] of PM at a large number of European sites (including both urban and rural locations) showed even larger fractions of carbonaceous material in $PM_{2.5}$, on average about 40%.

Carbonaceous aerosol particles consist largely of organic matter (OM; often denoted organic aerosol, OA) and so-called elemental carbon (EC; sometimes denoted "black carbon", BC, because it is usually strongly light-absorbing); some types of mineral dust particles also contain carbonate carbon.

Carbonaceous aerosols may include a huge number of different components, with varying properties (light-absorption, volatility, hygroscopicity etc.). Many different sources, both anthropogenic and natural (biogenic) contribute to carbonaceous particles; they may either be directly emitted to the atmosphere, e.g. during incomplete combustion, or be formed in the atmosphere from gaseous precursors.

1.2 The EMEP MSC-W model

The EMEP MSC-W model [11] is a chemical transport model (CTM) developed within the European Monitoring and Evaluation Programme for Transboundary Long-Range Transported Air Pollutants (EMEP; www.emep.int) at the Meteorological Synthesizing Centre-West (MSC-W). The model is used to simulate a wide variety of air pollutants, including photochemical oxidants and inorganic and organic aerosol particles. It is used within the EMEP programme to provide scientific support to the convention on long-range transboundary air pollution (CLRTAP, see e.g. [12]). The EMEP MSC-W model is an important tool for European policy making regarding air pollution; in the initial years of the EMEP programme the main focus was on transboundary transport of acidifying and eutrophying pollutants. Later photochemical ozone pollution also became an important issue. More recently the potential impact of particulate matter on human health has led to an increased interest in being able to model also PM and its different constituents with the model.

A thorough description of the standard EMEP MSC-W model, including the driving meteorological data from numerical weather prediction models, is given in [11]. The model has been extensively compared with measurements of many different compounds (e.g. [13]–[18]; and Papers I and IV in this thesis). A research version, including a new treatment of organic aerosol, is described in detail in Paper I; details about the modelling of elemental carbon are given in Paper IV and [19].

The model domain used in this thesis covers all of Europe and some surrounding areas (see Fig. 4.1 in Sect. 4.4.1). It has a horizontal resolution of ca. 50 km × 50 km (at Lat. 60°N). Twenty vertical levels are used to cover the troposphere; the lowest model level is ca. 90 m thick and the top of the model is at 100 hPa.

The EMEP MSC-W model assumes a very simplified size distribution of particulate matter. The model uses two size modes for particles, fine and coarse aerosol; fine particles are assumed to be in the accumulation mode, and to have a log-normal size-distribution with a mass-median diameter of 330 nm and geometric standard deviation of 1.8; the assigned sizes for coarse mode particles vary somewhat with compound [11]. The simplified treatment of the aerosol size-distribution in the EMEP model is justified by the fact that the model is mainly designed to calculate PM_{10} and $PM_{2.5}$ mass closure (concentrations and chemical composition), which has been the main priority within the EMEP/CLRTAP framework.

The EMEP model includes several different photo-oxidant and aerosol chemistry schemes; in this thesis the standard chemical mechanism “EmChem09” from [11] was used for treating the chemistry of inorganic compounds and the gas-phase chemistry of volatile organic compounds (VOCs). The chemistry scheme is based on the “lumped molecule” approach to handle VOC-emissions and chemistry, which means that a small number of surrogate VOCs are used to represent the huge number of different VOCs that are emitted to the atmosphere, e.g. o-xylene represents all aromatic VOCs and n-butane all alkanes heavier than ethane. A detailed description of the EmChem09 chemistry scheme, including lists of all reactions and reaction rates can be found in [11]. A major part of the work presented in this thesis deals with the extension of the EmChem09 scheme with models to treat the organic aerosol.

The EMEP model treats both anthropogenic and natural emissions of various organic and inorganic gases and particles. In this work, anthropogenic emissions of VOCs, and inorganic

pollutants (NO_x, SO_2, NH_3 etc.), from different source sectors were taken from the standard EMEP emission inventory, mainly based on officially reported national emission data from the countries that are parties to the CLRTAP. These emission data are available from www.emep.int. Detailed information about the anthropogenic emission data can be found in the annual Inventory Review reports published by the EMEP Centre on Emission Inventories and Projections (CEIP; www.ceip.at).

Carbonaceous aerosol emissions from anthropogenic sources were mainly taken from an inventory by Denier van der Gon et al. (the EUCAARI-inventory; see Papers I, IV and V) but for residential wood combustion emissions a new inventory was developed and tested in Papers IV and V (see Sect. 5).

Vegetation is an important source of organic aerosols. Biogenic emissions of isoprene (C_5H_8) and monoterpenes ($C_{10}H_{16}$) from vegetation are calculated in the model taking into account effects of light and temperature etc. Biogenic VOC (BVOC) emissions are discussed further in Sect. 4.4.1.

Vegetation fires (open-burning wildfires, agricultural fires and prescribed burning) are also important sources of carbonaceous aerosol particles. Two different emission inventories, based on satellite observations of fires, have been used in this thesis. In Paper I the Global Fire Emission Database (GFEDv2, [20]) with 1° × 1° spatial resolution and 8-day temporal resolution was used. In the later studies (Papers III-V) the "Fire INventory from NCAR version 1.0" (FINNv1, [21]) was used; this inventory provides daily emissions with a high horizontal resolution (1 km × 1km).

2 Measurements of carbonaceous aerosol

2.1 Terminology

The terminology for carbonaceous aerosol can be confusing, especially regarding the strongly light-absorbing component of the particles (often denoted black carbon, BC) [22].

In this thesis the term "soot" is used for light-absorbing particles emitted from combustion sources, which is a common usage of the term [23]. Depending on the source and the combustion efficiency, and atmospheric processing of the particles, soot particles may have varying composition and light-absorbing properties. Sometimes the term "soot carbon" is used for carbon particles with the typical properties of (fresh and uncoated) soot particles from combustion, consisting of aggregates of almost purely carbon 10–50 nm spherules [24].

The following definitions are used for "organic carbon", "elemental carbon" and "black carbon" in this work:

- Organic Carbon (OC) is the particulate carbon that volatilise in an inert atmosphere below a defined temperature; OC-concentrations (and concentrations of elemental and total carbon) are determined by thermal analysis techniques (Sect. 2.2).
- Elemental Carbon (EC) is the particulate carbon that does *not* volatilise in an inert atmosphere below a defined temperature.
- Black Carbon (BC) concentration is the estimated concentration of light-absorbing particles based on optical (light-absorption) measurements (Sect. 2.3).

The relation between EC and BC concentrations is not simple as is discussed in detail in Paper IV. Sometimes the terms BC and EC (and even soot) are used as synonyms, since EC is often assumed to consist entirely of light-absorbing carbon; however this is not necessarily true, as discussed in Sect. 2.2.

Both optical and thermal measurement techniques are important. Optical methods measure climate-relevant properties of the particles while the thermal methods measures the carbonaceous aerosol mass, which is usually what is modelled in chemical transport models.

2.2 Thermal analysis techniques - TC, OC and EC

The total carbon (TC) content of particulate matter, and the OC and EC concentrations, can be measured using thermal analysis of particles collected on filters (see e.g. [25] and Papers II and IV).

The thermal analysis methods are usually reliable for determining the total carbon concentration in the filter sample [26]. The separation of the TC into EC and OC fractions is more problematic. Many different EC/OC separation methods have been employed (see e.g. [26]); in most of them the collected particle sample is heated in a step-wise procedure, initially usually in an oxygen free atmosphere and at later steps with oxygen added. The evolved carbon is converted into CO_2, which can be measured using infrared spectroscopy, or reduced to CH_4, and measured using a flame ionization detector. Organic components are assumed to leave the filter at lower temperature (< 500°C) than the EC and this difference in thermal stability can be used to separate the OC from the EC in the sample.

There are a number of problems with the EC/OC separation techniques (e.g. [25], [27] and references therein) that leads to large uncertainties in the EC/OC split of the TC. Many intermethod and interlaboratory studies have been performed and EC concentrations are often found to differ by a factor of 2 between commonly used methods (e.g. [28]) and differences up to a factor of 7 have been reported [25].

Potential problems include:

- some organic material may be highly refractory and have similar thermal and oxidative properties as EC and thus may be measured as (false) EC; this would lead to overestimation of EC and underestimation of OC and may be especially important for biomass burning aerosols (e.g. [24], [29])
- EC can be oxidised earlier than expected, e.g. due to presence of species that catalyse the oxidation, such as K and Na; this could lead to an underestimation of EC (and corresponding overestimation of OC) [30]
- pyrolysis of organic compounds (charring) on the filter during the heating phase may transform the OC to EC (e.g. [31], [32]) leading to an overestimation of EC

Some of these problems can be reduced (at least partially) by using various correction techniques. To correct for the charring problem, thermal optical analysis (TOA) techniques have been developed that monitor the reflectance or transmission of the filter during analysis (see e.g. [25]). However, charring correction techniques are based on faulty assumptions regarding the behaviour of the charred organics and the "native" EC [31]; this limits the possibility to accurately separate OC from native EC for particles that contain OC components that are prone to charring. Charring corrections may lead to an underestimation of EC due to the fact that pyrolytic carbon may have a greater attenuation coefficient than EC [31]. It is interesting to note that the EC-concentrations determined using the same temperature protocol for the TOA, and only differ in the choice of reflectance or transmission based charring correction, can be very different; reflectance based EC has been found to be much higher than transmission based EC (e.g. a factor of 1.7 higher in [32] and about a factor of two in [31]).

The agreement between different TOA measurement protocols seems to be especially poor for wood smoke samples (e.g. [33] and references therein), which is not surprising since wood smoke typically include substantial amounts of alkali metals (that may catalyse the combustion of EC so that it occurs simultaneously with OC volatilisation in the thermal analysis) and may include varying amounts of refractory organic components that could be detected as EC in the analysis (e.g. [29], [30]).

Note that the EC measured by thermal analysis methods (including TOA) may include some refractory *organic* compounds that are *not* strongly light-absorbing. The names *elemental* and *organic* carbon are thus somewhat misleading since they give the impression that the OC-fraction contains *all* the organic compounds of the particles and that EC-fraction consists of pure ("inorganic") carbon. The amount of truly elemental carbon (i.e. graphite, diamond or fullerenes) in the atmosphere is very low and the EC-fraction can contain significant amounts of non-carbon atoms; it consists at least partly of organic compounds. More precise names would be refractory carbon (instead of EC) and non-refractory carbon (for OC) [23].

Another potential complication when using thermal analysis methods is that, in addition to OC and EC, particulate matter may also contain carbonate carbon, mostly from various types of mineral dust [34]. Unless the carbonate carbon is taken into account in the thermal analysis method applied (e.g. by removal of the carbonate by acid pre-treatment of the filter) any carbonate captured on the filter may be detected as either EC or OC, depending on the form of the carbonate and the measurement protocol used [32]. The fraction of carbonate carbon in TC is expected to be low in Europe; at regional background sites usually < 5% according to [32] but higher contributions can occur, especially in regions affected by windblown dust, and in southern Europe carbonate carbon concentrations are expected to be significant [35], [36]. Mineral dust was not investigated in the work included in this thesis and carbonates are thus not included in the modelling presented here.

In addition to uncertainties related to the EC/OC separation there are also substantial uncertainties related to OC collection artefacts [37] — organic gas-phase compounds may adsorb to the quartz fiber filter, used to collect the particles, and be detected as OC in the thermal analysis (or as EC if they are pyrolysed), this effect also leads to an overestimation of the total particulate carbon concentration (positive artefact); since many organic aerosol components are semi-volatile negative artefacts may also occur due to evaporation of collected particulate OC. OC sampling artefacts are often handled by using backup filters to estimate the positive artefact and/or denuders to remove as much as possible of the organic vapours before the particle collection (e.g. [38] and Paper II). Usually the positive artefact is more important than the negative ([37], [38] and references therein). The positive artefact can be substantial, e.g. it has been estimated to contribute between 25 and 50% to OC for wood smoke measured on bare quartz filters [38]; in the same study even larger artefacts were observed for diesel exhaust.

The uncertainties involved in the EC/OC separation and the very poor agreement between thermal analysis methods using different measurement protocols have led Reid et al. [27] to the, rather disappointing, realization that reported EC and OC concentrations must be considered only as semi-quantitative, and that the best one can hope for is consistency. This should be remembered when comparing modelled OC and EC concentrations to measurements. Since EC concentrations are usually much lower than OC the *relative* uncertainty of the measured EC is much larger than for OC. Introduction of a standard procedure for thermal analysis of carbonaceous aerosol in Europe would at least mean a step towards consistency [32].

2.3 Light-absorbing carbon and optical measurements – BC

Various forms of light-absorbing carbonaceous particles are formed during combustion. Major sources include diesel engines, power plants and ship engines using heavy fuel oil or coal, residential (small scale) burning of solid fuels (wood, coal), agricultural field burning and vegetation fires [39]. The light-absorbing carbon emissions include both strongly absorbing soot particles and various moderately-to-weakly absorbing particle components – so called brown carbon [24], [40]. Brown carbon may include a large number of different compounds and can both be produced during low-temperature and/or inefficient combustion (for example tarry material or char, from biomass burning and lignite combustion (e.g. [41], [42]), and through heterogeneous or condensed phase atmospheric reactions [40].

Often the concentration of light-absorbing carbon is estimated from optical (light-absorption) measurements. There are several different optical measurement techniques available to determine the light-absorption of the aerosol; either the particles can be collected on filters before the analysis or the absorption can be directly measured in the aerosol (in situ) [43]. In Paper IV only data from filter-based instruments were used. These have some advantages over in situ measurements (simplicity, low-price, insensitivity to gaseous absorption) but they are prone to a number of artefacts (e.g. [24], [43]); based on studies comparing different filter based techniques with more reliable in situ instruments systematic errors of up to a factor of two in the absorption coefficient can be expected [24].

The light absorption (unit: m^{-1}) can be transferred into a BC mass concentration (in $\mu g\ m^{-3}$) using some mass absorption cross section (MAC) [23] corresponding to a certain type of light-absorbing particles (e.g. MAC=7.5 $m^2\ g^{-1}$ at 550nm, has been suggested for fresh (uncoated) BC [23]). Once in the atmosphere the fresh BC-emissions may become coated with various non-absorbing compounds (e.g. sulfate, organic molecules, water). Such coatings may lead to enhanced absorption and it has been estimated that the absorption of aged BC is about 1.5 times greater than that of freshly emitted (externally mixed) particles [44]. Other studies have indicated even greater absorption enhancements – a factor of two or more (see e.g. [24] and references therein).

Light-absorption measurements may also to some degree be influenced by other absorbing components than black carbon, including brown carbon and absorbing mineral dust [24].

The BC concentrations determined by optical methods using a constant MAC-value are thus not corresponding to the real mass concentrations of the light-absorbing particle components but to the mass of the "reference" particles (used to determine the MAC-value) that would lead to the same absorption as the observed samples [23], [24].

Paper IV includes a comparison of EC-concentrations determined by thermal analysis methods and BC-concentrations determined by simultaneous optical measurements at seven sites in northern, western and central Europe. The relationship between the EC and BC (as given by MAC values) differs widely between the sites, and the correlation between EC and BC also varies a lot between the stations, with a high correlation at three sites ($r \sim 0.9$) but poor correlation ($r \leq 0.6$) at three of the others. These variations can, at least partly, be due to the uncertainties discussed above for both measurement types but they also illustrate the fact that BC measurements are not easily comparable to model EC results.

2.4 Source apportionment (Paper II)

It is often interesting to know not only the total concentration of particulate matter, or total concentration of organic aerosol or elemental carbon, but also the contributions from different sources to these concentrations. A number of different source apportionment methods have been developed, see for example the review of source apportionment of PM in Europe by Viana et al. [45].

The source apportionment data used in this thesis are based on a tracer methodology initially developed for the CARBOSOL project [46]. It is based on measurements of various tracers for different emission sources; examples of tracers include levoglucosan from wood burning emissions [47], cholesterol from meat cooking (e.g. [48]), mannitol from fungal spores [49],

cellulose from plant debris [50], and the ratio of the radioactive isotope ^{14}C to the stable ^{12}C to estimate what fractions of the measured carbon are of fossil and modern origin [51]. The methodology includes an uncertainty analysis by taking into account measurement uncertainties and uncertainties/variabilities of the different tracer-to-source type concentrations relationships; this is described in detail in [46]. A variant of the methodology was used in Paper II to estimate the contributions of biomass combustion, other biogenic sources and fossil fuel sources to elemental and organic carbon at a rural site in southern Sweden. These results were also used for evaluating the EMEP model performance. One of the conclusions of the study was that the model severely underestimated OC from biomass combustion during winter. The source apportionment data from Paper II were also used in Papers IV and V when evaluating a new emission inventory for residential wood combustion (Sect. 5).

An extensive review has recently been published by Nozière et al. [52] covering the molecular identification of organic compounds in the atmosphere. This includes a lot of information about different compounds that can be useful as tracers (or in their terminology "markers") of different organic aerosol sources, including both primary emissions and secondary organic aerosol.

A major uncertainty for source apportionment studies aiming at separating fossil fuel sources from modern carbon sources is that ^{14}C measurements may be contaminated by so called "hot carbon" or "super-modern carbon", i.e. higher ^{14}C concentrations than the one expected in the contemporary atmosphere [53]. ^{14}C contamination can e.g. occur near nuclear installations, incinerators burning radioactive waste or at facilities using ^{14}C as a tracer. If the ^{14}C-contamination is high the source apportionment would indicate > 100% modern carbon in the particles. This should be taken as an indication that the site should not be used for sampling PM, with the intention of making ^{14}C-based analysis. Lower levels of ^{14}C contamination are much more difficult to detect and will lead to overestimation of the biogenic contributions to OC and EC, and underestimation of the fossil fuel sources. Presently, the extent of this problem is unknown; Buchholz et al. [53] suggest that "Super modern $PM_{2.5}$ samples are uncommon, but not rare" and they have seen "unnaturally elevated ^{14}C levels in PM in at least some samples from about 10% of the sites surveyed". Even relatively remote sites may occasionally show elevated ^{14}C concentrations [53] but the problem is likely more common in industrial/urban areas — even in the highly polluted Mexico City region, with very large emissions from fossil fuel sources, CO_2 is usually enriched in ^{14}C [54], which makes it impossible to separate fossil from non-fossil sources by radiocarbon analysis. Considering these problems it seems that radiocarbon techniques may be of more limited use for determining the contributions from fossil and modern sources to carbonaceous aerosol particles in urban areas than previously realised, at least without supporting measurement of other source specific tracers. High apparent contributions from biogenic sources may be due to ^{14}C-contamination. This issue also seems to affect some rural sites in Europe, but the causes and extent are still under investigation [55].

Another issue is that the most commonly used tracer for wood combustion, levoglucosan (produced during low temperature combustion of cellulose and hemicellulose [56]) may not be stable in the atmosphere. Recent studies have shown that it may react with OH both in the gas-phase [57], [58] and aqueous phase (deliquescent particles and cloud droplets) [59], [60]

leading to relatively short estimated atmospheric life-times of ca 1–5 days, depending on season and atmospheric conditions. The importance of this degradation of levoglucosan in the ambient aerosol is still not clarified [61] but, especially during summer, it may lead to a depletion of levoglucosan during long range transport. This would lead to an underestimation of the biomass burning contribution to OC and EC in the source apportionment studies, especially for sources far away from the sampling site, and a corresponding overestimation of the biogenic secondary organic aerosol contribution to OC.

Levoglucosan may also be emitted during combustion of lignite (brown coal) and levoglucosan emission factors from lignite have been found to be similar or even somewhat higher than for wood burning [62]. This means that source apportionment studies using levoglucosan as a tracer for wood burning will also apportion carbonaceous particles from lignite burning to the "wood burning" fraction. Since lignite is a fossil fuel, and all of the "wood burning carbon" is considered non-fossil in the source apportionment method applied, the biogenic secondary organic aerosol contribution to OC will be underestimated by the same amount as the wood burning OC is overestimated. In regions where lignite is used as fuel (e.g. parts of Poland, the Czech Republic and Bulgaria) levoglucosan should thus be considered as an indicator of a mixture of burning wood and lignite [62]. A possible way to discriminate between wood and lignite combustion could be to include other tracers of biomass burning — galactosan and mannosan seem to be absent or be emitted to a lower degree during lignite combustion [62].

Source apportionment studies are more complicated than just measuring total concentrations; they also often involve large uncertainties in the source-determination. Regardless of this, they are crucial when evaluating the performance of chemical transport models and emission inventories as discussed in Sect. 5. Without source apportionment data it is difficult to determine likely causes of model deviation from observed concentration and almost impossible to determine if "good" agreement between model results and measurements for OA-concentrations are for the right reasons or if it is because of "fortuitous" cancellation of errors or tuning of model parameters and/or emissions. It seems that only source apportionment data can constrain model parameters and emission estimates, in a reasonable way, for atmospheric organic aerosol modelling.

3 Elemental Carbon (EC) modelling (Paper IV)

The deposition efficiency determines the atmospheric residence time (and thereby the potential for long-distance transport) of non-volatile and unreactive particulate matter, such as most of the EC in the ambient atmosphere. Dry deposition is slow for accumulation mode particles and the most efficient removal is often by wet deposition.

Freshly emitted soot particles are often hydrophobic or have limited hygroscopicity (e.g. [63]–[65]). This means that they do not easily become cloud condensation nuclei (CCN), and thus do not contribute to cloud formation, and that they are not very efficiently removed by precipitation.

Hydrophobic soot particles can become hydrophilic after processing ("aging") in the atmosphere (e.g. [66]). Important processes include condensation of hydrophilic material (e.g. inorganic or organic vapours), coagulation with hydrophilic particles, and heterogeneous oxidation that can transform hydrophobic surface coatings into hydrophilic forms.

The timescale for the conversion of soot from hydrophobic to hydrophilic forms is variable and uncertain. Modelling studies have used different assumptions. A number of studies have assumed simple exponential decay rates for the conversion with life-times of about 1-2 days (e.g. [66], [67]) while other models have included more physical schemes taking into account coagulation and condensation to estimate the aging time (for an intercomparison and evaluation of BC in seventeen different global aerosol models, see [68]).

Some EC-containing particles may be hygroscopic already at the point of emission if they contain enough hydrophilic material, e.g. sulphuric acid from fuels with relatively high sulphur content (e.g. [69]) or inorganic salts common in biomass burning emissions (e.g. [27], [70]).

3.1 The EMEP MSC-W model for EC

The EMEP MSC-W model treatment of EC is relatively simple. Emissions of EC in $PM_{2.5}$ ($EC_{2.5}$) are split into a hydrophilic and a hydrophobic fraction. The hydrophilic fraction is assumed to be internally mixed with the soluble inorganic and organic aerosol components and for these particles in-cloud scavenging is assumed to be very efficient (scavenging coefficient $W_{in} = 1 \times 10^6$, see [11], corresponding to an exponential life time of 1 hour in a precipitating cloud with precipitation rate = 1 kg m^{-2} $hour^{-1}$). In Paper IV the hydrophobic EC was assumed to have a low in-cloud scavenging coefficient ($W_{in}=5 \times 10^4$) (4 times lower than the value assumed by Simpson et al. [11] but higher than the zero in-cloud scavenging used by Tsyro et al. [19]). The collection efficiency for below-cloud scavenging is low for all fine particles in the model, so wet deposition is inefficient for the hydrophobic EC. Dry deposition is also slow for accumulation mode particles under most conditions.

In the standard model version all anthropogenic $EC_{2.5}$ emissions from fossil fuel sources and residential combustion are assumed to consist of 80% hydrophobic and 20% hydrophilic EC. This split was initially used in the ECHAM general circulation model [71] and has then been widely used in different models (see e.g. [66]).

In contrast to the anthropogenic emissions, all of the EC emitted from open biomass fires (wildfires and agricultural burning) is treated as hydrophilic in the model version used in

Paper IV. Many studies have shown that biomass burning particles tend to be CCN active already at the point of emission or age very rapidly in the atmosphere so that they may be considered as hydrophilic in regional scale models (e.g. [72]–[74]).

The rate of transformation of hydrophobic EC to hydrophilic (the aging rate), initially introduced in the EMEP model in [19], is loosely based on the work by Riemer et al. [75]. They simulated aging of diesel soot in a polluted environment and constructed a simple parameterization of aging rates dependent on time of day and altitude. Aging was most efficient during daylight hours, when condensation of sulphuric acid and ammonium nitrate on the soot particles dominated. Aging was slower at low altitudes (close to the sources) than above the source region. In the standard EMEP model, the timescale (e-folding time) for EC aging is 8 h (rate 3.5×10^{-5} s^{-1}) for the three lowest model levels (up to ~300 m). At higher altitudes aging is more rapid with a lifetime of 2 h for the fresh EC. During the dark hours (sun below the horizon) the EC aging rate is low, 9.2×10^{-6} s^{-1}, corresponding to a lifetime of 30 h. The slow rate at night is due to aging by coagulation (condensation was not effective during night in [75]). Sensitivity tests of the aging assumptions were performed in Paper IV.

Support for the rapid hydrophobic to hydrophilic transformation of soot in daytime has been given by a number of recent field studies; the conversion rate can be quite fast during daytime and CCN activation of soot may occur on a timescale of hours (e.g. [76]–[78]). This is also supported by a recent laboratory study by Lambe et al. [79], who investigated the transformation of soot particles from hydrophobic to hydrophilic by heterogeneous OH oxidation and condensation of hydrophilic organic or inorganic coatings on the soot particles. The results of Lambe et al. suggest that the CCN activation of soot is primarily due to secondary coatings. Another recent study [80] indicates that heterogeneous oxidation by OH and ozone of organic coatings on soot particles may be fairly rapid during daytime, in moderately polluted environments, and can occur on comparable timescales as the aging by condensation.

The parameterisation of the aging rate in the EMEP model is based on simulations for polluted conditions and this could mean that the rate is too high in cleaner regions of the atmosphere. On the other hand the largest EC emissions occur in polluted regions and, at least in some areas, rapid aging of EC may also occur by condensation of biogenic secondary organic aerosol on the soot particles [79], [81].

3.2 Modelled EC

In Paper IV elemental carbon concentrations in Europe were modelled for the years 2005–2010. The model results were compared to EC concentrations at eight sites in northern, western and central Europe (measured by thermal analysis techniques) and at seven of the sites also to optical (BC) measurements.

To evaluate the model sensitivity to the assumptions regarding EC hygroscopicity and aging, three different model setups were tested in Paper IV. In addition to the standard aging scheme described above (Sect. 3.1) the model was also run with two alternative schemes:

- "FRESH" assuming that all EC is hydrophobic (treated as externally mixed, neglecting aging). This leads to more efficient long-range transport of EC than the standard version and gives a maximum estimate of EC.

- "AGED" assuming that all EC is internally mixed and hygroscopic when emitted.

Fig. 3.1a shows the modelled six-year mean surface level concentration of $EC_{2.5}$ (2005–2010) using the standard model setup. The highest modelled EC concentrations are found in urban and industrialized areas; in densely populated parts of western and central Europe the mean concentration of EC generally range from 0.4 to 1.2 μg m^{-3} (or somewhat higher in emission hotspots). Fossil fuel sources dominate the modelled surface level $EC_{2.5}$ (more than 70% in most countries, see Fig. 3.1b). Residential wood combustion contributes substantially to EC in some countries (e.g. France, Austria, Norway, Finland, Latvia and Romania), where 30–50 % or more of the modelled $EC_{2.5}$ come from this source. Open biomass fires may also emit substantial amounts of EC into the atmosphere during fire episodes but, according to the model simulations, the long-term (six–year mean) contributions from these emissions to near-ground $EC_{2.5}$ is relatively low (<10%) except in parts of the Ukraine and Russia. The total modelled $EC_{2.5}$ from biomass burning (residential combustion + open fires) is shown in Fig. 3.1c.

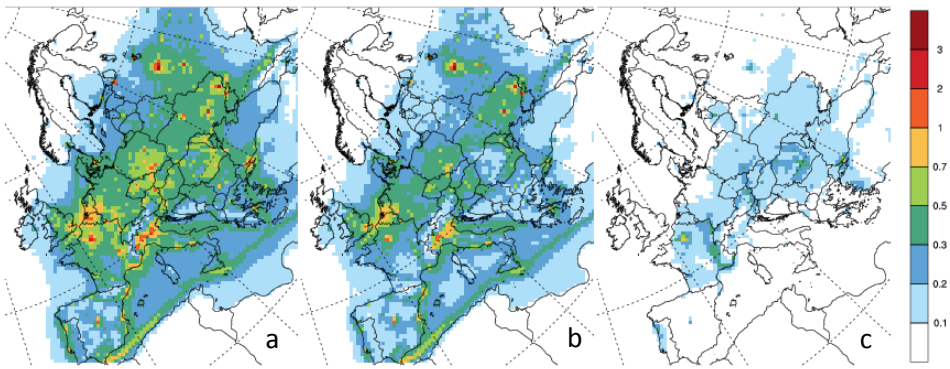

Figure 3.1 (a) *Six-year mean concentration of elemental carbon in $PM_{2.5}$ ($EC_{2.5}$) for 2005–2010, calculated with the standard model setup,* ***(b)*** *$EC_{2.5}$ from fossil fuel combustion,* ***(c)*** *$EC_{2.5}$ from biomass combustion. Unit: μg (C) m^{-3}.*

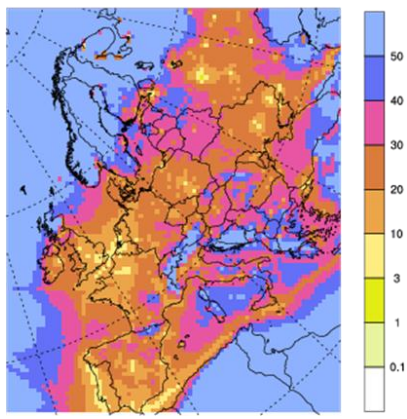

Figure 3.2 *Relative difference in model calculated elemental carbon in PM_{10} (EC_{10}) between a model version that treats all EC as hydrophobic (FRESH) and the standard model version that includes aging of EC. Unit: % higher model simulated EC_{10} with the FRESH version. Six-year average for the years 2005–2010.*

The model performed well when compared to (long-term average) EC concentrations for most of the sites examined in Paper IV (especially when considering the large uncertainties in EC measurements discussed in Sect. 2.2); the model bias was low (within ±20%) for six of the eight sites (Fig. 3.3). The model variability was lower than the observed one (Fig. 3.4), and the mean absolute error of the modelled concentrations compared to the EC measurements was 36–45% at five of the eight sites, but higher for the three others (64–75%); the correlation coefficients r between modelled and measured EC, ranged from 0.45 to 0.91 (Table 3.1).

The AGED model version gave very similar results to the standard model version. This is due to the relatively rapid aging rate used in the model. For most of the investigated sites the bias, mean absolute error and correlation were slightly better with the standard model version than with the AGED version.

The FRESH model version leads to substantially higher EC-concentrations than the standard version (Figs. 3.2 and 3.3). At most of the sites included in Paper IV the FRESH model overestimated EC concentrations, and the standard model version led to better agreement for average EC concentrations. For the more remote sites the measured EC concentration was in between the modelled EC using standard aging and the FRESH scenario. Considering the limited number of sites included in the study, the relatively small differences in model results between the different model versions, and uncertainties in both emissions and measurements, it is difficult to draw firm conclusions regarding the aging rates based on the data presented in Paper IV. However, the results for the majority of sites investigated indicate that the standard aging scheme may lead to somewhat too-rapid aging of the EC. This confirms that the aging scheme, which was originally constructed to simulate EC aging in polluted environments, may be less realistic for the cleaner parts of Europe.

Table 3.1 *Comparison of modelled EC to measured EC. N=number of measurements, Obs=Measured average EC-concentration, Model (r)=Modelled average EC concentration for the same time periods (r=correlation coefficient), MAE=Mean Absolute Error. Observed, Model, and MAE are given in µg/m³. Relative MAE values are given in parentheses (relative to the observed mean). Data from the years 2005–2010 but data coverage differs greatly between the stations.*

Station	N	Obs	Model (r)	MAE
Aspvreten (SE)	357	0.25	0.22 (0.63)	0.11(43 %)
Birkenes EC_{PM10} (NO)	537	0.13	0.11 (0.76)	0.06(44 %)
Birkenes $EC_{PM2.5}$(NO)	534	0.11	0.094 (0.71)	0.05(45 %)
Harwell (GB)	672	0.52	0.45 (0.45)	0.33(64 %)
Hyytiälä (FI)	248	0.18	0.16 (0.71)	0.07(41 %)
Mace Head (IE)	9	0.11	0.11 (0.91)	0.04(36 %)
Melpitz EC_{PM10} (DE)	2157	1.71	0.53 (0.55)	1.20(70 %)
Melpitz $EC_{PM2.5}$ (DE)	2100	1.43	0.45 (0.64)	0.99(70 %)
Overtoom (NL)	224	0.76	0.89 (0.51)	0.31(41 %)
Vavihill (SE)	143	0.19	0.32 (0.53)	0.14(75 %)

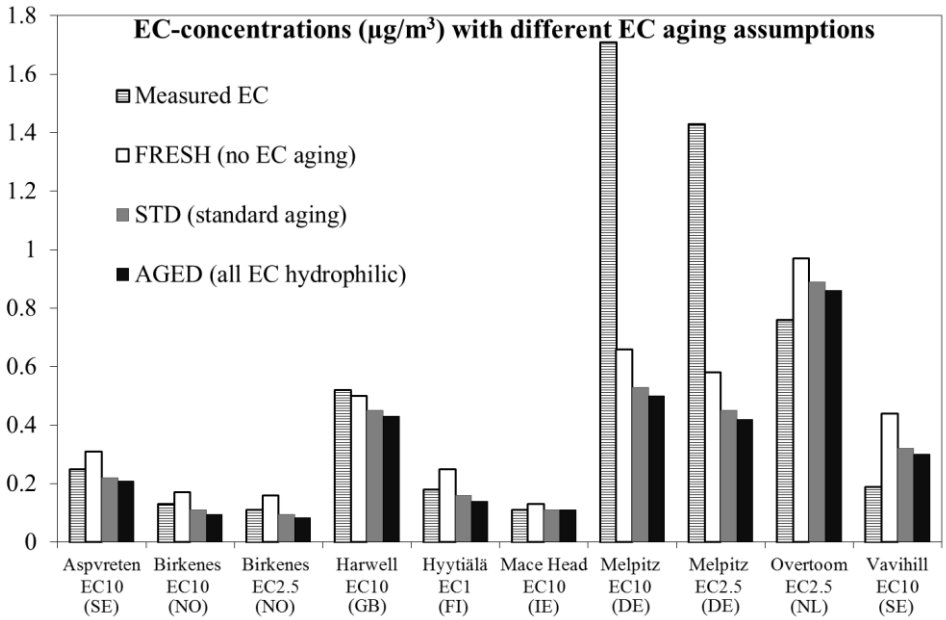

Figure 3.3 *Comparison of measured EC to model results from simulations using three different assumptions regarding the EC hygroscopicity and atmospheric aging. The diagram shows average EC concentrations for the periods with measurements: measured (striped); FRESH = model with all EC treated as externally mixed and hydrophobic, no aging (white); STD = standard model version, including atmospheric aging of EC (grey); AGED = model with all EC treated as hydrophilic already at emission (black); unit: µg (C) m^{-3}. Note that data are from different periods for different stations (see Paper IV).*

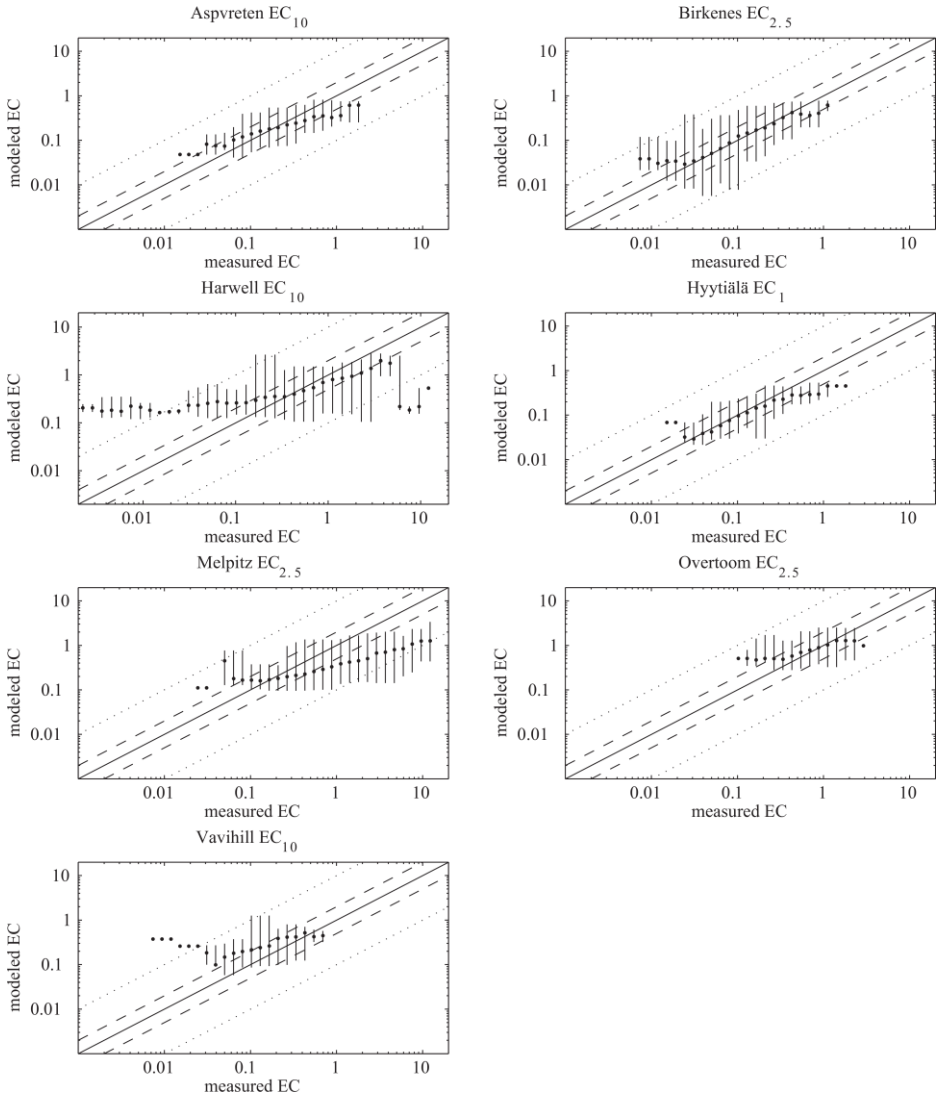

Figure 3.4 *Scatterplots of measured and modelled EC for seven European measurement stations:* ***(a)*** *Aspvreten* EC_{10}, ***(b)*** *Birkenes* $EC_{2.5}$, ***(c)*** *Harwell* EC_{10}, ***(d)*** *Hyytiälä* EC_{1}, ***(e)*** *Melpitz* $EC_{2.5}$, ***(f)*** *Overtoom* $EC_{2.5}$, *and* ***(g)*** *Vavihill* EC_{10}. *The measured EC are divided into logarithmically spaced concentration bins. Each order of magnitude is divided into 10 bins. The points represent the median of the model results for each concentration bin of measured EC. The vertical lines show the range of model results for each bin. Solid lines represent 1 : 1 lines. Dashed lines represent 2 : 1 and 1 : 2 lines, and dotted lines represent 10 : 1 and 1 : 10 lines. Unit: μg (C)* m^{-3}.

4 Organic aerosol (Paper I)

Organic compounds usually make up most of the carbonaceous aerosol; e.g. about 90% of the carbonaceous material in PM_{10} was organic matter, while only 10% was EC, at 12 rural sites in Europe [9]. Organic components are also major contributors to submicron particulate matter (PM_1). A recently published study, using aerosol mass spectrometry showed that 20–63% of the total PM_1 mass was due to organic aerosol at 17 European sites [82].

The chemistry of atmospheric organic aerosols is highly complex and an extremely large number of different chemical components may be involved (e.g. [83]–[87]). The complexity means that any attempt at large scale modelling of organic aerosol needs to be simplified. For overviews of both chemically detailed (explicit and semi-explicit) models and empirical models, see [84], [88]. Increased model complexity does not necessarily lead to improved agreement with observations as shown in a recent evaluation and intercomparison of organic aerosol in thirty-one global models [89].

A new model for treating organic aerosols was implemented and tested in the EMEP MSC-W model (Paper I). The new organic aerosol scheme is based on a semi-empirical approach, the so called volatility basis set (VBS) approach [90], further described in Sects. 4.3 and 4.4.

Organic aerosol is often divided into two types: primary organic aerosol (POA) — directly emitted organic particles; and secondary organic aerosol (SOA) — formed in the atmosphere after oxidation of organic molecules initially emitted in the gas-phase [91]. POA will be discussed in Sects. 4.1 and 4.3, and SOA in Sect. 4.4.

4.1 Primary organic aerosol (POA) emissions

4.1.1 Combustion

Different forms of combustion are the dominant anthropogenic sources of primary organic aerosol. Small-scale (residential) combustion is a very important source (see Sect. 5), partly because a lot of wood burning is used and partly because the emissions are usually not cleaned efficiently in the small scale appliances used. Another important source is emissions from vehicles - both from the fuel and lubrication oil [92]. Older vehicles are typically emitting much more than modern cars with (well-functioning) modern exhaust cleaning technology [93], [94]. Small off-road engines (e.g. lawnmowers, trimmers, diesel generators) can have very high emissions per amount of fuel used, but the total POA emissions from these sources are likely relatively small compared to emissions from road traffic [95], but see [96]. Shipping also emits substantial amounts of particulate matter, including a large fraction organic aerosol [97]; the OA (and total particle) emissions are expected to decrease due to new fuel regulations leading to a change from heavy fuel oil, with high sulphur content, to low-sulphur fuel (e.g. [97], [98]).

Vegetation fires (open biomass fires; including both agricultural burning and natural wildfires) are large sources of organic aerosol (e.g. [21], [27]) on the global scale and in some parts of Europe.

Primary organic aerosol emissions from combustion sources are semi-volatile [99], [100]. The emissions consist of a large number of different organic compounds with varying

volatilities. Most of these components have not been individually identified so the emissions are largely uncharacterized, consisting of an "unresolved complex mixture" [100]. However, emission inventories have so far assumed fixed POA emission factors for different sources, and chemical transport models have usually treated the organic emissions as consisting of a completely non-volatile fraction (the POA emissions from the inventory) and a completely volatile fraction (VOC, entirely in the gas-phase).

Since emission measurements typically have been done at high concentrations (small dilution) a substantial part of the POA emissions may evaporate when the emission plume is diluted in the atmosphere [100], [101]. The "traditional" assumption that the POA-emissions in the inventory are entirely non-volatile may lead to substantial overestimation of particulate POA-concentrations in the atmosphere (e.g. [101], [102]). The real particulate POA concentration will depend on the degree of dilution (and the background concentration of OA that the emitted semi-volatile compounds can partition to) and temperature.

4.1.2 Other primary organic aerosol emissions

A number of natural sources of primary organic aerosol particles exists [103]. Important examples include: pollen and pollen fragments, fungal spores, bacteria, viruses, plant debris (cellulose), animal debris, oceanic OA [104], lichen. Many of the primary biological aerosol particles (PBAP) are relatively large (> PM_{10}) and deposit efficiently, but at least at some locations a significant fraction of PM_{10} may consist of PBAP (e.g. [105]). In the work presented in this thesis the PBAP are not explicitly included.

Cooking (e.g. frying and charbroiling) may be an important source of primary organic aerosol, especially in urban areas. Aerosol mass spectrometry studies in Europe have found large OA contributions from cooking in a number of cities (Zürich, London, Manchester, Barcelona and Paris [82], [106]–[109]). The emission inventories used in this thesis only included small contributions from cooking and this source has not been explicitly studied here. Addition of cooking emissions to the inventory would raise the model calculated OA in urban areas but the impacts this source could have in Europe on regional scale are still unknown.

4.2 Gas-particle partitioning of the organic aerosol

To large extent organic aerosol particles consist of molecules that are semi-volatile, which means that they can exist simultaneously in the gas-phase and particulate phase. Gas-to-particle partitioning of organic molecules can occur by absorption into an organic solution or adsorption on particle surfaces [110]. Absorption is usually assumed to be the dominant partitioning mechanism for ambient aerosols (e.g. [83], [90], [111]).

A common simplifying assumption is that the organic components in the particles can be described as a (pseudo-ideal) mixture in equilibrium with the atmosphere [88]. Assuming that the gas-particle partitioning of the semi-volatile organic compounds occurs through absorption into a condensed organic aerosol phase, the fraction of a compound, i, in the condensed phase, ξ_i, can be written [90]:

$$\xi_i = \left(1 + \frac{C_i^*}{C_{OA}}\right)^{-1} ; \; C_{OA} = \sum_i C_i \, \xi_i \,, \qquad (1)$$

where C_{OA} is the total mass concentration of absorbing organic aerosol; C_i is the total concentration (gas + particle phase) of the compound i; and C_i^* is the effective saturation concentration of compound i. C_i^* is the inverse of the frequently used gas-particle partitioning coefficient, K_p, (e.g. [112]),

$$C_i^* = \frac{C_i^{gas} C_{OA}}{C_i^{part}} = \frac{1}{K_p}, \quad (2)$$

where C_i^{gas} and C_i^{part} are the concentrations of compound i in the gas-phase and particulate phase. Eq. 1 is a convenient way of expressing the gas-particle partitioning but it is important to remember that the effective saturation concentrations (C_i^*) are semi-empirical properties of the organic aerosol components, and they include the activity coefficients of the compounds in the organic aerosol mixture. If one assumes that the individual activity coefficients remain constant under different atmospheric conditions (i.e. that the organic aerosol behaves as a pseudo-ideal solution), then the C_i^* for a given component will also remain constant [91].

The gas-particle partitioning depends on the total organic mass concentration C_{OA} (Eq. 1). This means that the fraction of a given semi-volatile compound that is in the particle phase will be higher near large emission sources than in remote parts of the atmosphere – the organic aerosol will tend to evaporate upon dilution [90].

The partitioning is also temperature dependent; the volatilities of the organic compounds decrease with temperature. An expression for the temperature dependence of C_i^* can be derived from the Clausius-Clapeyron equation [113],

$$C_i^*(T) = C_i^*(T_{ref}) \frac{T_{ref}}{T} \exp\left[\frac{\Delta H_{vap,i}}{R}\left(\frac{1}{T_{ref}} - \frac{1}{T}\right)\right], \quad (3)$$

where T is the temperature; $C_i^*(T_{ref})$ is the effective saturation concentration, at a reference temperature T_{ref}; $\Delta H_{vap,i}$ is the enthalpy of vaporisation; and R is the ideal gas constant.

Compounds with effective saturation concentrations C^*(298K) in the range 0.01–1 000 μg m^{-3} are denoted SVOCs – semi-volatile organic compounds, since they can occur simultaneously in the gas and particle phase at least in some parts of the atmosphere; sometimes the term LVOC (low volatility organic compounds) is used for the C^*-range 0.01–0.1 μg m^{-3} [91]. Higher volatility compounds with C^* from 10^4 μg m^{-3} to 10^6 μg m^{-3} are usually called IVOCs – intermediate volatility compounds; these are almost entirely in the gas-phase except at very extreme conditions. However, due to their relatively low volatility, IVOCs (and SVOCs in the gas-phase) are expected to easily form secondary organic aerosol after oxidation in the atmosphere (see Sect. 4.4).

4.3 Volatility basis set (VBS) treatment of POA

To be able to take the effects of volatility into account Donahue et al. [90] suggested that the static description of POA emissions as a fixed non-volatile emission is replaced by a dynamic treatment of the emissions as a set of lumped/surrogate species that span a wide range of volatilities, using a VBS of effective saturation concentrations (C^*) from 0.01 μg m^{-3} to 1 000 000 μg m^{-3}, with the different volatility bins separated by powers of 10 (at 298K).

Emissions of organic compounds more volatile than $C^* = 3\times10^6$ μg m^{-3} are assumed to be included in the VOC-emissions in the emission inventories but a large fraction of the lower-volatility organics ($C^* \leq 3\times10^6$ μg m^{-3}) are likely missing in the traditional emission inventories; the amount of low-volatility organics that is missing is uncertain but it has been estimated that these are underestimated by a factor 2–3 [91].

To be able to better describe the evolution of OA in the atmosphere the primary organic aerosol emissions should thus not be described as non-volatile emissions but as emissions of varying volatilities (SVOC and IVOC emissions; possibly including some fraction of non-volatile OC). Until recently, volatility distribution estimates were only available for a few emission sources [100], [114], and, since they were based on measurements of mass collected on quartz filters, IVOCs were not included (except as a "positive" measurement artefact [38]). The volatility distributions were constructed from gas-particle partitioning data for the POA measured at varying temperatures or exhaust concentrations [101], [114]. This approach has several drawbacks [101] and the volatility distributions determined from fits of gas-particle partitioning data are not unique; many different combinations of volatility distributions, total emissions and enthalpies of vaporisation can satisfy the same data [115], [116].

In Paper I, the VBS approach to treating the primary organic aerosol emissions was introduced in the EMEP MSC-W model. All POA emission sources were assumed to have the same volatility distribution for the semi- and intermediate volatility OC (S/IVOC) emissions; the distribution was initially determined for diesel exhaust and assuming that the mass of the missing IVOC-emissions is 150% of the POA-inventory emissions [100], [102].

Recently a number of new studies of the gas-particle partitioning of different emission sources have been performed at the Carnegie Mellon University [101], [116]–[118]; just as in earlier works, only the SVOC part of the emissions is covered in these studies — detailed knowledge of the IVOC emissions is still missing.

4.4 Secondary organic aerosol (SOA)

Secondary organic aerosol may form in the atmosphere after chemical transformations of relatively volatile (primary emitted) organic compounds into less volatile compounds that partition to the particle phase. Here a brief overview will be given of some aspects of SOA important for this thesis, and of the way SOA formation was implemented in the EMEP model. For reviews of SOA formation (and other aspects of SOA) see [84], [85], [119].

Volatile organic compounds may form SOA after oxidation in the atmosphere. SOA formed after gas-phase oxidation of VOCs has been studied (and modelled) for a long time and until fairly recently most chemical transport models only considered SOA from VOCs (VOC-SOA) [88]. Sometimes the VOC-SOA is called "traditional" SOA, to separate it from SOA formed from primary emissions of S/IVOCs. There is no fundamental difference between the formation of SOA from S/IVOCs and that from VOCs but some confusion may arise from the fact that SVOCs can be both primary OA and at the same time precursors for SOA.

Important SOA precursors include both VOCs emitted from vegetation (biogenic VOCs, or BVOCs; discussed in more detail below) and VOCs of anthropogenic origin (AVOCs). Usually aromatic compounds are the most important AVOC-precursors; e.g. SOA-yields from photo-oxidation of toluene can be very high [120].

Since S/IVOCs are relatively low-volatile compounds they have a large potential to form particulate SOA after oxidation in the atmosphere [96], [100], [121]. This means that the major anthropogenic primary OA sources are important anthropogenic SOA (ASOA) sources as well.

4.4.1 SOA from biogenic VOC-emissions

Globally, emissions of biogenic VOCs by forests and other vegetation are the major sources of organic compounds to the atmosphere; Guenther et al. [122] estimated that the annual total global BVOC emissions are about 1000 Tg, which can be compared to an estimate of the total anthropogenic VOC-emissions of ca 130 Tg for the year 2000 [123]. The global BVOC emissions are dominated by isoprene (~50%), monoterpenes (~15%) and methanol (~10%) according to the MEGAN2.1 model estimates [122]. However, there are large regional variations in the emissions; in a recently published BVOC emission model for Europe [124] the European BVOC emissions are estimated to be dominated by oxygenated VOCs (methanol, formaldehyde, formic acid, ethanol, acetaldehyde, acetone, acetic acid) (43-45% of the total BVOC emissions) and monoterpenes (33-36%) while the isoprene emissions are somewhat lower (18-21%). In most of the papers included in this thesis only BVOC emissions of monoterpenes and isoprene were included. For the whole EMEP model domain the annual total (2007) monoterpene emissions were about 20 Tg and the isoprene emissions 9 Tg (Fig. 4.1).

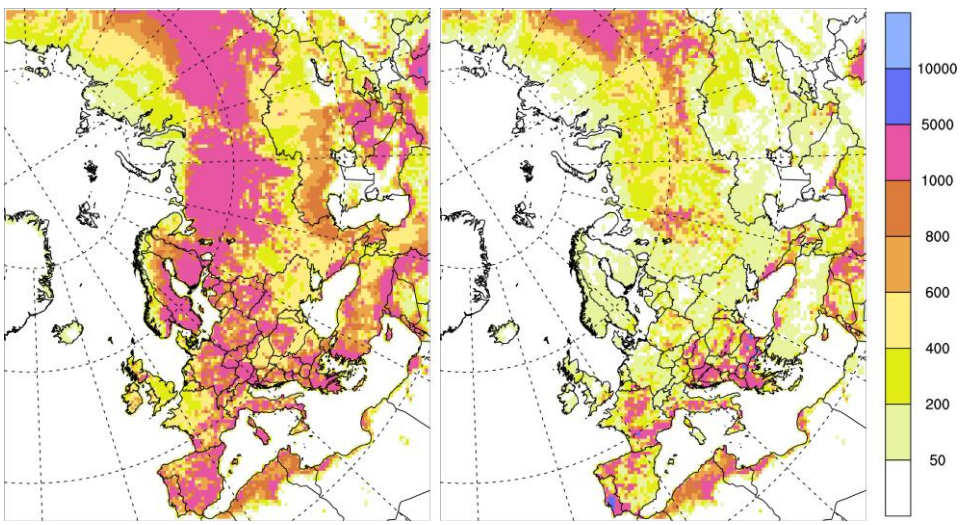

Figure 4.1 *Biogenic emissions of monoterpenes (left) and isoprene (right) in the EMEP model domain for the year 2007. Unit: mg m^{-2}.*

The uncertainties of the BVOC-emissions estimates are large — Guenther et al. [122] estimate that for a few compounds (including isoprene and methanol) the uncertainties in the *annual global* emissions are about a factor of two while the uncertainties for the most abundant monoterpenes (and a few other compounds) are about a factor of three; for most other species uncertainties are higher. It should also be noted that the uncertainties for specific times and locations can be much larger than those for the annual global emissions.

Emissions of BVOCs are considered as being constitutive if produced and released by unperturbed (non-stressed) vegetation. Most BVOC-emission algorithms for regional scale application include only constitutive emissions and these are assumed to be controlled by meteorology (especially temperature and light) and phenological cycles [11], [122]. Induced BVOC-emissions from stressed plants will be discussed in Sect. 6.

Oxidation of BVOCs in the atmosphere contributes to the formation of ozone and leads to formation of biogenic SOA (BSOA) [84]. Many BVOCs are unsaturated (e.g. isoprene, α-pinene and sesquiterpenes) and react with all of the main oxidants in the atmosphere (OH, O_3, NO_3). Some of the BVOC oxidation products have low vapour pressures and may form SOA by gas-to-particle transformation.

Monoterpenes have been considered as the most important BSOA precursors due to large emissions combined with high SOA-yields seen in smog-chamber experiments (e.g. [83], [85] and references therein). Although isoprene emissions can be very large, the SOA-formation from this compound has been thought to be minor due to high volatilities of its oxidation products [125]. However, during the last decade a number of studies have indicated that isoprene oxidation may potentially lead to substantial SOA-formation via a number of different mechanisms [126]. Chamber studies of the SOA yield from isoprene show a high degree of variability and the reasons for this are not fully understood. A very recent study [127] suggests that the light-source used in the experiments could be an important factor, and that studies using natural light or artificial lamps with emissions similar to the solar spectrum produce substantially less SOA than studies using fluorescent lamps with no emissions at long (> 400 nm) wavelengths; this was interpreted as an indication that SOA mass yields from isoprene in the atmosphere could be lower than suggested by a number of chamber studies.

The SOA-yields from oxidation of sesquiterpenes (SQT) are high (e.g [128], [129]) but SQT emission estimates are very uncertain [130], global SQT-emissions have been estimated to be relatively low [122] and the SQT-emissions may to a large extent not be constitutive, but rather induced by stress (e.g. caused by insect infestations [130]–[132]; see Sect. 6); for these reasons many SOA-models have neglected SQT emissions. In this thesis SQT emissions were only included in Paper III and in some further sensitivity tests presented in Sect. 7.

A number of studies have shown that BSOA is often a major contributor to ambient OA at rural, and even some urban, sites in Europe (e.g., [46], [105], [133], [134] and Paper II). BSOA has been estimated to contribute approximately half of the total OC on a global scale [84]; the uncertainty of this estimate is very large – BSOA contributions as small as 1/8 and as large as 2/3 were also considered plausible.

4.4.2 Volatility basis set treatment of SOA

SOA formation from S/IVOCs

A simplified approach to treat SOA formation from S/IVOCs was introduced in the EMEP model in Paper I. The method is based on the POA oxidation scheme by Robinson et al. [100] and Shrivastava et al. [102]. The POA emissions are distributed over different volatilities, using a 9-bin VBS as described in Sect. 4.3. The gas-phase fraction of the S/IVOCs reacts with OH radicals and each reaction results in a shift of the compound to the next lower volatility bin (one order of magnitude lower volatility; this is a conservative volatility reduction typical

of the addition of a carbonyl group to the reacting compound [102]). In addition, a small increase in mass is included for each oxidation step (+7.5% to account for added oxygen and other non-carbon atoms [100]).

Separate model components are used for three different S/IVOC sources: fossil fuel sources, residential biomass combustion and vegetation fires. Separate model species are also used for primary components and oxidised (aged) components, to be able to separate POA from SOA.

As an example of how the S/IVOC reactions are treated in the model, reactions R1 and R2 show the first two oxidation steps for the surrogate species for fossil fuel OA emissions with effective saturation concentration $C^* = 10^3$ µg m^{-3} (denoted FFUEL_ug1000):

$$\text{FFUEL\_ug1000(g)} + \text{OH} \rightarrow \text{oxFFUEL\_ug100} + 0.075\ \text{O\_FFUEL\_ug100} \quad \text{(R1)}$$

$$\text{oxFFUEL\_ug100(g)} + \text{OH} \rightarrow \text{oxFFUEL\_ug10} + 0.075\ \text{O\_FFUEL\_ug10} \quad \text{(R2)}$$

The oxFFUEL_ugX model compounds also partition between the gas and particle phases and the particulate fraction of these contribute to the SOA concentration. The additional model species (O_FFUEL_ugX) are used to keep track of the 7.5% mass increase.

The reaction rate for the OH-oxidation (both R1 and R2) is set to 4×10^{-11} cm^3 $molecule^{-1}$ s^{-1} (taken from [100]). This rate is about a factor of 2 higher than typical OH-reaction rates for large n-alkanes [135]. Reducing the rate by a factor of two led to underestimation of SOA-formation, when comparing to a smog-chamber study of diesel exhaust, while the original scheme reproduced the SOA *mass* fairly well after about 1-3 hours of oxidation but overpredicted SOA at longer times [102]. An alternative scheme with slower reaction rate (2×10^{-11} cm^3 $molecule^{-1}$ s^{-1}) in combination with more added mass per reaction (+40%) and a larger drop in volatility (two orders of magnitude per reaction) has been constructed [136] to fit observed oxygen-to-carbon ratios in laboratory experiments on oxidation of wood smoke better than the scheme from [100].

These atmospheric reactions mean that the initially emitted IVOCs will gradually be transformed into less volatile compounds that start to contribute to the particulate OA.

The simple VBS-based S/IVOC scheme for primary OA emissions and SOA formation is a first attempt at including the effect of unspeciated (IVOC) emissions and treating the organic aerosol in a more realistic way than to assume non-volatile POA emissions and to only include SOA-formation from VOCs. Unfortunately the scheme is poorly constrained by available experimental data. The volatility distributions of the POA emissions from different sources are not uniquely defined (Sect. 4.3), the amount of IVOC emissions from different sources is uncertain, and most of the IVOCs are unspeciated, which means that their reactivities and SOA-forming potentials are uncertain.

An alternative to this way of treating the unspeciated organic emissions has been proposed by Jathar et al. [94]. They determined the SOA yield of the unspeciated organics from different sources and for each source they chose a single surrogate n-alkane species, with as similar SOA-formation potential as possible as the mixture of unspeciated organics in smog chamber experiments. These surrogate species can be used in chemical transport models to represent the total amount of unspeciated emissions, including evaporated semi-volatile POA emissions.

SOA formation from VOCs

A VBS-scheme for treating SOA formation from oxidation of VOCs was also added to the EMEP model in Paper I. A small 4-bin VBS is used to model SOA formed both from anthropogenic and biogenic VOCs [137]. The four bins include only SVOCs and cover the effective saturation concentration (C^*) range 1 – 1000 μg m^{-3}. The parameterisation of the SOA-formation from a given model-VOC can be written:

VOC + oxidant → VOC-peroxy radical (R3)

VOC-peroxy radical + NO → $\alpha_{1,\text{high-NOx}}P_1 + \alpha_{2,\text{high-NOx}}P_{10} + \alpha_{3,\text{high-NOx}}P_{100} + \alpha_{4,\text{high-NOx}}P_{1000}$ (R4)

VOC-peroxy radical + HO_2 → $\alpha_{1,\text{low-NOx}}P_1 + \alpha_{2,\text{low-NOx}}P_{10} + \alpha_{3,\text{low-NOx}}P_{100} + \alpha_{4,\text{low-NOx}}P_{1000}$ (R5)

where P_1, P_{10}, P_{100} and P_{1000} are the four different semi-volatile surrogate species, with $C^* = 1$, 10, 100 and 1000 μg m^{-3}, and the yield coefficients α_1-α_4 may be different for low- and high-NO_x conditions. Table 4.1 shows the mass yields α_i used for the different SOA precursor VOCs.

SOA formation from monoterpenes can be initiated by gas-phase oxidation by any of the three oxidants O_3, OH or NO_3 but for isoprene only oxidation by OH leads to SOA formation in the model. The isoprene + NO_3 reaction has been shown to produce SOA in laboratory studies with fairly high yields (4-24%) [138] but isoprene is only emitted during daytime and it reacts rapidly with OH so only a minor fraction of it will remain at night when the concentration of NO_3 radicals can be significant. For all anthropogenic VOCs the SOA-formation is initiated by OH-reactions; model alkenes (surrogate species propene) also react with ozone but this reaction does not lead to SOA-formation in the model.

Table 4.1 *Mass yields (α) of semi-volatile surrogate species, with saturation concentrations, C^*(298K), of 1, 10, 100 and 1000 μg m^{-3}, for the EMEP model SOA precursors for the high- and low-NO_x cases (corresponding to peroxy radical reaction with NO and HO_2, respectively).*

Precursor	**α-values (mass based stoichiometric yields)**							
	High-NO_x Case (R4)				Low-NO_x Case (R5)			
	1	10	100	1000	1	10	100	1000
Alkanes	0	0.038	0	0	0	0.075	0	0
Alkenes	0.001	0.005	0.038	0.15	0.005	0.009	0.06	0.225
Aromatics	0.002	0.195	0.3	0.435	0.075	0.3	0.375	0.525
Isoprene	0.001	0.023	0.015	0	0.009	0.03	0.015	0
Terpenes	0.012	0.122	0.201	0.5	0.107	0.092	0.359	0.608

Notes: yields are based on [139], and references therein. Alkanes (excluding C_2H_6), alkenes (excluding C_2H_4) and aromatics are represented by the surrogates n-butane, propene, o-xylene in the EMEP-chemistry.

4.4.3 Atmospheric aging of SOA

An important issue regarding SOA-formation is the longer-term evolution of the SOA in the atmosphere. Most smog-chamber experiments have a relatively short duration and the SOA particle mass yields determined from these studies may be due to only a few reaction-steps following the initial oxidation of the VOC by O_3, OH or NO_3. Many of the products from the

oxidation of common BVOCs (and AVOCs) are semi-volatile; a large fraction of this semi-volatile SOA will be in the gas-phase under normal atmospheric conditions. Most of these gas-phase molecules likely react rapidly with OH (and in some cases also with other oxidants). These reactions may lead to addition of functional groups to the molecule (e.g. carbonyls, hydroxyl or nitrate groups); when this happens the products will have lower volatilities than the reacting molecule and they will partition to the particulate phase to a higher degree [119]. The oxidation can also lead to fragmentation of the molecule into smaller pieces usually with higher volatility than the reacting molecule. Fragmentation reactions become increasingly important as the oxidation state of the organic aerosol component increases and given enough time the final outcome of oxidation of organic molecules would be CO_2 [140].

The atmospheric oxidation of the aerosol, consisting of both functionalization and fragmentation reactions, is often called aging and it may potentially lead to large changes in the degree of oxidation of the particulate OA, compared to the fresh particles, and also to substantial increase in particulate SOA-mass [141].

Many types of reactions can occur in the condensed phase (see e.g. [84], [119]) but in the models used in this thesis only gas-phase reactions have been included (note however that some effects of rapid condensed phase reactions may be included in the SOA-yields in the experiments used in the VBS-parameterisation [85]). The homogeneous gas-phase aging by reaction with OH-radicals is likely much faster than aging in the particle phase by heterogeneous uptake of oxidants, except for molecules with very low volatilities [88]; but the time scale of heterogeneous reactions is shorter than typical atmospheric residence times for submicron particles so these reactions may also be important during long-range transport of the particulate organic compounds [88], [141]. At least two studies [142], [143] have shown that UV radiation may lead to fragmentation of α-pinene SOA and this could potentially be an important sink process for SOA in the atmosphere.

In Paper I different assumptions regarding the aging of SOA were explored. For S/IVOC species, from primary OA emissions, multi-generational aging was allowed without fragmentation (as described in Sect. 4.4.2); this simplification was based on the assumption that the POA emissions to a large extent consist of large relatively unsubstituted alkanes for which fragmentation reactions are uncommon [102].

Three different model schemes (based on [144] and [145]) were implemented for VOC-SOA:

- No aging of VOC-SOA, i.e. only including the first-generation products (4-bin VBS; Table 4.1.
- Aging of both biogenic and anthropogenic VOC-SOA; the 4-bin VBS SVOC-surrogate species, produced in reactions of type R4 and R5, were allowed to react with OH radicals in the gas-phase with the reaction rate 4×10^{-12} cm^3 $molecule^{-1}$ s^{-1}, with each oxidation reaction leading to a reduction of the volatility by a factor of 10 and a net mass increase of 7.5% to account for addition of oxygen. This scheme allows multi-generational aging of the VOC-SOA, and no fragmentation is included. This can lead to very large SOA-yields, since eventually most of the first-generation SVOC products will be transformed into LVOC (C^*=0.1 μg m^{-3}) that partition almost completely to the particle phase. The use of a very low aging rate (an order of magnitude lower than the aging rate for the S/IVOC-SOA species) delays this

process but Lane et al. [144] anyway found that this aging scheme led to serious overestimation of OC concentrations in rural areas in eastern USA.

- No aging of biogenic VOC-SOA but aging of anthropogenic VOC-SOA, using the OH-reaction rate 1×10^{-11} cm^3 $molecule^{-1}$ s^{-1} as suggested in [145].

4.4.4 Dry deposition of SOA vapours

The particulate phase OA from the VBS-scheme is assumed to be in the accumulation mode (and internally mixed with the inorganic aerosol). The particles are assumed to be hygroscopic, which means that wet deposition through in-cloud scavenging is efficient (see Sect. 3.1). Wet deposition is usually the most important removal mechanism for non-volatile accumulation mode particles, since dry deposition is very slow under most conditions. However, for semi-volatile components (such as SOA) deposition losses can also occur in the gas-phase. The dry deposition velocities of most of the semi-volatile SOA components (and IVOCs) are unknown and it is difficult to estimate appropriate deposition velocities for the lumped species representing the complex mixture of SOA-components in the VBS-based schemes used in this thesis. Neglecting dry deposition of SVOC(g) may lead to overestimation of the particulate OA concentration [146]–[149]. The importance of dry deposition of anthropogenic organic vapours from long-chained alkanes (typical primary S/IVOC-emission components) seems to be limited [147] while the semi-volatile gas-phase products from oxidation of biogenic and anthropogenic VOCs may be highly water soluble and may be efficiently taken up through plant stomata and by wet surfaces, leading to efficient dry deposition [146], [148], [149]. In the work presented in this thesis the dry deposition velocity of all oxidised semi- and intermediate volatile organic components in the gas-phase was assumed to be the same as for acetaldehyde (see [11] for a detailed description of the handling of dry deposition in the model). This means very low deposition velocities during winter (typically less than 0.1 cm s^{-1}) and slightly higher during summer (ca 0.1 – 0.4 cm s^{-1}). These low deposition velocities may lead to overestimated atmospheric residence times for SOA in the model. A sensitivity test assuming very efficient dry deposition of biogenic SOA components in the gas phase is included in Sect. 7.

4.5 Results – out of wood?

In Paper I four different VBS-based organic aerosol schemes were implemented in the EMEP model and tested in long-term simulations for Europe covering the six years 2002-2007. Model results were compared to various types of measurements at 27 sites in Europe. Here some of the findings/conclusions of Paper I are briefly summarised.

Several sources contributed significantly to organic aerosol in Europe. Biogenic and anthropogenic SOA and vegetation fires were all important contributors to modelled OA during summertime. During winter both residential wood burning and fossil fuel sources contributed substantially to organic aerosol in Europe, according to the model simulations.

Model results were very sensitive to the assumptions regarding the partitioning of the POA emissions and the aging of primary S/IVOC species and SOA components. The treatment of POA as S/IVOCs, subject to atmospheric aging, had a large impact on the results with a lot of evaporation of POA in emission areas, followed by gas-phase oxidation of the evaporated

components and transformation into ASOA. The evaporation led to a substantial decrease in modelled total organic aerosol in urban high-emission areas — on the *regional* scale the ASOA formation from the aging of the S/IVOC emissions more than compensated for the evaporation losses, and led to increased total OA concentrations and a higher degree of oxidation of the model OA. The traditional treatment of POA as completely non-volatile is unrealistic (as discussed above) but large uncertainties are introduced by the addition of a poorly constrained amount of IVOCs and an uncertain aging scheme.

Adding aging of the VOC-SOA to the model increased the calculated OA concentrations further, especially over the Mediterranean Sea; here, large amounts of highly oxidised SOA accumulated in these model versions, as a consequence of multigenerational aging without fragmentation reactions. Some of the SOA-yields found when adding multi-generational aging are very high, higher than those seen in smog-chambers, and it is likely that the neglect of fragmentation reactions for highly oxidised SOA-components leads to overestimation of SOA formation.

For summer periods the VBS-scheme that included multi-generational aging of all SOA tended to give results in slightly better agreement with observations than the other model versions (Fig. 4.2). There is a clear possibility that the results were improved for the wrong reasons – e.g. increased BVOC-emissions might give similar effects as increased aerosol yields or aging rates for BSOA; high ASOA yields predicted by the VBS-scheme might be masking problems with missing or underestimated POA emissions.

Although Paper I showed that simple VBS-based organic aerosol models can give good agreement with measured concentrations of OC (and TC) for summer conditions, it is clear that more observational studies are needed to constrain the VBS parameterisations and to help improve emission inventories.

None of the model/emission combinations tested was able to reproduce winter levels of particulate carbonaceous matter in Europe. At most sites OC concentrations during winter were underestimated (Fig. 4.2), and the comparisons to source-apportionment studies showed very poor agreement for OC from wood burning. Large overestimation occurred at two Norwegian sites but large underestimation at all other sites. These results from Paper I (also supported by results from Paper II) were an important motivation for the development and testing of a new European emission inventory for residential wood combustion (Papers IV and V).

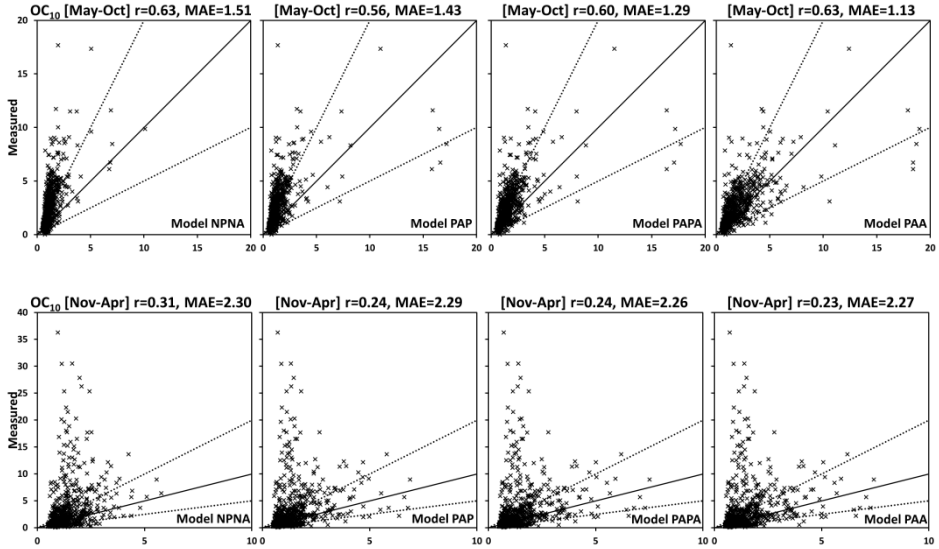

Figure 4.2 *Organic carbon concentration in PM_{10} (OC_{10}). Filter measurements from European sites (2002–2007) and corresponding model concentrations. The upper plots show data from the summer half-years (May–October; 671 measurements), and the lower plots data from winter half-years (November–April; 687 measurements). Model versions (from left to right):* ***NPNA*** *– non-volatile primary OA emissions, no aging of SOA;* ***PAP*** *- POA emissions (including additional IVOCs) distributed over different volatilities (9-bin VBS) and subject to atmospheric aging reactions, no aging of VOC-SOA;* ***PAPA*** *– similar to PAP but including aging of anthropogenic VOC-SOA (oxidation rate 1×10^{-11} cm^3 $molecule^{-1}$ s^{-1});* ***PAA*** *– similar to PAP but including aging of all VOC-SOA (oxidation rate 4×10^{-12} cm^3 $molecule^{-1}$ s^{-1}). For details see text. Unit: µg (C) m^{-3}. Correlation coefficients (r) and mean absolute error (MAE) for the four different model versions are given above the plots.*

5 Emissions from residential wood combustion (Papers IV and V)

Small scale combustion of biomass fuels (especially wood) has long been recognized as a major source of particulate matter during the cold seasons in large parts of Europe (e.g. [150] and references therein). Several modelling studies have indicated that winter-time emissions of PM may have been severely underestimated in the past (e.g. Papers I and II, [151], [152]).

It is difficult to estimate total emissions from residential wood combustion (RWC) for several reasons. For example, it is hard to obtain reliable statistics for fuel wood use, since it is often non-commercial and falls outside the economic administration; this has led to substantial underestimations of fuel wood consumption. Another complication is that many different types of appliances are used for residential wood combustion, with large differences in particle emissions per unit of fuel burnt; modern combustion equipment emits much less than old stoves and fireplaces. The actual combustion conditions (and thereby emissions) depend a lot on the user, and different customs regarding how to burn wood may have a large influence on emissions.

Emission inventories based on national reporting (e.g. the emissions available at the EMEP Centre on Emission Inventories and Projections, CEIP; www.ceip.at) may also include large inconsistencies between different countries due to differences in assumed emission factors even for the same appliance types. This can partly be due to the influence of the combustion type, fuel parameters and different operating conditions, including ignition methods [153]. Another very important factor is the different sampling and measurement protocols or techniques used by different countries. Some methodologies sample particles on a heated filter, through a probe, from undiluted flue gas at relatively high temperatures (e.g. 160°C), thereby only capturing non- or low-volatile particles, often denoted “solid particles” (SP) in the emission sampling studies [153], while others include some dilution and cooling of the sample in a dilution tunnel and measure particles at relatively low temperatures (e.g. < 35°C in the Norwegian standard NS 3058-2 [154]) and thereby capture both the solid particles and a larger fraction of the condensable (semi-volatile) particles.

5.1 A new emission inventory

A new bottom-up emission inventory for carbonaceous aerosol emissions from residential combustion of biofuels in Europe is described in Papers V and IV. In this new inventory, emission factors for different appliance types were based on dilution tunnel sampling. For a given appliance type the same emission factor was used for *all* countries (the average (dilution tunnel) emission factor from the different reported values). This means that the new inventory has a consistent approach for residential wood combustion, independent of individual country emission factor choices used for official reporting.

The new emission inventory (TNO-newRWC) is based on an EC and OA emission inventory developed within the EUCAARI project (for further details about the EUCAARI inventory see Paper V). The inventory covers Europe from 10°W to 60°E and 35°N to 70°N; it includes Turkey but emissions in Africa and Kazakhstan are not included. The inventory has a relatively high spatial resolution, using a 1/8° × 1/16° longitude–latitude grid (ca 7 × 7 km). The RWC emissions within each country are distributed based on population density,

weighted with estimated local wood-availability (based on forest land-cover maps) and with a higher weight for rural than urban areas since urban houses are less likely to have wood stoves [155]. It should be noted that the spatial distribution of the emissions does not take into account local factors such as legal restrictions, cultural traditions and the availability of energy distribution networks. This likely leads to overestimated emissions in some urban areas (e.g. the larger cities in the UK, where residential combustion of solid fuels is restricted) and, as a consequence, underestimated emissions in rural areas.

The new emission inventory changed the total primary organic aerosol emissions from wood combustion substantially, but not in the same way for all countries. The total OC-emissions from residential wood combustion (for the whole UNECE-Europe domain) in the EUCAARI emission inventory were about 350 Gg C / year — in the new emission inventory the estimated emissions are almost three times larger: ca 980 Gg C / year. For all countries except Norway the new inventory has higher emissions than the old inventory. Fig. 5.1 illustrates how the total anthropogenic primary particulate OC emissions differ between the new inventory and the EUCAARI inventory for some selected countries. According to the new inventory, residential wood combustion is the totally dominant anthropogenic source of primary organic aerosol emissions in Europe – about 60% of the POA is estimated to be emitted by RWC (Fig. 5.2a).

The model impact of the large differences in total emissions between the two inventories is illustrated in Fig, 5.3, which shows model simulated annual average organic aerosol concentrations in Europe using the two inventories (using a model version including aging of both primary S/IVOC-components and SOA-components in the gas-phase; the PAA model scheme from Paper I).

Although emission estimates based on dilution tunnel measurements capture a lot more of the emitted OC than solid particle measurements, a large fraction of the semi- and intermediate-volatility organic compounds emitted from RWC will be in the gas-phase also at the temperatures achieved in the dilution tunnel (e.g. ~30°C). Since residential combustion is especially important during periods with low temperatures it is likely that some of the SVOCs that do not condense at the dilution tunnel conditions will do so at cold winter temperatures. The more volatile S/IVOCs may be oxidised in the atmosphere and the oxidation-products may condense as particulate SOA (see Sect. 4.4).

In Paper V the TNO-newRWC inventory and the (older) EUCAARI inventory were used in model simulations with the EMEP model for the three-year period 2007–2009. Comparisons of modelled wood burning OC to Scandinavian source apportionment studies showed much better agreement with the new inventory than with the EUCAARI inventory. However, only a relatively limited amount of source apportionment data, from five sites, was used in Paper V and further evaluation of the new inventory is needed, using additional measurements for other regions in Europe; such work is planned for the near future.

The modelled total particulate organic carbon concentrations were also compared to long-term measurements at six sites in countries where the differences in emissions between the two inventories are large. At all sites the correlation between modelled and observed wintertime OC increased and the mean absolute error of the model OC was lower at most of the sites with the revised inventory than with the old one.

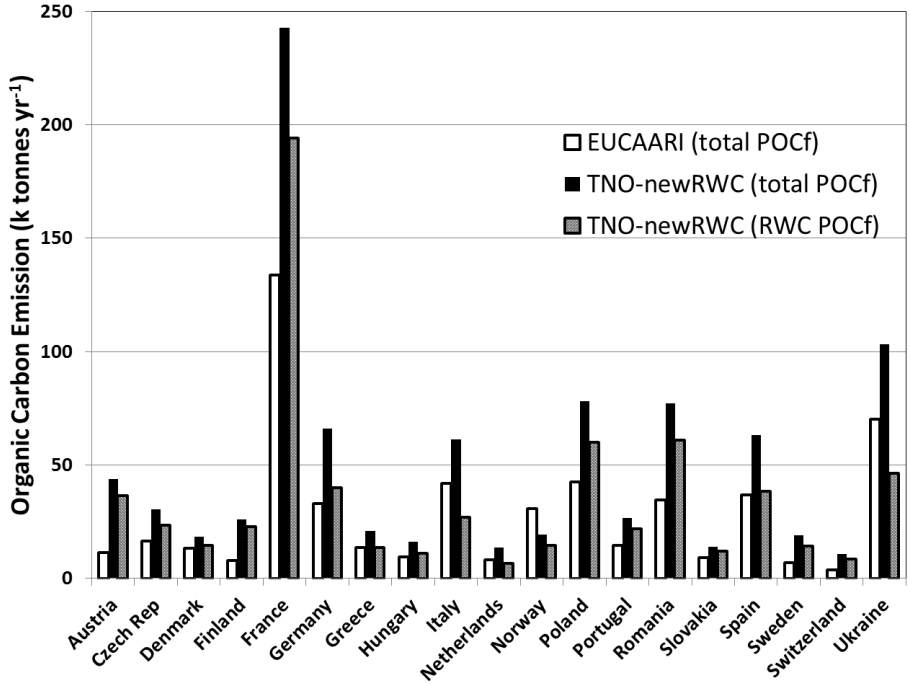

Figure 5.1 *Total emissions of particulate organic carbon (sum of all anthropogenic sources; $PM_{2.5}$-fraction) for selected countries according to the old (EUCAARI; white bars) and new (TNO-newRWC; black bars) emission inventories. For the new inventory the emissions from residential wood combustion (RWC) are also shown (grey bars). Unit: kt C yr^{-1}.*

For most countries the differences in estimated EC emissions from residential wood combustion between the TNO-newRWC and EUCAARI inventories are smaller than the changes in OC emissions (see Paper IV for a discussion about the reasons for the differences in the EC-emissions). Total European $EC_{2.5}$ emissions from RWC are 26% higher in the new inventory compared to the old one. However, for Norway the new inventory has substantially lower EC-emissions than the old inventory and model simulations with the new inventory led to much better agreement with source-apportionment data from Norwegian sites based on tracers of wood burning (Paper IV).

RWC emissions contribute about 1/5 of the total anthropogenic $EC_{2.5}$-emissions in UNECE-Europe according to the new emission inventory. This makes it the second largest source after road transport (Fig. 5.2b).

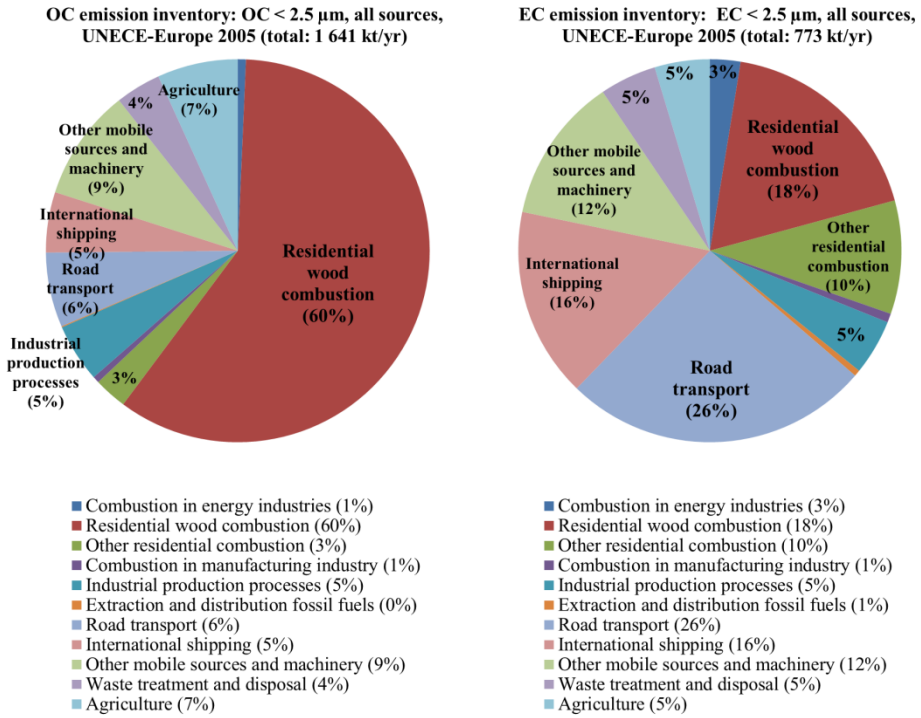

Figure 5.2 *Relative contribution from different source sectors to emissions of* ***(a)*** *particulate organic carbon ($OC_{2.5}$) [left] and* ***(b)*** *elemental carbon ($EC_{2.5}$) [right] in Europe in 2005. The emissions are based on the new emission inventory (TNO-newRWC) for residential wood combustion and the emission inventory developed within the EUCAARI project for other sources.*

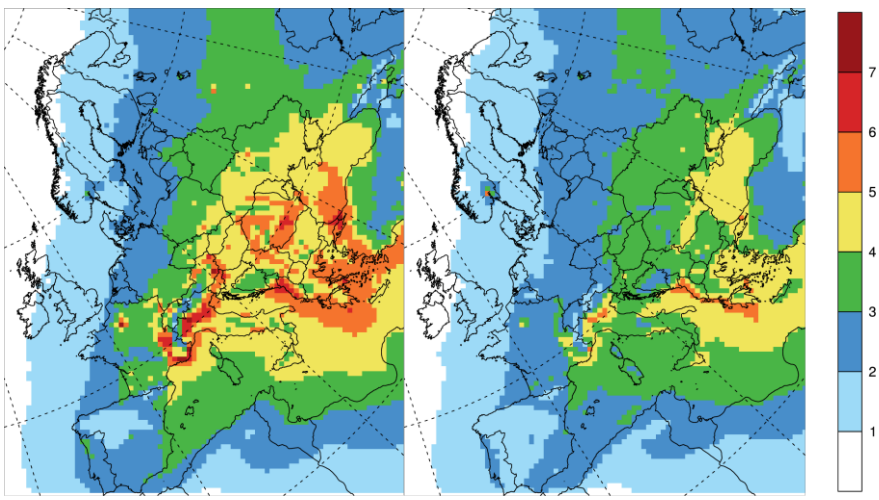

Figure 5.3 *Model simulated annual average concentration of total organic matter in $PM_{2.5}$ (2007) using two different emission inventories for residential wood combustion;* ***Left****: the revised TNO-newRWC inventory;* ***Right****: the "old" EUCAARI inventory. Unit: µg m^{-3}. For details about the model set-up and organic aerosol scheme used, see Paper V.*

6 Biotic stress-induced emissions (Paper III)

6.1 Stress-induced emissions

In addition to the constitutive BVOC-emissions, discussed in Sect. 4.4.1, vegetation also emits organic compounds in response to various types of stress — so called stress-induced emissions (SIE). Some types of stress lead to very large induced VOC-emissions and many of the emitted compounds are highly reactive and can form large amounts of organic aerosol after oxidation in the atmosphere [156]. The potential impact of SIE in northern and central Europe on organic aerosol concentrations is investigated in Paper III.

Stress factors that can lead to induced emissions can be divided into biotic factors (infestation by insects, fungi, viruses etc.) [157] and abiotic factors (e.g. heat stress [131], drought, exposure to ozone and other oxidants, and UV-radiation; for reviews of induced BVOC-emissions due to abiotic stress factors see [158], [159]).

The stress-induced emissions may aid the affected plant in several ways (e.g. [159]–[161]); induced VOCs may:

- reduce oxidative stress and increase the resistance to high temperatures (e.g., isoprene, monoterpenes and sesquiterpenes)
- deter herbivores from feeding and ovipositing
- attract herbivore predators and parasitoids
- have antimicrobial effects
- be used for internal, and plant-to-plant, signalling to stimulate defence mechanisms within the plants

Stress-induced emissions vary with the plant type affected, the severity of the stress and the cause of stress. A large number of different VOCs may be emitted, e.g. ethene, methanol, so called green leaf volatiles (various C_6 alcohols, aldehydes and esters), monoterpenes, sesquiterpenes and phenolic VOCs (e.g. [160], [161]).

The severity of the stress is an important factor [162]; e.g. severe heat stress that cause irreversible damage to the plant may lead to reduced emissions [131] and bark beetle attacks on trees may initially lead to a substantial increase of monoterpene (MT) emissions followed by a drastic decrease if the tree dies as a consequence of the attack [163].

Experiments at the Jülich Plant Atmosphere Chamber have shown that both methyl salicylate (MeSA) and sesquiterpenes (Fig. 6.1) released from trees infested by aphids are very efficient in forming SOA [132]; the SIE in the experiments were large compared to the constitutive emissions of monoterpenes and the particle mass yields for MeSA and SQT were about 3–4 times larger than for the MT. Inspections of European forests [164] suggest that non-infested and unstressed plants are uncommon — some degree of stress is the normal state of vegetation. This means that SIE may account for a significant part of the SOA formation in European forests.

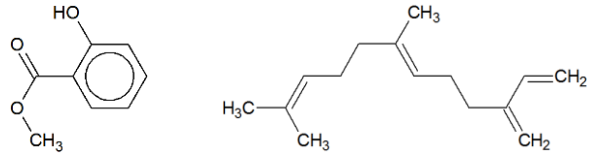

Figure 6.1 *Left: Methyl salicylate — MeSA. Right: β-farnesene, (a sesquiterpene) used as an alarm pheromone by aphids and also produced and emitted by many plants.*

Almost all large-scale modelling of organic aerosol so far has neglected stress-induced emissions and only considered constitutive BVOC-emissions. One reason for this is that the SIE are very uncertain, variable, and difficult to predict. Inherent difficulties include episodic character, time lags of emissions, dependencies on plant history, adaption to stresses and scaling of emissions from leaf level to regional scale; Arneth and Niinemets [157] discuss the difficulties of simulating insect induced emissions in dynamic vegetation models. Realistic, predictive detailed simulation of biotic SIE in regional scale models is presently not feasible. However, the potentially large impact of SIE on organic aerosol formation means that it is important to assess the order of magnitude of the impact of SIE. If SIE has a large impact on SOA, it is worth putting more effort into investigating this in detail.

Paper III is a first estimate of the potential impact of biotic stress induced emissions on organic aerosol concentrations in Europe. Plausible emission scenarios for current conditions were constructed and projections of possible effects of SIE in the future were investigated. In addition a special type of biotic SIE of more regional character was considered. A summary of the methodology and a brief discussion of the results are given in the following sections.

6.2 Emission factors for infested trees

Emissions, due to insect infestations on Northern/Central European trees were estimated based on plant-chamber experiments performed on infested trees in the Jülich Plant Atmosphere Chamber (JPAC) [132]. The emission factors for SIE from infested trees were based on the observed ratio of SIE to monoterpene emissions in the JPAC. Two emission scenarios were constructed:

- Case 1 was based on measurements on a Norway spruce infested by aphids; this tree was found to emit substantial amounts of sesquiterpenes. The SQT/MT emission ratio was 2.4.
- Case 2 was based on chamber data from experiments with a combined stand of birch, spruce and pine, with the spruce having a high degree of aphid infestation; this experiment showed large emissions of both methyl salicylate and sesquiterpenes. The emission ratios were MeSA/MT=3.5 and SQT/MT =4.9.

The stress induced SQT and MeSA emissions were of *de novo* type [131], which means that they are emitted in connection with biosynthesis and occur only during daylight hours. For this reason the SIE were only switched on during daytime in the model scenarios.

6.3 Fraction of infested trees

To construct continental scale emission scenarios for SIE (for Europe north of Lat. 45° N) the observed emission factors from infested trees in JPAC were combined with estimates of the fractions of infested trees in Central and Northern Europe. The estimate for present-day conditions was based on surveys of the European forests, presented in European and national forest damage reports, provided by ICP Forests (the International Co-operative Programme on Assessment and Monitoring of Air Pollution Effects on Forests operating under the UNECE Convention on Long-range Transboundary Air Pollution, http://www.icp-forests.org/) [164]–[166].

Insects are reported to be the most frequent cause of damage to trees in Europe and insect infestations are well distributed over northern and central European forests [165]. Further, Fischer et al. [165] state that tree defoliation may be a useful warning system for the response of forests to different stress factors; they rate trees with > 25% defoliation as being damaged. The fraction of damaged trees is relatively large in northern and central Europe: for northern (boreal) forests 11% of the trees were rated as damaged by [165] and similarly the Finnish forest damage report [166] stated that about 10–12% of the pines had a high degree (>25%) of defoliation; central and north-central forest types have even larger fractions of damaged trees (19–28% reported in [165]).

In Paper III (Case 1 and 2) the fraction of trees with significant defoliation was used as a rough estimate of the fraction of stressed trees. Since the JPAC experiments on infested trees only included central and northern European tree species only SIE in the area north of Lat. 45° N were considered. The fraction of currently stress-affected trees were assumed to be 10% for latitudes greater than 60° N and 20% between 45° N and 60° N.

Model emission scenarios with higher degrees of infestation were also considered. Hypothetical severe-case future scenarios of SIE were constructed by assuming that insect infestations affect trees that today are at >10% defoliation. This corresponds to about 2/3 of the trees in central Europe [165] and about 50% of the trees in boreal forests [166].

6.4 Regional episodic infestation by bark lice

A special type of regional insect infestation was also studied in Paper III — a two-month infestation of honeydew generating lice on spruce trees in Baden-Württemberg (south-west Germany). Honeydew produced by the spruce shoot aphid *Cinara pilicornis* (and other bark lice) is important for forest honey production and detailed observational data, collected by bee-keepers, exist in Baden-Württemberg (www.stockwaage.se). The relation between infestation and forest-honey production is well known to bee-keepers — in a good honey year the infestation is widespread and lasts through the summer months.

A Norway spruce infested by *Cinara pilicornis* was studied by Mentel et al. [132]. The coupled insect – tree system emitted large quantities of long chained C_{17}-alkenes (mainly 8-heptadecene; 6,9-heptadecadiene; and 3,6,9-heptadecatriene). These C_{17}-BVOCs were very reactive and the SOA-yield for the C_{17}-BVOCs was found to be very high: 33 mass-%. The amount of C_{17}-BVOCs emitted was also very high compared to the monoterpene emissions (emission ratio C_{17}-BVOC/MT = 18). Elevated SQT emissions were also observed in this experiment, the emission ratio was SQT/MT = 1.

Case 3 in Paper III simulates a year with wide-spread infestation (a good honey-year). All spruce in Baden-Württemberg (38% of all trees) were assumed to be heavily infested during June and July. This is an extreme case, but the bark lice may also infest other tree species, and some years even deciduous trees may be infested and contribute to honeydew production.

Since the day-time emissions of C_{17}-BVOCs in the experiment [132] were about 2–3 times higher than during night, only daytime emissions were included in the model (just as for SQT and MeSA in Case 1 and 2). This means that a potentially significant night-time production of SOA from C_{17}-BVOCs is neglected.

6.5 Stress-induced emission scenarios

Combining the emission factors for the infested trees with the estimated fractions of infested trees led to five different scenarios for stress induced emissions on large and regional scales.

The SIE in the scenarios are summarised in Table 6.1. The scenarios constructed to simulate present day stress-levels in central and northern Europe (Case 1 and Case 2) includes substantial emissions of SQT. In the "north–central" European region (45–60°N) SQT emissions are estimated to be ca 50% (Case 1) or 100% (Case 2) of the daytime MT emissions. MeSA-emissions may also be very large if stress induced emissions similar to those seen in the plant chamber experiments used as input for Case 2 are common in the European forests — for the boreal forests (Lat > 60N) MeSA emissions are estimated to be 35% of the daytime MT emissions and for the north–central European forests 70%.

Table 6.1 *Biotic stress-induced emissions (SIE) of sesquiterpenes (SQT), methyl salicylate (MeSA) and unsaturated C_{17}-BVOC (C17) in the different model scenarios. The SIE are expressed as mass based fractions of the daytime model emissions of monoterpenes (MT).*

Scenario	Area	SQT/MT	MeSA/MT	C17/MT
Case 0	everywhere	0.05	–	–
Case 1	Lat > 60° N	0.24	–	–
	45° N < Lat ≤ 60° N	0.48	–	–
	Lat ≤ 60° N	0.05	–	–
Case 2	Lat > 60° N	0.49	0.35	–
	45° N < Lat ≤ 60° N	0.98	0.70	–
	Lat ≤ 60° N	0.05	–	–
Case 1F	Lat > 60° N	1.2	–	–
	45° N < Lat ≤ 60° N	1.6	–	–
	Lat ≤ 60° N	0.05	–	–
Case 2F	Lat > 60° N	2.45	1.75	–
	45° N < Lat ≤ 60° N	3.27	2.33	–
	Lat ≤ 60° N	0.05	–	–
Case 3	Jun–Jul, Lat: 47.8–49.8° N, Lon: 8.0–10.2° E	0.38	–	6.8
	Elsewhere (and rest of year)	0.05	–	–

6.6 Modelling of SOA formation from biotic SIE

Simplified mechanisms for SOA formation from biotic stress-induced emissions of sesquiterpenes, methyl salicylate and unsaturated C_{17}-compounds were implemented in the EMEP model. The SOA yields for the SQT, MeSA and C_{17}-compounds were based on measured yields in the Jülich Plant Atmosphere Chamber [132].

Since limited information is available regarding SOA formation from these stress-induced BVOC-emissions, simple fixed SOA yields were used, based on the experimental data. The SIE-SOA was treated as non-volatile in the model simulations since no information about the volatility distribution of the SIE-SOA was available.

The following SOA-forming reactions were included in the model:

$$SQT + Ox \rightarrow 0.17\ SQT\text{-}SOA \quad (R6)$$

$$MeSA + OH \rightarrow 0.22\ MeSA\text{-}SOA \quad (R7)$$

$$C_{17}\text{-}BVOC + Ox \rightarrow 0.33\ C_{17}B\text{-}SOA \quad (R8)$$

where Ox denotes a general oxidant (OH, O_3 or NO_3).

For SQT the SOA-yield was based on the experimental yields from aphid-infested Norway Spruce trees (17 mass-%) [132]; the same SOA-yield was assumed for all SQT-emissions in the model. For MeSA and C_{17}-BVOC the SOA yields were 22 and 33%, respectively.

SOA-formation from SQT is rapid; in the model the OH and O_3 oxidation rates (R6) were set to 1.97×10^{-10} cm^3 $molecule^{-1}$ s^{-1} and 1.16×10^{-14} cm^3 $molecule^{-1}$ s^{-1}, respectively, based on the rates for β-caryophylllene oxidation from the Master Chemical Mechanism (MCM v3.2 [167], via website: http://mcm.leeds.ac.uk/MCM).

MeSA is much more stable in the atmosphere [168] and, based on experimental data from JPAC, the OH-reaction rate (R7) was set to 4×10^{-12} cm^3 $molecule^{-1}$ s^{-1}. This low rate means that a significant fraction of the MeSA will remain during night and reaction with NO_3 radicals should also be considered:

$$MeSA + NO_3 \rightarrow \alpha\ MeSA\text{-}SOA \quad (R9)$$

The reaction rate for the NO_3 reaction is not known and neither is the possible SOA-yield (α). Canosa-Mas et al. [168] assumed that MeSA could react as fast with NO_3 as phenol does but, as discussed in Paper III, MeSA may be more stable than phenol; for example, the MeSA+OH reaction (from the JPAC experiments) is seven times slower than the phenol+OH reaction. Since the atmospheric chemistry of MeSA is poorly known, several sensitivity tests were performed in Paper III, using different assumptions regarding the MeSA+NO_3 reaction and SOA yield. The MeSA+NO_3 reaction was either neglected ($k_{R9} = 0$) or assumed to occur with the rate $k_{R9} = 5.4 \times 10^{-13}$ cm^3 $molecule^{-1}$ s^{-1} (seven times slower than the phenol+NO_3 reaction; this is roughly in line with preliminary results from laboratory experiments at JPAC). The SOA-yield for the MeSA+NO_3 reaction was either assumed to be 0 or 22% (the same as for the OH-reaction). Sensitivity tests of different assumptions regarding the MeSA deposition losses were also performed (see Paper III).

In paper III, the constitutive BVOC-emissions (and the AVOC and primary OA emissions) were treated with a slightly modified version of one of the VBS-models described in Paper I; the PAP version (**P**artitioning and atmospheric **A**geing of **P**rimary S/IVOC emissions) was chosen as the base case. This means that atmospheric aging of semi-volatile compounds formed from the oxidation of biogenic and anthropogenic VOCs was excluded — only first-generation BSOA and ASOA from these reactions were included.

6.7 Impact of biotic stress-induced emissions in Europe

6.7.1 Current situation scenarios

A one-year simulation (for 2007) was performed with the EMEP model for each of the SIE-scenarios in Table 6.1. Since most of the BVOC-emissions (including the SIE) occur during the warmer seasons, results were extracted for the 6-month period April–September. In Fig. 6.2 the biogenic SOA due to only the constitutive BVOC-emissions (Case 0) is compared to the organic aerosol formed due to the stress-induced emissions in the two present-day scenarios (Case 1 and 2).

- Case 1-type stress-induced emissions (only SQT-emissions) at the estimated present-day level of infestation lead to moderate levels of SIE-SOA (< 0.3 μg m^{-3} in most of Europe for the 6-month (Apr–Sep) mean, corresponding to between 20 and 40% of the total modelled BSOA in most of Europe north of Lat. 45° N).
- Biotic SIA including MeSA (Case 2) leads to much higher modelled SIE-SOA concentrations, between 0.6 and 1 μg m^{-3} in large parts of eastern and central Europe — clearly higher than the modelled unstressed BSOA concentrations during the same period. For Case 2 between 50 and 80% of the total BSOA is SIE-SOA, for most of Europe north of Lat. 45° N.

Although the emission scenarios considered in Paper III for the current situation (Case 1 and 2) are rough estimates, they do not lead to unrealistic modelled organic aerosol concentrations. Modelled OC concentrations at the forested site Hyytiälä in south-central Finland were compared to measurements. Modelled OC using Case 2 emissions was slightly closer to observations than with Case 1 emissions and both SIE-scenarios were in better agreement with observations than the reference scenario that did not explicitly treat biotic stress emissions. It should be noted that the improved results for total OC when adding SIE does not prove that the stress-induced emissions are correctly modelled; the improvement could also be due to compensation of underestimated constitutive BVOC-emissions, or underestimated SOA-formation from the BVOC-emissions (e.g. due to neglect of aging reactions).

6.7.2 Regional episodic infestation of *Cinara pilicornis*

The model scenario simulating a two-month severe infestation of spruce in Baden-Württemberg by the forest-honey generating bark louse *Cinara pilicornis* (Case 3 in Paper III) leads to very large organic aerosol formation in the infested region. The calculated increase of background $PM_{2.5}$ concentration in Baden-Württemberg due to the SIE is about 3 μg m^{-3} and it is larger than 0.5 μg m^{-3} in all of southern Germany. For Baden-Württemberg this

corresponds to an increase in the calculated background $PM_{2.5}$ of about 50–70%. Although this model scenario can be considered a worst-case scenario for lice infestation in Baden-Württemberg (and best-case for honey production) it should be pointed out that the bark lice can also infect other tree species and that *Cinara pilicornis* (and other bark lice) are found throughout Europe (Fig. 6.3). If the type of C_{17}-BVOC emissions found in [132] (during 10 days) occurs over extended time periods also in real forests the impact on SOA-formation in Europe would be large. As pointed out by Mentel et al. [132] very little is known about biogenic emissions of C_{17}–compounds. Considering their very high SOA-forming potential, illustrated in Paper III, further studies seem worthwhile — a better understanding of the origin of the emissions (from the plant or insect) and whether other aphid species than *Cinara pilicornis* may emit the same (or similar) compounds are important issues to investigate.

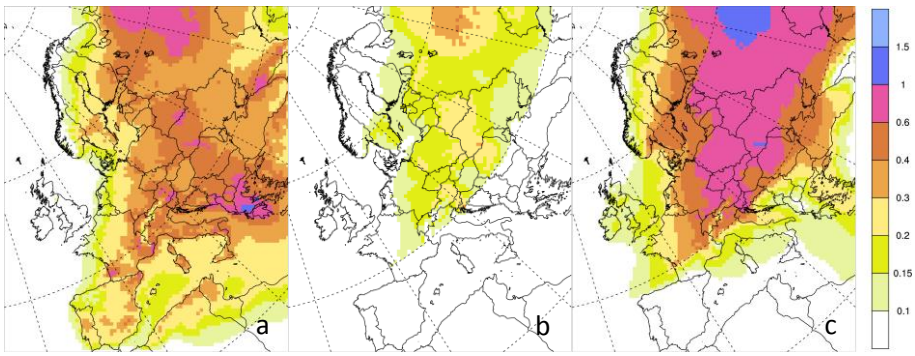

Figure 6.2 *Model calculated 6-month mean (Apr–Sep) concentrations of biogenic SOA and biotic stress-induced OA (SIE-OA);* ***(a)*** *BSOA from constitutive emissions (reference simulation, Case 0),* ***(b)*** *SIE-OA in Case 1 (biotic stress with sesquiterpene (SQT) emissions),* ***(c)*** *SIE-OA in Case 2 (biotic stress with emissions of SQT and methyl salicylate). Unit: µg m^{-3}.*

Figure 6.3 *Biotic stress* ***(a)*** *ant attended aphids on spruce shoot* ***(b)*** *spruce infested by pineapple gall adelgid* ***(c)*** *group of spruce shoot aphids, Cinara pilicornis(?).*

6.7.3 Implications of Paper III

A large number of different biotic stressors exist in the environment and many plants are obviously infested at least to some degree. The inspections of European forests suggest that totally non-infested plants are not likely to be common and thus some stress is the normal state of vegetation.

It is clear that SIE can dominate SOA formation on the laboratory scale but up-scaling of the laboratory results to large scale is uncertain. The SIE scenarios investigated in Paper III are based on experiments on a limited number of tree species and stressors. The large number of different stressors (both biotic and abiotic) in the environment means that the true stress-induced emissions that occur in nature will behave in a much more complicated way than in the simplified model scenarios, both regarding speciation and the temporal variation of the SIE. This approach used to model SIE-SOA in northern and central Europe is a first step, and may lead to over- or underestimations of the importance of SIE-SOA. However, without consideration of SIE-SOA, modelling scenarios will remain unrealistic.

The results from the European scale simulations with the EMEP model show that, for some periods, stress-induced emissions may be more important for organic aerosol production than the constitutive emissions of BVOC.

If growing conditions for trees change rapidly on the time-scale of the life span of individual trees, due to e.g. climate change, established vegetation may be unable to adapt to the new conditions and become more vulnerable to different stressors; this could lead to increased stress-induced emissions and as a consequence higher SIE-SOA concentrations.

MeSA is emitted by many different plants due to different types of stressors, both biotic and abiotic. Furthermore the MeSA + OH reaction has a high SOA-yield. This means that MeSA may be a very important BSOA-precursor in many areas. MeSA reacts rather slowly with OH and this means that the atmospheric residence time may be relatively long and that night-time reactions with NO_3 radicals may be important. However, the rate of the MeSA + NO_3 reaction is not known and neither is the SOA-yield for the reaction. Sensitivity tests performed in Paper III using different assumptions regarding the MeSA + NO_3 reaction indicate that it is worthwhile to try to determine the SOA-yield from the reaction experimentally, since a large fraction of MeSA may react with NO_3 rather than OH.

The results from Paper III point to the need to determine stress-induced emissions by field measurements. Such measurements are difficult for SQT, due to their high reactivities and resulting short atmospheric lifetimes, but MeSA should be easily detectable in the atmosphere, if the model assumptions in Paper III regarding emissions and reactivity are realistic. MeSA has indeed been observed [169] in and over a walnut forest canopy at levels comparable to those found in Paper III.

7 Putting it all together

During the work with this thesis many different model sensitivity tests have been performed; some of them were presented in Papers I and III–V. Based on the findings in Papers I-V, some additional model simulations have been performed to update the estimates of the organic aerosol concentrations in Europe and of the relative importance of the major sources of the aerosol. In this section some results from these recent model simulations are presented.

The organic aerosol schemes used here are based on the volatility basis set methods from Paper I, but some modifications have been done, to take into account findings from Paper I and further developments in Papers III–V:

- the new emission inventory for residential wood combustion (Paper IV+V) was used
- the general background concentration of organic aerosol was set to 0.4 μg m^{-3}, based on findings in Paper I
- emissions from open biomass fires were taken from the FINNv1 inventory [21], which has higher temporal and spatial resolution than the fire inventory used in Paper I
- a small emission of sesquiterpenes was added (equal to 5 % of the daytime monoterpene emissions; as in Paper III)

7.1 Method

Results from simulations using six different model set-ups are compared here. The first three versions (a–c) investigate the influence of atmospheric aging of VOC-SOA in the gas-phase:

(a) "PAP" — this version is intended to give a low estimate of the organic aerosol. It is based on the **PAP** method in Paper I (**P**artitioning and atmospheric **A**ging of **P**rimary semi- and intermediate-volatility OC emissions). No aging of VOC-SOA is included and no explicit stress-induced emissions. This scheme is identical to the base case simulation (Case 0) in Paper III.

(b) "Age1" — similar to PAP but allows one generation of aging of VOC-SOA; this gives an intermediate estimate of OA, and may be more realistic than no aging at all (laboratory experiments have shown considerable SOA enhancements due to OH-aging [141]).

(c) "PAA" — based on the **PAA** method in Paper I (**P**artitioning of primary OA and **A**ging of **A**ll semi-volatile OA components in the gas-phase). This model version allows for multi-generational aging of the semi-volatile OA; this may lead to unrealistically high SOA yields from VOC-oxidation, as discussed in Sect. 4.4.3. The PAA-version gives a high estimate of OA but no explicit SIE are included (which means that it is not a maximum estimate).

The remaining three model versions (d–f) include biotic stress-induced emissions of sesquiterpenes and methyl salicylate, MeSA (north of Lat. 45°N), using the emission assumptions from Case 2 in Paper III (see also Sect. 6) and includes SOA formation from the MeSA+NO_3 reaction, and loss of NO_3-radicals due to SOA-forming reactions (for details regarding the MeSA+NO_3 chemistry see Sect 6.6 and Paper III):

(d) "B2N-PAP"— similar to the PAP-scheme, but including stress-induced emissions.

(e) "B2N-Age1"— similar to the Age1-scheme, but including stress-induced emissions.

(f) "B2N-Age1-DD"— the same as (e) but including rapid dry deposition of biogenic SOA components in the gas-phase; the deposition is assumed to be as efficient as for HNO_3. This sensitivity test was included to investigate the potential impact of very efficient dry deposition of SOA-vapours, discussed in Sect. 4.4.4.

7.2 Model results

Fig. 7.1 shows the modelled organic aerosol concentrations (total organic matter in $PM_{2.5}$, $OM_{2.5}$; annual mean 2007) using the six model/emission scenarios. Scenario (c), the PAA scheme, gives clearly higher concentrations than the other model versions, especially in the southern part of the model domain. In western, central and northern Europe the total $OM_{2.5}$ concentrations calculated with the PAA scheme are about 15–30% higher than with the low-estimate PAP scheme (a); in Russia, Belarus, the Ukraine, and southern Europe the difference is >30% and over the Mediterranean Sea, and southern Italy and Greece, the difference is even larger (>40%).

The difference between the Age1 scheme (b) and the PAP scheme (a) is much smaller — total $OM_{2.5}$ is 5–15% higher with Age1 than PAP in almost all of Europe.

Introducing biotic stress induced emissions (scenarios d–f) leads to increased SOA-formation. The total $OM_{2.5}$ concentration in scenario (d) is between 10 and 25% higher than in scenario (a) in most of the area north of Lat. 45°N (smaller difference in western France and larger in the easternmost part of the domain shown in Fig. 7.1).

Scenario (e), which includes biotic stress induced emissions for Lat.>45°N and one generation of aging of VOC-SOA, leads to about as high $OM_{2.5}$ concentrations as the PAA-scheme (c) in the northern parts of Europe (within ± 5% in most of the land areas with Lat.>45°N).

The $OM_{2.5}$ concentrations are also fairly similar for case (b) and (f). These two model versions give intermediate OA concentrations (between the low estimate PAP (a) and high estimate PAA (c) model versions). It is likely that the dry deposition of semi-volatile SOA components in the gas phase is underestimated in the standard model version. This is expected to lead to a model overestimation of the organic aerosol, but this could be compensated by an underestimation of the BVOC-emissions — these two effects could be of similar magnitude (judging from the similarity between (b) and (f)).

The similarities in modelled OA, between different model schemes (c–e and b–f), illustrate that there are several different ways to get very similar model results for the OA concentrations.

A preliminary comparison of modelled organic aerosol concentrations at Finokalia (Crete) to AMS-data from May 2008 [82] indicates that the (high-estimate) model version PAA (c) overestimates the (ca 1 month long) campaign average OM concentration severely. The (low-estimate) PAP (a) underestimates it somewhat, and the other model versions tested for 2008 (Age1 (b), B2N-Age1 (e), B2N-Age1-DD (f)) all produce monthly mean OA-concentrations close to the observed average concentration of submicron organic aerosol (2.6 μg m^{-3}).

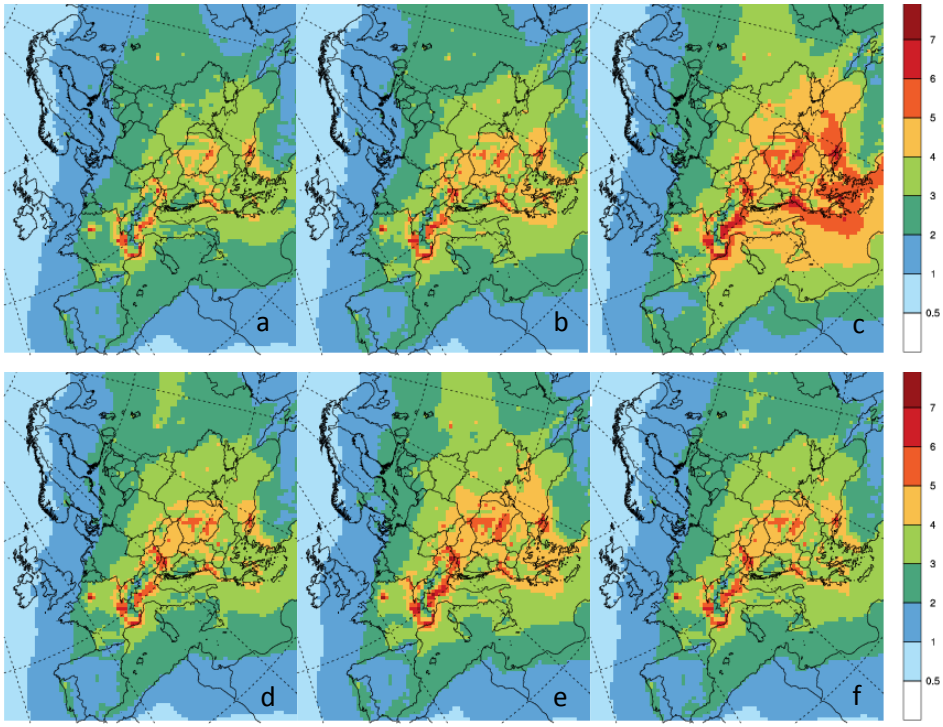

Figure 7.1 *Model simulated total concentration of organic aerosol in $PM_{2.5}$ (annual mean, 2007). Comparison of six different model set-ups (details see text), from left to right:* ***(a)*** *PAP, no aging of VOC-SOA;* ***(b)*** *Age1, single-generation aging of VOC-SOA;* ***(c)*** *PAA, multi-generational aging of VOC-SOA;* ***(d)*** *B2N-PAP, PAP-scheme + biotic stress-induced emissions;* ***(e)*** *B2N-Age1, Age1-scheme + biotic SIE;* ***(f)*** *B2N-Age1-DD, Age1 + biotic SIE, and rapid dry deposition of BSOA components in the gas phase. Unit: μg m^{-3}.*

In the following, results from the 1-generation aging model version ("Age1", without stress-induced emissions, i.e. Case (b) above) are investigated in some more detail to illustrate the model estimated contributions from different sources to the organic aerosol in Europe.

In Fig. 7.2 the modelled organic carbon concentration in $PM_{2.5}$ ($OC_{2.5}$), and the relative contributions from different sources to $OC_{2.5}$ are shown. Many different sources contribute significantly to the model calculated $OC_{2.5}$. Residential wood combustion is the largest source in most areas (Fig. 7.2b). Biogenic SOA contributes substantially (>30%) in parts of Russia, Finland and Sweden (Fig. 7.2e). Fossil fuel sources are important over several ocean areas (the Mediterranean Sea, North Sea, English Channel and Bay of Biscay) and in Italy, England, Belgium, the Netherlands and the NW parts of Germany and France, as well as in some high-emission areas in the Ukraine and Russia (Fig. 7.2d). Open biomass fires also contribute a lot to the modelled $OC_{2.5}$ in regions affected by fires during the year that was modelled; for 2007 the major influence of fires were seen in eastern and south-eastern Europe (Fig. 7.2c).

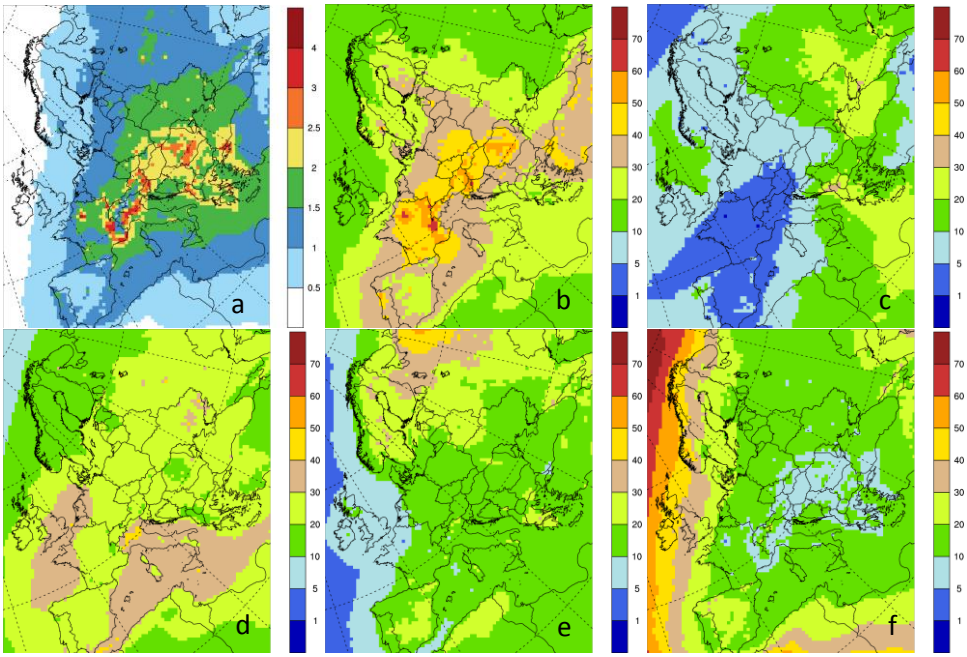

Figure 7.2 (a) *Organic carbon in $PM_{2.5}$ ($OC_{2.5}$) Unit: µg(C) m^{-3}; and relative contribution from different sources (in % of the total $OC_{2.5}$):* ***(b)*** *residential wood combustion;* ***(c)*** *open biomass fires;* ***(d)*** *fossil fuel sources;* ***(e)*** *biogenic SOA;* ***(f)*** *model background OC. Based on annual mean concentration for 2007 from a model simulation allowing only a single generation aging of VOC-SOA ("Age1"-model see text).*

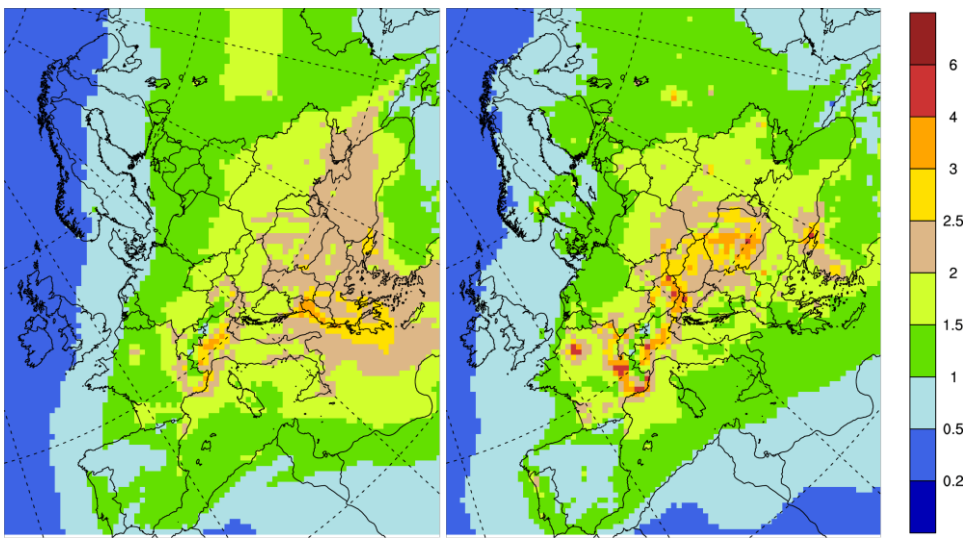

Figure 7.3 *Organic carbon in $PM_{2.5}$ ($OC_{2.5}$) — Left:* ***Summer*** *(May–Oct), Right:* ***Winter*** *(Nov–Apr). Six-month mean concentrations for 2007, from a model simulation using the "Age1"-model (see text). Unit: µg(C) m^{-3}.*

7.2.1 Seasonal variation

Several important carbonaceous aerosol sources have large seasonal variations. Residential combustion for heating occurs mostly during the cold seasons while the biogenic emissions from vegetation are highest during the summer half-year [11]. Vegetation fires are most common during spring and summer months.

Organic carbon

Fig. 7.3 shows the modelled summer (May–Oct) and winter (Nov–Apr) six-month mean concentrations of $OC_{2.5}$. In most of northern, central, and western Europe the total $OC_{2.5}$ concentrations are about 0.2–3 μg(C) m^{-3} higher during winter than summer due to residential wood combustion. In south-eastern Europe and over the eastern Mediterranean Sea and Black Sea summer concentrations are about 0.5–2 μg(C) m^{-3} higher than the winter concentrations, due to a combination of relatively high concentrations of biogenic SOA, influences of open biomass fires, and contributions from anthropogenic SOA during summer in this region (Figs. 7.5a,b,c).

Residential wood combustion is the dominant OC-source in essentially all of Europe during winter, contributing more than 50% to the model OC in large parts of Europe (Figs. 7.4e and 7.5e). Substantial contributions from fossil fuel sources (>1 μg(C) m^{-3}) occur in northern Italy (Figs. 7.4f and 7.5f).

During the summer half-year, fossil fuel sources, biomass burning and biogenic SOA all contribute noticeably to OC. OC-contributions from fossil fuel sources are larger during summer than winter, according to the model simulation (compare Figs. 7.5c and f). They are "high" (>0.5 μg(C) m^{-3}) over the Mediterranean Sea and in parts of southern and central/eastern Europe; the highest concentrations are found in northern Italy (>1.5 μg(C) m^{-3}; Fig. 7.5c). Biomass burning OC (from vegetation fires + residential combustion) influence much the same area (for 2007) as the fossil fuel OC, but with larger impacts in Albania, south-eastern Europe, and in France (Fig. 7.5b). Modelled biogenic SOA is especially important (>0.5 μg(C) m^{-3}) in parts of eastern and south-eastern Europe (Fig. 7.5a).

The model results for $OC_{2.5}$ indicate that non-fossil sources contribute more to OC than fossil fuel sources, on the *regional scale*, during both summer and winter, with the exception of northern Italy (the Po Valley) where modelled OC contributions from fossil fuel sources are larger than the non-fossil OC during summer.

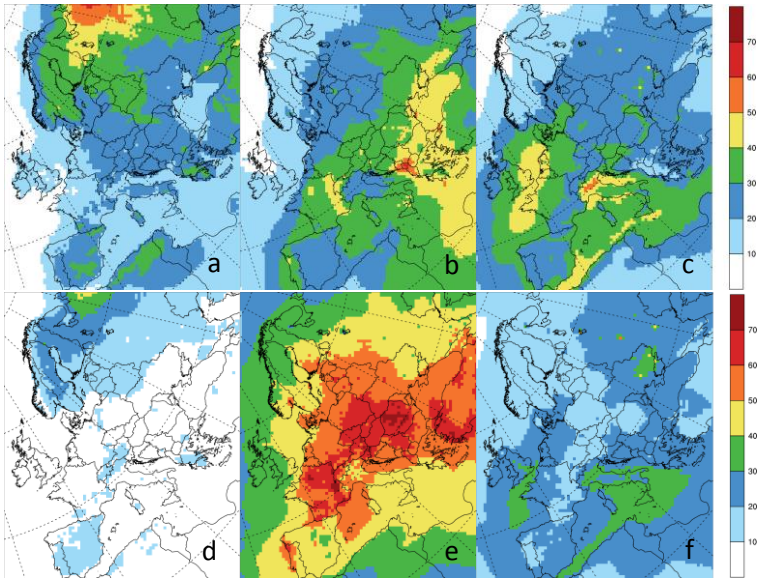

Figure 7.4 *Modelled relative contributions to organic carbon ($OC_{2.5}$) from major source categories.* ***Summer*** *(May–Oct) $OC_{2.5}$ from:* ***(a)*** *biogenic SOA,* ***(b)*** *biomass burning (residential wood combustion + open biomass fires),* ***(c)*** *fossil fuel sources;* ***Winter*** *(Nov–Apr) $OC_{2.5}$ from:* ***(d)*** *biogenic SOA,* ***(e)*** *biomass burning,* ***(f)*** *fossil fuel sources. Six-month mean concentration for 2007, from a model simulation using the "Age1"- model (see text). Unit: % of the total $OC_{2.5}$.*

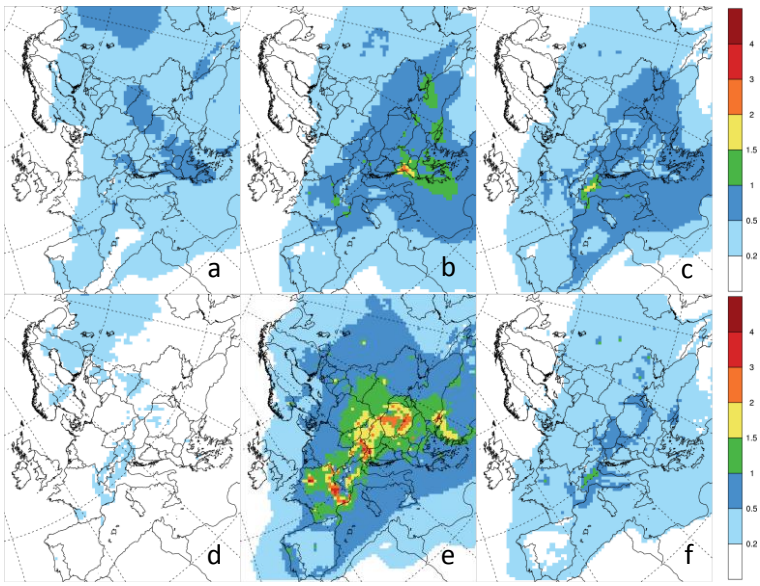

Figure 7.5 *Modelled absolute contributions to $OC_{2.5}$ from major source categories.* ***Summer*** *(May–Oct) $OC_{2.5}$ from:* ***(a)*** *biogenic SOA,* ***(b)*** *biomass burning (residential wood combustion + open biomass fires),* ***(c)*** *fossil fuel sources;* ***Winter*** *(Nov–Apr) $OC_{2.5}$ from:* ***(d)*** *biogenic SOA,* ***(e)*** *biomass burning,* ***(f)*** *fossil fuel sources. Six-month mean concentration for 2007, from a model simulation using the "Age1"-model (see text). Unit: μg(C) m^{-3}.*

Elemental carbon

In contrast to the major influence of non-fossil sources for OC, long-term average modelled elemental carbon is dominated by fossil fuel sources in almost all of Europe (Fig. 3.1, Sect. 3.2). However, during winter residential wood combustion is also an important EC-source. Fig. 7.6 shows model simulated concentrations of $EC_{2.5}$, and the contributions from biomass combustion and fossil fuel sources, for summer (a)–(c) and winter (d)–(f) six-month periods (2007). Concentrations are higher during winter than summer; in most of western, central and eastern Europe typically between 0.1 and 1 μg m^{-3} higher — more in a few emission hot-spots. Over some ocean areas, especially the Mediterranean Sea, the modelled summer concentrations of $EC_{2.5}$ are somewhat higher than the winter concentrations.

During the summer half-year almost all of the modelled EC comes from fossil fuel sources (Fig. 7.6c), except in France, Austria and a few other areas where there is some influence from residential wood combustion (Fig. 7.6b).

During winter, residential heating is much more important. In some countries, where the wood burning emissions are especially high in the new inventory (Papers IV, V), e.g. France and Romania, the modelled contribution from this source is higher than that from fossil fuel sources (Fig. 7.6e,f).

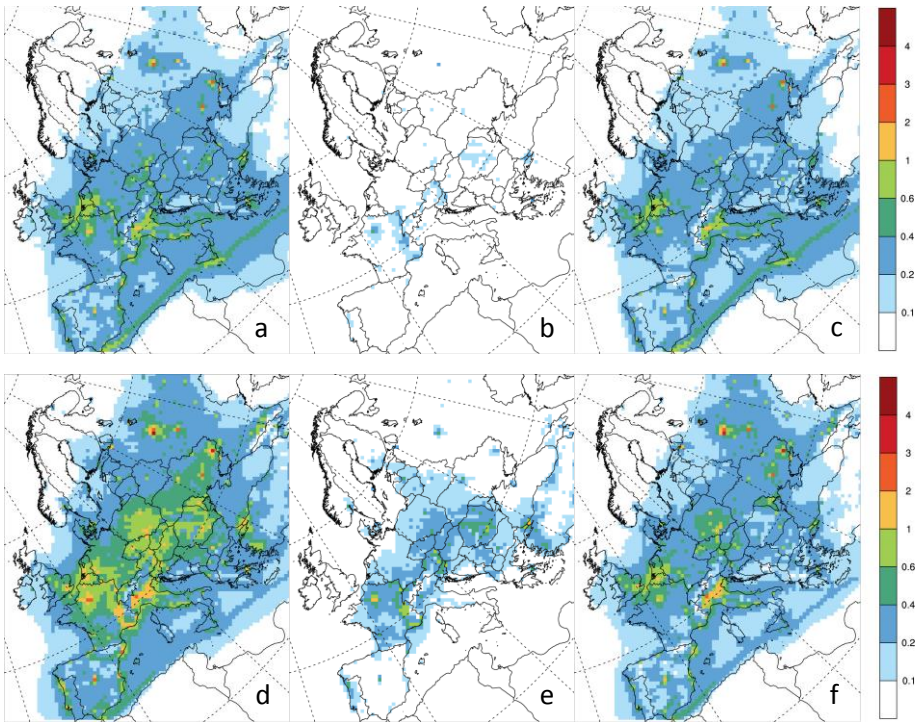

Figure 7.6 *Elemental carbon in $PM_{2.5}$ ($EC_{2.5}$) – comparison of summer (May–Oct) and winter (Nov–Apr) concentrations.* ***Summer****:* ***(a)*** *Total $EC_{2.5}$,* ***(b)*** *biomass burning (residential wood combustion + open biomass fires),* ***(c)*** *fossil fuel sources;* ***Winter****:* ***(d)*** *Total $EC_{2.5}$,* ***(e)*** *biomass burning,* ***(f)*** *fossil fuel sources. Based on six-month mean concentration for 2007. Unit: μg(C) m^{-3}.*

8 Concluding remarks

A long-term goal of regional scale chemical transport modelling is to be able to describe the composition of particulate matter in the atmosphere, to track different sources, estimate their relative importance, and to give realistic predictions of responses to changes in emissions (both anthropogenic and natural) and atmospheric conditions. Many different sources (with different seasonal variation etc.) contribute to the organic aerosol and elemental carbon concentrations in the atmosphere, as shown in this thesis.

The modelled source contributions to the organic aerosol vary substantially depending on the model assumptions (Paper I). It is possible to model total organic carbon concentrations (and total carbon) to match measured concentrations for summer periods, in parts of Europe where measurement data are available (mean absolute error < 50%, Paper I; considering the measurement uncertainties and sampling artefacts, this can be considered "good"). However, the agreement between model and measurements may be fortuitous — there are too few detailed source apportionment studies available (and these techniques have large uncertainties as well) to be able to say with certainty that the model (and emissions) accurately describe the real organic aerosol in the atmosphere on the European scale.

Biogenic and anthropogenic emissions of primary organic aerosol and secondary organic aerosol forming VOCs are highly uncertain (see e.g. Papers I, III, IV, V). In my opinion, the most important objective at the moment within the field of regional scale carbonaceous aerosol modelling, is a better description of emissions – both anthropogenic (e.g. the volatility distribution of different OA-emission sources, and quantification of emissions of intermediate volatility organic compounds from different sources) and biogenic (both constitutive emissions and stress-induced emissions). Currently, it is difficult to determine how uncertain different emission estimates are, and as long as emissions are poorly known it will be hard to construct reliable regional scale model systems.

The uncertainties in organic aerosol modelling need to be acknowledged. If chemical transport model results are used as input for other studies or models (e.g. ecosystem impact studies, population exposure estimates, data assimilation etc.), or for policy purposes, it is important that the users of the CTM results are made aware of the uncertainties.

To make substantial further progress in describing the atmospheric aerosol in chemical transport models, I believe that more effort has to be put on measurements – both in the field and laboratory. Detailed measurements for reasonably extended time periods are needed (including source apportionment tracers) to constrain the emissions and model parameters of semi-empirical models of the type used in the work presented in this thesis.

For semi-empirical models with a number of parameters that are not well constrained by laboratory measurements, comparisons to field measurements may be the best, or only, way to choose between different parameter values. If model parameters have been tuned to get agreement with a very limited set of field measurements there is a risk that the model will give poor results for very different conditions (other emissions, other locations, other meteorological conditions). For this reason, models that are to be applied on large scales need to be evaluated for long time periods and at as many locations as possible. In addition, it is necessary to compare model results not only to measured OC, EC and TC, but also to more

detailed measurements, such as source apportionment studies (e.g. Paper II) that give information about the relative contributions from different sources.

As shown in this thesis, chemical transport models in combination with detailed measurements can be very useful to evaluate emission inventories for different sources, and to suggest improvements. A good example of this is the problems discovered with poor agreement between modelled and measured concentrations of OC, and tracers of wood-burning during winter (e.g. Papers I, II), which led to the development and testing of a new inventory for residential wood combustion (Papers IV, V).

Modelling studies are useful to investigate potential impacts of newly discovered sources of organic aerosol, as demonstrated in Paper III, for some types of biotic stress-induced emissions. Although these types of model simulations, based on up-scaling of laboratory results, are uncertain they help estimate the potential importance of these sources on the regional scale and they suggest important areas of future research.

9 Acknowledgements

Many thanks to David Simpson, my main supervisor during this thesis work. It has been a pleasure working with you Dave!

Thanks to my other supervisors over the last 24 years or so: Mattias, Cecilia, Sten, Karin, Petter, Oscar, Leif, and of course Pascal, my most persistent supervisor! You have all contributed to this, directly or indirectly.

Thanks also to my family, friends and colleagues, both past and present, in Göteborg, Norrköping, Uppsala, and many other places!

Special thanks to my co-authors and to Anna for lots of help!

Thanks to SMHI, for leave of absence and some travel support.

This work was supported by the Swedish Clean Air Research Programme (SCARP).

Now, let's get out of the blue and back into the woods!

10 References

[1] A. I. Calvo, C. Alves, A. Castro, V. Pont, A. M. Vicente, and R. Fraile, "Research on aerosol sources and chemical composition: Past, current and emerging issues," *Atmos. Res.*, vol. 120–121, pp. 1–28, Feb. 2013.

[2] S. Fuzzi, U. Baltensperger, K. Carslaw, S. Decesari, H. Denier van der Gon, M. C. Facchini, D. Fowler, I. Koren, B. Langford, U. Lohmann, E. Nemitz, S. Pandis, I. Riipinen, Y. Rudich, M. Schaap, J. G. Slowik, D. V. Spracklen, E. Vignati, M. Wild, M. Williams, and S. Gilardoni, "Particulate matter, air quality and climate: lessons learned and future needs," *Atmos. Chem. Phys.*, vol. 15, no. 14, pp. 8217–8299, 2015.

[3] A. M. Fiore, V. Naik, and E. M. Leibensperger, "Air Quality and Climate Connections," *J. Air Waste Manage. Assoc.*, vol. 65, no. 6, pp. 645–685, Jun. 2015.

[4] M. R. Heal, P. Kumar, and R. M. Harrison, "Particles, air quality, policy and health," *Chem. Soc. Rev.*, vol. 41, no. 19, pp. 6606–6630, 2012.

[5] J. G. Watson, "Visibility: Science and Regulation," *J. Air Waste Manage. Assoc.*, vol. 52, no. 6, pp. 628–713, Jun. 2002.

[6] P. Matson, K. A. Lohse, and S. J. Hall, "The globalization of nitrogen deposition: consequences for terrestrial ecosystems.," *Ambio*, vol. 31, no. 2, pp. 113–119, 2002.

[7] J. S. Brown, T. Gordon, O. Price, and B. Asgharian, "Thoracic and respirable particle definitions for human health risk assessment," *Part. Fibre Toxicol.*, vol. 10, art. 12, 2013.

[8] EU, "Directive 2008/50/EC of the European Parliament and of the Council of 21 May 2008 on ambient air quality and cleaner air for Europe," *Off. J. Eur. Union*, vol. L 152, pp. 1–44 (EN), 2008.

[9] K. E. Yttri, W. Aas, A. Bjerke, J. N. Cape, F. Cavalli, D. Ceburnis, C. Dye, L. Emblico, M. C. Facchini, C. Forster, J. E. Hanssen, H. C. Hansson, S. G. Jennings, W. Maenhaut, J. P. Putaud, and K. Tørseth, "Elemental and organic carbon in PM10: a one year measurement campaign within the European Monitoring and Evaluation Programme EMEP," *Atmos. Chem. Phys.*, vol. 7, pp. 5711–5725, 2007.

[10] J. P. Putaud, R. Van Dingenen, A. Alastuey, H. Bauer, W. Birmili, J. Cyrys, H. Flentje, S. Fuzzi, R. Gehrig, H. C. Hansson, R. M. Harrison, H. Herrmann, R. Hitzenberger, C. Huglin, A. M. Jones, A. Kasper-Giebl, G. Kiss, A. Kousa, T. A. J. Kuhlbusch, G. Loschau, W. Maenhaut, A. Molnar, T. Moreno, J. Pekkanen, C. Perrino, M. Pitz, H. Puxbaum, X. Querol, S. Rodriguez, I. Salma, J. Schwarz, J. Smolik, J. Schneider, G. Spindler, H. ten Brink, J. Tursic, M. Viana, A. Wiedensohler, and F. Raes, "A European aerosol phenomenology-3: Physical and chemical characteristics of particulate matter from 60 rural, urban, and kerbside sites across Europe," *Atmos. Environ.*, vol. 44, no. 10, pp. 1308–1320, 2010.

[11] D. Simpson, A. Benedictow, H. Berge, R. Bergström, L. D. Emberson, H. Fagerli, C. R. Flechard, G. D. Hayman, M. Gauss, J. E. Jonson, M. E. Jenkin, A. Nyíri, C. Richter, V. S. Semeena, S. Tsyro, J. P. Tuovinen, A. Valdebenito, and P. Wind, "The EMEP MSC-W chemical transport model – Technical description," *Atmos. Chem. Phys.*, vol. 12, no. 16, pp. 7825–7865, 2012.

[12] S. Reis, P. Grennfelt, Z. Klimont, M. Amann, H. ApSimon, J.-P. Hettelingh, M. Holland, A.-C. LeGall, R. Maas, M. Posch, T. Spranger, M. A. Sutton, and M. Williams, "From Acid Rain to Climate Change," *Science*, vol. 338, no. 6111, pp. 1153–1154, Nov. 2012.

[13] J. E. Jonson, D. Simpson, H. Fagerli, and S. Solberg, "Can we explain the trends in European ozone levels?," *Atmos. Chem. Phys.*, vol. 6, no. 1, pp. 51–66, Jan. 2006.

[14] D. Simpson, H. Fagerli, S. Hellsten, J. C. Knulst, and O. Westling, "Comparison of modelled and monitored deposition fluxes of sulphur and nitrogen to ICP-forest sites in Europe," *Biogeosciences*, vol. 3, no. 3, pp. 337–355, Jul. 2006.

[15] H. Fagerli and W. Aas, "Trends of nitrogen in air and precipitation: Model results and observations at EMEP sites in Europe, 1980-2003," *Env. Poll.*, vol. 154, pp. 448–461, 2008.

[16] W. Aas, S. Tsyro, E. Bieber, R. Bergström, D. Ceburnis, T. Ellermann, H. Fagerli, M. Frölich, R. Gehrig, U. Makkonen, E. Nemitz, R. Otjes, N. Perez, C. Perrino, A. S. H. Prévôt, J.-P. Putaud, D. Simpson, G. Spindler, M. Vana, and K. E. Yttri, "Lessons learnt from the first EMEP intensive measurement periods," *Atmos. Chem. Phys.*, vol. 12, no. 17, pp. 8073–8094, Sep. 2012.

[17] A. Sakalli and D. Simpson, "Towards the use of dynamic growing seasons in a chemical transport model," *Biogeosciences*, vol. 9, no. 12, pp. 5161–5179, 2012.

[18] M. Gauss, S. Tsyro, B. M. Steensen, and A.-G. Hjellbrekke, "EMEP/MSC-W model performance for acidifying and eutrophying components, photo-oxidants and particulate matter in 2012.

Supplementary material to EMEP status report 1/2014, The Norwegian Meteorological Institute, Oslo, Norway, www.emep.int," 2014.

[19] S. Tsyro, D. Simpson, L. Tarrasón, Z. Klimont, K. Kupiainen, C. Pio, and K. E. Yttri, "Modeling of elemental carbon over Europe," *J. Geophys. Res.*, vol. 112, no. D23, D23S19, Sep. 2007.

[20] G. R. van der Werf, J. T. Randerson, L. Giglio, G. J. Collatz, M. Mu, P. S. Kasibhatla, D. C. Morton, R. S. DeFries, Y. Jin, and T. T. van Leeuwen, "Global fire emissions and the contribution of deforestation, savanna, forest, agricultural, and peat fires (1997–2009)," *Atmos. Chem. Phys.*, vol. 10, no. 23, pp. 11707–11735, Dec. 2010.

[21] C. Wiedinmyer, S. K. Akagi, R. J. Yokelson, L. K. Emmons, J. A. Al-Saadi, J. J. Orlando, and A. J. Soja, "The Fire INventory from NCAR (FINN): a high resolution global model to estimate the emissions from open burning," *Geosci. Model Dev.*, vol. 4, no. 3, pp. 625–641, 2011.

[22] A. Petzold, J. A. Ogren, M. Fiebig, P. Laj, S. M. Li, U. Baltensperger, T. Holzer-Popp, S. Kinne, G. Pappalardo, N. Sugimoto, C. Wehrli, A. Wiedensohler, and X. Y. Zhang, "Recommendations for reporting black carbon measurements," *Atmos. Chem. Phys.*, vol. 13, pp. 8365–8379, 2013.

[23] T. C. Bond and R. W. Bergstrom, "Light Absorption by Carbonaceous Particles: An Investigative Review," *Aerosol Sci. Technol.*, vol. 40, no. 1, pp. 27–67, Jan. 2006.

[24] M. O. Andreae and A. Gelencser, "Black carbon or brown carbon? The nature of light-absorbing carbonaceous aerosols," *Atmos. Chem. Phys.*, vol. 6, pp. 3131–3148, Jul. 2006.

[25] J. G. Watson, J. C. Chow, and L.-W. A. Chen, "Summary of organic and elemental carbon/black carbon analysis methods and intercomparisons," *Aerosol Air Qual. Res.*, vol. 5, pp. 65–102, 2005.

[26] H. Schmid, L. Laskus, H. Jurgen Abraham, U. Baltensperger, V. Lavanchy, M. Bizjak, P. Burba, H. Cachier, D. Crow, J. Chow, T. Gnauk, A. Even, H. M. ten Brink, K.-P. Giesen, R. Hitzenberger, C. Hueglin, W. Maenhaut, C. Pio, A. Carvalho, J.-P. Putaud, D. Toom-Sauntry, and H. Puxbaum, "Results of the 'carbon conference' international aerosol carbon round robin test stage I," *Atmos. Environ.*, vol. 35, no. 12, pp. 2111–2121, Apr. 2001.

[27] J. S. Reid, R. Koppmann, T. F. Eck, and D. P. Eleuterio, "A review of biomass burning emissions, part II: intensive physical properties of biomass burning particles," *Atmos. Chem. Phys.*, vol. 5, no. 3, pp. 799–825, 2005.

[28] G. R. McMeeking, S. M. Kreidenweis, S. Baker, C. M. Carrico, J. C. Chow, J. L. Collett, W. M. Hao, A. S. Holden, T. W. Kirchstetter, W. C. Malm, H. Moosmüller, A. P. Sullivan, and C. E. Wold, "Emissions of trace gases and aerosols during the open combustion of biomass in the laboratory," *J. Geophys. Res.*, vol. 114, no. D19, D19210, Oct. 2009.

[29] O. L. Mayol-Bracero, P. Guyon, B. Graham, G. Roberts, M. O. Andreae, S. Decesari, M. C. Facchini, S. Fuzzi, and P. Artaxo, "Water-soluble organic compounds in biomass burning aerosols over Amazonia - 2. Apportionment of the chemical composition and importance of the polyacidic fraction," *J. Geophys. Res.*, vol. 107, no. D20, art. 8091, 2002.

[30] T. Novakov and C. E. Corrigan, "Thermal characterization of biomass smoke particles," *Mikrochim. Acta*, vol. 119, no. 1–2, pp. 157–166, 1995.

[31] R. Subramanian †, A. Y. Khlystov, and A. L. Robinson, "Effect of Peak Inert-Mode Temperature on Elemental Carbon Measured Using Thermal-Optical Analysis," *Aerosol Sci. Technol.*, vol. 40, no. 10, pp. 763–780, Oct. 2006.

[32] F. Cavalli, M. Viana, K. E. Yttri, J. Genberg, and J.-P. Putaud, "Toward a standardised thermal-optical protocol for measuring atmospheric organic and elemental carbon: the EUSAAR protocol," *Atmos. Meas. Tech.*, vol. 3, no. 1, pp. 79–89, 2010.

[33] R. Subramanian, C. A. Roden, P. Boparai, and T. C. Bond, "Yellow Beads and Missing Particles: Trouble Ahead for Filter-Based Absorption Measurements," *Aerosol Sci. Technol.*, vol. 41, no. 6, pp. 630–637, May 2007.

[34] N. Jankowski, C. Schmidl, I. L. Marr, H. Bauer, and H. Puxbaum, "Comparison of methods for the quantification of carbonate carbon in atmospheric PM10 aerosol samples," *Atmos. Environ.*, vol. 42, no. 34, pp. 8055–8064, Nov. 2008.

[35] A. Karanasiou, E. Diapouli, F. Cavalli, K. Eleftheriadis, M. Viana, A. Alastuey, X. Querol, and C. Reche, "On the quantification of atmospheric carbonate carbon by thermal/optical analysis protocols," *Atmos. Meas. Tech.*, vol. 4, no. 11, pp. 2409–2419, Nov. 2011.

[36] M. Sillanpää, A. Frey, R. Hillamo, A. S. Pennanen, and R. O. Salonen, "Organic, elemental and inorganic carbon in particulate matter of six urban environments in Europe," *Atmos. Chem. Phys.*, vol. 5, no. 11, pp. 2869–2879, Nov. 2005.

[37] R. Subramanian, A. Y. Khlystov, J. C. Cabada, and A. L. Robinson, "Positive and Negative Artifacts in Particulate Organic Carbon Measurements with Denuded and Undenuded Sampler Configurations," *Aerosol Sci. Technol.*, vol. 38, no. 12 supp 1, pp. 27–48, 2004.

[38] E. M. Lipsky and A. L. Robinson, "Effects of Dilution on Fine Particle Mass and Partitioning of Semivolatile Organics in Diesel Exhaust and Wood Smoke," *Environ. Sci. Technol.*, vol. 40, no. 1, pp. 155–162, Jan. 2006.

[39] N. A. Janssen, M. E. Gerlofs-Nijland, T. Lanki, R. O. Salonen, F. Cassee, G. Hoek, P. Fischer, B. Brunekreef, and M. Krzyzanowski, "Health effects of black carbon," *World Heal. Organ. Reg. Off. Eur. Report, ISBN 978 92 890 0265 3, available http//www.euro.who.int/en/health-topics/environment-and-health/air-quality/publications/2012/health-effects-of-black-carbon*, 2012.

[40] A. Laskin, J. Laskin, and S. A. Nizkorodov, "Chemistry of Atmospheric Brown Carbon," *Chem. Rev.*, vol. 115, no. 10, pp. 4335–4382, May 2015.

[41] J. L. Hand, W. C. Malm, A. Laskin, D. Day, T. Lee, C. Wang, C. Carrico, J. Carrillo, J. P. Cowin, J. Collett, and M. J. Iedema, "Optical, physical, and chemical properties of tar balls observed during the Yosemite Aerosol Characterization Study," *J. Geophys. Res.*, vol. 110, no. D21, D21210, 2005.

[42] Y. M. Han, J. J. Cao, S. C. Lee, K. F. Ho, and Z. S. An, "Different characteristics of char and soot in the atmosphere and their ratio as an indicator for source identification in Xi'an, China," *Atmos. Chem. Phys.*, vol. 10, no. 2, pp. 595–607, 2010.

[43] H. Moosmüller, R. K. Chakrabarty, and W. P. Arnott, "Aerosol light absorption and its measurement: A review," *J. Quant. Spectrosc. Radiat. Transf.*, vol. 110, pp. 844–878, 2009.

[44] T. C. Bond, G. Habib, and R. W. Bergstrom, "Limitations in the enhancement of visible light absorption due to mixing state," *J. Geophys. Res. Atmos.*, vol. 111, no. 20, pp. 1–13, 2006.

[45] M. Viana, T. A. J. Kuhlbusch, X. Querol, A. Alastuey, R. M. Harrison, P. K. Hopke, W. Winiwarter, M. Vallius, S. Szidat, A. S. H. Prévôt, C. Hueglin, H. Bloemen, P. Wåhlin, R. Vecchi, A. I. Miranda, A. Kasper-Giebl, W. Maenhaut, and R. Hitzenberger, "Source apportionment of particulate matter in Europe : A review of methods and results," vol. 39, no. 3, pp. 827–849, 2008.

[46] A. Gelencsér, B. May, D. Simpson, A. Sánchez-Ochoa, A. Kasper-Giebl, H. Puxbaum, A. Caseiro, C. Pio, and M. Legrand, "Source apportionment of PM2.5 organic aerosol over Europe: Primary/secondary, natural/anthropogenic, and fossil/biogenic origin," *J. Geophys. Res.*, vol. 112, no. D23, D23S04, Sep. 2007.

[47] B. R. T. Simoneit, J. J. Schauer, C. G. Nolte, D. R. Oros, V. O. Elias, M. P. Fraser, W. F. Rogge, and G. R. Cass, "Levoglucosan, a tracer for cellulose in biomass burning and atmospheric particles," *Atmos. Environ.*, vol. 33, no. 2, pp. 173–182, 1999.

[48] M. J. Kleeman, M. A. Robert, S. G. Riddle, P. M. Fine, M. D. Hays, J. J. Schauer, and M. P. Hannigan, "Size distribution of trace organic species emitted from biomass combustion and meat charbroiling," *Atmos. Environ.*, vol. 42, no. 13, pp. 3059–3075, 2008.

[49] H. Bauer, M. Claeys, R. Vermeylen, E. Schueller, G. Weinke, A. Berger, and H. Puxbaum, "Arabitol and mannitol as tracers for the quantification of airborne fungal spores," *Atmos. Environ.*, vol. 42, no. 3, pp. 588–593, 2008.

[50] A. Sánchez-Ochoa, A. Kasper-Giebl, H. Puxbaum, A. Gelencser, M. Legrand, and C. Pio, "Concentration of atmospheric cellulose: A proxy for plant debris across a west-east transect over Europe," *J. Geophys. Res.*, vol. 112, no. D23, D23S08, Aug. 2007.

[51] K. E. Yttri, D. Simpson, K. Stenström, H. Puxbaum, and T. Svendby, "Source apportionment of the carbonaceous aerosol in Norway - quantitative estimates based on ^{14}C, thermal-optical and organic tracer analysis," *Atmos. Chem. Phys.*, vol. 11, pp. 9375–9394, 2011.

[52] B. Nozière, M. Kalberer, M. Claeys, J. Allan, B. D'Anna, S. Decesari, E. Finessi, M. Glasius, I. Grgić, J. F. Hamilton, T. Hoffmann, Y. Iinuma, M. Jaoui, A. Kahnt, C. J. Kampf, I. Kourtchev, W. Maenhaut, N. Marsden, S. Saarikoski, J. Schnelle-Kreis, J. D. Surratt, S. Szidat, R. Szmigielski, and A. Wisthaler, "The Molecular Identification of Organic Compounds in the Atmosphere: State of the Art and Challenges," *Chem. Rev.*, vol. 115, no. 10, pp. 3919–3983, May 2015.

[53] B. A. Buchholz, S. J. Fallon, P. Zermeño, G. Bench, and B. A. Schichtel, "Anomalous elevated radiocarbon measurements of PM2.5," *Nucl. Instruments Methods Phys. Res. Sect. B Beam Interact. with Mater. Atoms*, vol. 294, pp. 631–635, Jan. 2013.

[54] S. A. Vay, S. C. Tyler, Y. Choi, D. R. Blake, N. J. Blake, G. W. Sachse, G. S. Diskin, and H. B. Singh, "Sources and transport of Δ14C in CO2 within the Mexico City Basin and vicinity," *Atmos. Chem. Phys.*, vol. 9, no. 14, pp. 4973–4985, Jul. 2009.

[55] K. E. Yttri, "Personal communication." 2015.

[56] L.-J. Kuo, B. E. Herbert, and P. Louchouarn, "Can levoglucosan be used to characterize and quantify char/charcoal black carbon in environmental media?," *Org. Geochem.*, vol. 39, no. 10, pp. 1466–1478, Oct. 2008.

[57] C. J. Hennigan, A. P. Sullivan, J. L. Collett, and A. L. Robinson, "Levoglucosan stability in biomass burning particles exposed to hydroxyl radicals," *Geophys. Res. Lett.*, vol. 37, no. 9, L09806, 2010.

[58] A. A. May, R. Saleh, C. J. Hennigan, N. M. Donahue, and A. L. Robinson, "Volatility of Organic Molecular Markers Used for Source Apportionment Analysis: Measurements and Implications for Atmospheric Lifetime," *Environ. Sci. Technol.*, vol. 46, no. 22, pp. 12435–12444, Nov. 2012.

[59] D. Hoffmann, A. Tilgner, Y. Iinuma, and H. Herrmann, "Atmospheric Stability of Levoglucosan: A Detailed Laboratory and Modeling Study," *Environ. Sci. Technol.*, vol. 44, pp. 694–699, 2010.

[60] R. Zhao, E. L. Mungall, A. K. Y. Lee, D. Aljawhary, and J. P. D. Abbatt, "Aqueous-phase photooxidation of levoglucosan – a mechanistic study using aerosol time-of-flight chemical ionization mass spectrometry (Aerosol ToF-CIMS)," *Atmos. Chem. Phys.*, vol. 14, no. 18, pp. 9695–9706, Sep. 2014.

[61] K. E. Yttri, J. Schnelle-Kreis, W. Maenhaut, G. Abbaszade, C. Alves, A. Bjerke, N. Bonnier, R. Bossi, M. Claeys, C. Dye, M. Evtyugina, D. García-Gacio, R. Hillamo, A. Hoffer, M. Hyder, Y. Iinuma, J.-L. Jaffrezo, A. Kasper-Giebl, G. Kiss, P. L. López-Mahia, C. Pio, C. Piot, C. Ramirez-Santa-Cruz, J. Sciare, K. Teinilä, R. Vermeylen, A. Vicente, and R. Zimmermann, "An intercomparison study of analytical methods used for quantification of levoglucosan in ambient aerosol filter samples," *Atmos. Meas. Tech.*, vol. 8, no. 1, pp. 125–147, Jan. 2015.

[62] D. Fabbri, C. Torri, B. R. T. Simoneit, L. Marynowski, A. I. Rushdi, and M. J. Fabiańska, "Levoglucosan and other cellulose and lignin markers in emissions from burning of Miocene lignites," *Atmos. Environ.*, vol. 43, no. 14, pp. 2286–2295, May 2009.

[63] T. Tritscher, Z. Jurányi, M. Martin, R. Chirico, M. Gysel, M. F. Heringa, P. F. DeCarlo, B. Sierau, A. S. H. Prévôt, E. Weingartner, and U. Baltensperger, "Changes of hygroscopicity and morphology during ageing of diesel soot," *Environ. Res. Lett.*, vol. 6, no. 3, art. 034026, 2011.

[64] C. Wittbom, J. H. Pagels, J. Rissler, A. C. Eriksson, J. E. Carlsson, P. Roldin, E. Z. Nordin, P. T. Nilsson, E. Swietlicki, and B. Svenningsson, "Cloud droplet activity changes of soot aerosol upon smog chamber ageing," *Atmos. Chem. Phys.*, vol. 14, no. 18, pp. 9831–9854, 2014.

[65] M. Laborde, M. Crippa, T. Tritscher, Z. Jurányi, P. F. Decarlo, B. Temime-Roussel, N. Marchand, S. Eckhardt, A. Stohl, U. Baltensperger, A. S. H. Prévôt, E. Weingartner, and M. Gysel, "Black carbon physical properties and mixing state in the European megacity Paris," *Atmos. Chem. Phys.*, vol. 13, no. 11, pp. 5831–5856, Jun. 2013.

[66] B. Croft, U. Lohmann, and K. von Salzen, "Black carbon ageing in the Canadian Centre for Climate modelling and analysis atmospheric general circulation model," *Atmos. Chem. Phys.*, vol. 5, no. 7, pp. 1931–1949, 2005.

[67] W. F. Cooke, C. Liousse, H. Cachier, and J. Feichter, "Construction of a 1 ° × 1 ° fossil fuel emission data set for carbonaceous aerosol and implementation and radiative impact in the ECHAM4 model," *J. Geophys. Res.*, vol. 104, no. D18, pp. 22137–22162, Sep. 1999.

[68] D. Koch, M. Schulz, S. Kinne, C. McNaughton, J. R. Spackman, Y. Balkanski, S. Bauer, T. Berntsen, T. C. Bond, O. Boucher, M. Chin, A. Clarke, N. De Luca, F. Dentener, T. Diehl, O. Dubovik, R. Easter, D. W. Fahey, J. Feichter, D. Fillmore, S. Freitag, S. Ghan, P. Ginoux, S. Gong, L. Horowitz, T. Iversen, A. Kirkevag, Z. Klimont, Y. Kondo, M. Krol, X. Liu, R. Miller, V. Montanaro, N. Moteki, G. Myhre, J. E. Penner, J. Perlwitz, G. Pitari, S. Reddy, L. Sahu, H. Sakamoto, G. Schuster, J. P. Schwarz, O. Seland, P. Stier, N. Takegawa, T. Takemura, C. Textor, J. A. van Aardenne, and Y. Zhao, "Evaluation of black carbon estimations in global aerosol models," *Atmos. Chem. Phys.*, vol. 9, no. 22, pp. 9001–9026, 2009.

[69] M. Gysel, S. Nyeki, E. Weingartner, U. Baltensperger, H. Giebl, R. Hitzenberger, A. Petzold, and C. W. Wilson, "Properties of jet engine combustion particles during the PartEmis experiment: Hygroscopicity at subsaturated conditions," *Geophys. Res. Lett.*, vol. 30, no. 11, art. 1566, 2003.

[70] G. J. Engelhart, C. J. Hennigan, M. A. Miracolo, A. L. Robinson, and S. N. Pandis, "Cloud condensation nuclei activity of fresh primary and aged biomass burning aerosol," *Atmos. Chem. Phys.*, vol. 12, no. 15, pp. 7285–7293, Aug. 2012.

[71] U. Lohmann, J. Feichter, C. C. Chuang, and J. E. Penner, "Prediction of the number of cloud droplets in the ECHAM GCM," *J. Geophys. Res.*, vol. 104, no. D8, pp. 9169–9198, 1999.

[72] M. D. Petters, C. M. Carrico, S. M. Kreidenweis, A. J. Prenni, P. J. DeMott, J. L. Collett, and H. Moosmüller, "Cloud condensation nucleation activity of biomass burning aerosol," *J. Geophys. Res.*, vol. 114, no. D22, D22205, Nov. 2009.

[73] K. A. Pratt, S. M. Murphy, R. Subramanian, P. J. DeMott, G. L. Kok, T. Campos, D. C. Rogers, A. J. Prenni, A. J. Heymsfield, J. H. Seinfeld, and K. A. Prather, "Flight-based chemical characterization of biomass burning aerosols within two prescribed burn smoke plumes," *Atmos. Chem. Phys.*, vol. 11, no. 24, pp. 12549–12565, Dec. 2011.

[74] T. L. Lathem, A. J. Beyersdorf, K. L. Thornhill, E. L. Winstead, M. J. Cubison, A. Hecobian, J. L. Jimenez, R. J. Weber, B. E. Anderson, and A. Nenes, "Analysis of CCN activity of Arctic aerosol and Canadian biomass burning during summer 2008," *Atmos. Chem. Phys.*, vol. 13, no. 5, pp. 2735–2756, Mar. 2013.

[75] N. Riemer, H. Vogel, and B. Vogel, "Soot ageing time scales in polluted regions during day and night," *Atmos. Chem. Phys.*, vol. 4, pp. 1885–1893, 2004.

[76] R. C. Moffet and K. A. Prather, "In-situ measurements of the mixing state and optical properties of soot with implications for radiative forcing estimates," *Proc. Natl. Acad. Sci.*, vol. 106, no. 29, pp. 11872–11877, Jul. 2009.

[77] J. Wang, M. J. Cubison, A. C. Aiken, J. L. Jimenez, and D. R. Collins, "The importance of aerosol mixing state and size-resolved composition on CCN concentration and the variation of the importance with atmospheric aging of aerosols," *Atmos. Chem. Phys.*, vol. 10, pp. 7267–7283, 2010.

[78] Y. F. Cheng, H. Su, D. Rose, S. S. Gunthe, M. Berghof, B. Wehner, P. Achtert, A. Nowak, N. Takegawa, Y. Kondo, M. Shiraiwa, Y. G. Gong, M. Shao, M. Hu, T. Zhu, Y. H. Zhang, G. R. Carmichael, A. Wiedensohler, M. O. Andreae, and U. Pöschl, "Size-resolved measurement of the mixing state of soot in the megacity Beijing, China: diurnal cycle, aging and parameterization," *Atmos. Chem. Phys.*, vol. 12, no. 10, pp. 4477–4491, May 2012.

[79] A. T. Lambe, A. T. Ahern, J. P. Wright, D. R. Croasdale, P. Davidovits, and T. B. Onasch, "Oxidative aging and cloud condensation nuclei activation of laboratory combustion soot," *J. Aerosol Sci.*, vol. 79, pp. 31–39, 2015.

[80] E. C. Browne, J. P. Franklin, M. R. Canagaratna, P. Massoli, T. W. Kirchstetter, D. R. Worsnop, K. R. Wilson, and J. H. Kroll, "Changes to the Chemical Composition of Soot from Heterogeneous Oxidation Reactions," *J. Phys. Chem. A*, vol. 119, no. 7, pp. 1154–1163, Feb. 2015.

[81] Y. Ma, S. D. Brooks, G. Vidaurre, A. F. Khalizov, L. Wang, and R. Zhang, "Rapid modification of cloud-nucleating ability of aerosols by biogenic emissions," *Geophys. Res. Lett.*, vol. 40, no. 23, pp. 6293–6297, Dec. 2013.

[82] M. Crippa, F. Canonaco, V. A. Lanz, M. Äijälä, J. D. Allan, S. Carbone, G. Capes, D. Ceburnis, M. Dall'Osto, D. A. Day, P. F. DeCarlo, M. Ehn, A. Eriksson, E. Freney, L. Hildebrandt Ruiz, R. Hillamo, J. L. Jimenez, H. Junninen, A. Kiendler-Scharr, A.-M. Kortelainen, M. Kulmala, A. Laaksonen, A. A. Mensah, C. Mohr, E. Nemitz, C. O'Dowd, J. Ovadnevaite, S. N. Pandis, T. Petäjä, L. Poulain, S. Saarikoski, K. Sellegri, E. Swietlicki, P. Tiitta, D. R. Worsnop, U. Baltensperger, and A. S. H. Prévôt, "Organic aerosol components derived from 25 AMS data sets across Europe using a consistent ME-2 based source apportionment approach," *Atmos. Chem. Phys.*, vol. 14, no. 12, pp. 6159–6176, Jun. 2014.

[83] M. Kanakidou, J. H. Seinfeld, S. N. Pandis, I. Barnes, F. J. Dentener, M. C. Facchini, R. Van Dingenen, B. Ervens, A. Nenes, C. J. Nielsen, E. Swietlicki, J. P. Putaud, Y. Balkanski, S. Fuzzi, J. Horth, G. K. Moortgat, R. Winterhalter, C. E. L. Myhre, K. Tsigaridis, E. Vignati, E. G. Stephanou, and J. Wilson, "Organic aerosol and global climate modelling: a review," *Atmos. Chem. Phys.*, vol. 5, pp. 1053–1123, 2005.

[84] M. Hallquist, J. C. Wenger, U. Baltensperger, Y. Rudich, D. Simpson, M. Claeys, J. Dommen, N. M. Donahue, C. George, A. H. Goldstein, J. F. Hamilton, H. Herrmann, T. Hoffmann, Y. Iinuma, M. Jang, M. E. Jenkin, J. L. Jimenez, A. Kiendler-Scharr, W. Maenhaut, G. McFiggans, T. F. Mentel, A. Monod, A. S. H. Prevot, J. H. Seinfeld, J. D. Surratt, R. Szmigielski, and J. Wildt, "The formation, properties and impact of secondary organic aerosol: current and emerging issues," *Atmos. Chem. Phys.*, vol. 9, no. 14, pp. 5155–5236, 2009.

[85] J. H. Kroll and J. H. Seinfeld, "Chemistry of secondary organic aerosol: Formation and evolution of low-volatility organics in the atmosphere," *Atmos. Environ.*, vol. 16, pp. 3593–3624, 2008.

[86] A. H. Goldstein and R. E. Galbally, "Known and unexplored organic constituents in the Earth's atmosphere," *Environ. Sci. Technol.*, vol. 41, pp. 1514–1521, 2007.

[87] N. M. Donahue, S. A. Epstein, S. N. Pandis, and A. L. Robinson, "A two-dimensional volatility basis set: 1. organic-aerosol mixing thermodynamics," *Atmos. Chem. Phys.*, vol. 11, no. 7, pp. 3303–3318, Apr. 2011.

[88] N. M. Donahue, A. L. Robinson, E. R. Trump, I. Riipinen, and J. H. Kroll, "Volatility and Aging of Atmospheric Organic Aerosol," *Top. Curr. Chem.*, vol. 339, pp. 97–143, 2012.

[89] K. Tsigaridis, N. Daskalakis, M. Kanakidou, P. J. Adams, P. Artaxo, R. Bahadur, Y. Balkanski, S. E. Bauer, N. Bellouin, A. Benedetti, T. Bergman, T. K. Berntsen, J. P. Beukes, H. Bian, K. S. Carslaw, M. Chin, G. Curci, T. Diehl, R. C. Easter, S. J. Ghan, S. L. Gong, A. Hodzic, C. R. Hoyle, T. Iversen, S. Jathar, J. L. Jimenez, J. W. Kaiser, A. Kirkevåg, D. Koch, H. Kokkola, Y. H. Lee, G. Lin, X. Liu, G. Luo, X. Ma, G. W. Mann, N. Mihalopoulos, J.-J. Morcrette, J.-F. Müller, G. Myhre, S. Myriokefalitakis, N. L. Ng, D. O'Donnell, J. E. Penner, L. Pozzoli, K. J. Pringle, L. M. Russell, M. Schulz, J. Sciare, Ø. Seland, D. T. Shindell, S. Sillman, R. B. Skeie, D. Spracklen, T. Stavrakou, S. D. Steenrod, T. Takemura, P. Tiitta, S. Tilmes, H. Tost, T. van Noije, P. G. van Zyl, K. von Salzen, F. Yu, Z. Wang, Z. Wang, R. A. Zaveri, H. Zhang, K. Zhang, Q. Zhang, and X. Zhang, "The AeroCom evaluation and intercomparison of organic aerosol in global models," *Atmos. Chem. Phys.*, vol. 14, no. 19, pp. 10845–10895, Oct. 2014.

[90] N. M. Donahue, A. L. Robinson, C. O. Stanier, and S. N. Pandis, "Coupled Partitioning, Dilution, and Chemical Aging of Semivolatile Organics," *Environ. Sci. Technol.*, vol. 40, no. 8, pp. 2635–2643, 2006.

[91] N. M. Donahue, A. L. Robinson, and S. N. Pandis, "Atmospheric organic particulate matter: From smoke to secondary organic aerosol," *Atmos. Environ.*, vol. 43, no. 1, pp. 94–106, 2009.

[92] D. R. Worton, G. Isaacman, D. R. Gentner, T. R. Dallmann, A. W. H. Chan, C. Ruehl, T. W. Kirchstetter, K. R. Wilson, R. A. Harley, and A. H. Goldstein, "Lubricating Oil Dominates Primary Organic Aerosol Emissions from Motor Vehicles," *Environ. Sci. Technol.*, vol. 48, pp. 3698–3706, 2014.

[93] T. D. Gordon, A. A. Presto, N. T. Nguyen, W. H. Robertson, K. Na, K. N. Sahay, M. Zhang, C. Maddox, P. Rieger, S. Chattopadhyay, H. Maldonado, M. M. Maricq, and A. L. Robinson, "Secondary organic aerosol production from diesel vehicle exhaust: impact of aftertreatment, fuel chemistry and driving cycle," *Atmos. Chem. Phys.*, vol. 14, no. 9, pp. 4643–4659, May 2014.

[94] S. H. Jathar, T. D. Gordon, C. J. Hennigan, H. O. T. Pye, G. Pouliot, P. J. Adams, N. M. Donahue, and A. L. Robinson, "Unspeciated organic emissions from combustion sources and their influence on the secondary organic aerosol budget in the United States," *Proc. Natl. Acad. Sci.*, vol. 111, no. 29, pp. 10473–10478, Jul. 2014.

[95] T. D. Gordon, D. S. Tkacik, A. A. Presto, M. Zhang, S. H. Jathar, N. T. Nguyen, J. Massetti, T. Truong, P. Cicero-Fernandez, C. Maddox, P. Rieger, S. Chattopadhyay, H. Maldonado, M. M. Maricq, and A. L. Robinson, "Primary Gas- and Particle-Phase Emissions and Secondary Organic Aerosol Production from Gasoline and Diesel Off-Road Engines," *Environ. Sci. Technol.*, vol. 47, no. 24, pp. 14137–14146, Dec. 2013.

[96] Y. Zhao, C. J. Hennigan, A. A. May, D. S. Tkacik, J. A. de Gouw, J. B. Gilman, W. C. Kuster, A. Borbon, and A. L. Robinson, "Intermediate-Volatility Organic Compounds: A Large Source of Secondary Organic Aerosol," *Environ. Sci. Technol.*, vol. 48, no. 23, pp. 13743–13750, Dec. 2014.

[97] D. A. Lack, J. J. Corbett, T. Onasch, B. Lerner, P. Massoli, P. K. Quinn, T. S. Bates, D. S. Covert, D. Coffman, B. Sierau, S. Herndon, J. Allan, T. Baynard, E. Lovejoy, A. R. Ravishankara, and E. Williams, "Particulate emissions from commercial shipping: Chemical, physical, and optical properties," *J. Geophys. Res.*, vol. 114, D00F04, 2009.

[98] J. Moldanová, E. Fridell, H. Winnes, S. Holmin-Fridell, J. Boman, A. Jedynska, V. Tishkova, B. Demirdjian, S. Joulie, H. Bladt, N. P. Ivleva, and R. Niessner, "Physical and chemical characterisation of PM emissions from two ships operating in European Emission Control Areas," *Atmos. Meas. Tech.*, vol. 6, no. 12, pp. 3577–3596, Dec. 2013.

[99] M. K. Shrivastava, E. M. Lipsky, C. O. Stanier, and A. L. Robinson, "Modeling Semivolatile Organic Aerosol Mass Emissions from Combustion Systems," *Environ. Sci. Technol.*, vol. 40, no. 8, pp. 2671–2677, 2006.

[100] A. L. Robinson, N. M. Donahue, M. K. Shrivastava, E. A. Weitkamp, A. M. Sage, A. P. Grieshop, T. E. Lane, J. R. Pierce, and S. N. Pandis, "Rethinking organic aerosols: semivolatile emissions and photochemical aging.," *Science*, vol. 315, no. 5816, pp. 1259–1262, 2007.

[101] A. A. Presto, C. J. Hennigan, N. T. Nguyen, and A. L. Robinson, "Determination of Volatility Distributions of Primary Organic Aerosol Emissions from Internal Combustion Engines Using Thermal Desorption Gas Chromatography Mass Spectrometry," *Aerosol Sci. Technol.*, vol. 46, no. 10, pp. 1129–1139, Oct. 2012.

[102] M. K. Shrivastava, T. E. Lane, N. M. Donahue, S. N. Pandis, and A. L. Robinson, "Effects of gas particle partitioning and aging of primary emissions on urban and regional organic aerosol concentrations," *J. Geophys. Res. Atmos.*, vol. 113, no. 18, pp. 1–16, 2008.

[103] V. R. Després, J. Alex Huffman, S. M. Burrows, C. Hoose, A. S. Safatov, G. Buryak, J. Fröhlich-Nowoisky, W. Elbert, M. O. Andreae, U. Pöschl, and R. Jaenicke, "Primary biological aerosol

particles in the atmosphere: A review," *Tellus, Ser. B Chem. Phys. Meteorol.*, vol. 64, art. 15598, 2012.

[104] S. Myriokefalitakis, E. Vignati, K. Tsigaridis, C. Papadimas, J. Sciare, N. Mihalopoulos, M. C. Facchini, M. Rinaldi, F. J. Dentener, D. Ceburnis, N. Hatzianastasiou, C. D. O'Dowd, M. van Weele, and M. Kanakidou, "Global Modeling of the Oceanic Source of Organic Aerosols," *Adv. Meteorol.*, vol. 2010, pp. 1–16, 2010.

[105] K. E. Yttri, D. Simpson, J. K. Nøjgaard, K. Kristensen, J. Genberg, K. Stenström, E. Swietlicki, R. Hillamo, M. Aurela, H. Bauer, J. H. Offenberg, M. Jaoui, C. Dye, S. Eckhardt, J. F. Burkhart, A. Stohl, and M. Glasius, "Source apportionment of the summer time carbonaceous aerosol at Nordic rural background sites," *Atmos. Chem. Phys.*, vol. 11, pp. 13339–13357, 2011.

[106] V. A. Lanz, M. R. Alfarra, U. Baltensperger, B. Buchmann, C. Hueglin, and A. S. Prevot, "Source apportionment of submicron organic aerosols at an urban site by factor analytical modelling of aerosol mass spectra," *Atmos. Chem. Phys.*, vol. 7, no. 6, pp. 1503–1522, 2007.

[107] J. D. Allan, P. I. Williams, W. T. Morgan, C. L. Martin, M. J. Flynn, J. Lee, E. Nemitz, G. J. Phillips, M. W. Gallagher, and H. Coe, "Contributions from transport, solid fuel burning and cooking to primary organic aerosols in two UK cities," *Atmos. Chem. Phys.*, vol. 10, pp. 647–668, 2010.

[108] C. Mohr, P. F. DeCarlo, M. F. Heringa, R. Chirico, J. G. Slowik, R. Richter, C. Reche, A. Alastuey, X. Querol, R. Seco, J. Peñuelas, J. L. Jiménez, M. Crippa, R. Zimmermann, U. Baltensperger, and A. S. H. Prévôt, "Identification and quantification of organic aerosol from cooking and other sources in Barcelona using aerosol mass spectrometer data," *Atmos. Chem. Phys.*, vol. 12, no. 4, pp. 1649–1665, 2012.

[109] M. Crippa, P. F. DeCarlo, J. G. Slowik, C. Mohr, M. F. Heringa, R. Chirico, L. Poulain, F. Freutel, J. Sciare, J. Cozic, C. F. Di Marco, M. Elsasser, J. B. Nicolas, N. Marchand, E. Abidi, A. Wiedensohler, F. Drewnick, J. Schneider, S. Borrmann, E. Nemitz, R. Zimmermann, J.-L. Jaffrezo, A. S. H. Prévôt, and U. Baltensperger, "Wintertime aerosol chemical composition and source apportionment of the organic fraction in the metropolitan area of Paris," *Atmos. Chem. Phys.*, vol. 13, no. 2, pp. 961–981, Jan. 2013.

[110] J. F. Pankow, "Review and comparative analysis of the theories on partitioning between the gas and aerosol particulate phases in the atmosphere," *Atmos. Environ.*, vol. 21, pp. 2275–2283, 1987.

[111] Y. Andersson-Sköld and D. Simpson, "Secondary organic aerosol formation in northern Europe: A model study," *J. Geophys. Res.*, vol. 106, no. D7, pp. 7357–7374, Apr. 2001.

[112] J. F. Pankow, "An absorption model of gas/particle partitioning of organic compounds in the atmosphere," *Atmos. Environ.*, vol. 28, no. 2, pp. 185–188, 1994.

[113] P. E. Sheehan and F. M. Bowman, "Estimated effects of temperature on secondary organic aerosol concentrations," *Environ. Sci. Technol.*, vol. 35, no. 11, pp. 2129–2135, Jun. 2001.

[114] A. P. Grieshop, M. A. Miracolo, N. M. Donahue, and A. L. Robinson, "Constraining the Volatility Distribution and Gas-Particle Partitioning of Combustion Aerosols Using Isothermal Dilution and Thermodenuder Measurements," *Environ. Sci. Technol.*, vol. 43, pp. 4750–4756, 2009.

[115] C. D. Cappa and J. L. Jimenez, "Quantitative estimates of the volatility of ambient organic aerosol," *Atmos. Chem. Phys.*, vol. 10, pp. 5409–5424, 2010.

[116] A. A. May, E. J. T. Levin, C. J. Hennigan, I. Riipinen, T. Lee, J. L. Collett, J. L. Jimenez, S. M. Kreidenweis, and A. L. Robinson, "Gas-particle partitioning of primary organic aerosol emissions: 3. Biomass burning," *J. Geophys. Res. Atmos.*, vol. 118, pp. 11327–11338, 2013.

[117] A. A. May, A. A. Presto, C. J. Hennigan, N. T. Nguyen, T. D. Gordon, and A. L. Robinson, "Gas-Particle Partitioning of Primary Organic Aerosol Emissions: (2) Diesel Vehicles," *Environ. Sci. Technol.*, vol. 47, pp. 8288–8296, 2013.

[118] A. A. May, A. A. Presto, C. J. Hennigan, N. T. Nguyen, T. D. Gordon, and A. L. Robinson, "Gas-particle partitioning of primary organic aerosol emissions: (1) Gasoline vehicle exhaust," *Atmos. Environ.*, vol. 77, pp. 128–139, Oct. 2013.

[119] P. J. Ziemann and R. Atkinson, "Kinetics, products, and mechanisms of secondary organic aerosol formation," *Chem. Soc. Rev.*, vol. 41, no. 19, pp. 6582–6605, 2012.

[120] L. Hildebrandt, N. M. Donahue, and S. N. Pandis, "High formation of secondary organic aerosol from the photo-oxidation of toluene," *Atmos. Chem. Phys.*, vol. 9, no. 9, pp. 2973–2986, 2009.

[121] E. A. Weitkamp, A. M. Sage, J. R. Pierce, N. M. Donahue, and A. L. Robinson, "Organic aerosol formation from photochemical oxidation of diesel exhaust in a smog chamber," *Environ. Sci. Technol.*, vol. 41, no. 20, pp. 6969–6975, 2007.

[122] A. B. Guenther, X. Jiang, C. L. Heald, T. Sakulyanontvittaya, T. Duhl, L. K. Emmons, and X. Wang, "The model of emissions of gases and aerosols from nature version 2.1 (MEGAN2.1): An

extended and updated framework for modeling biogenic emissions," *Geosci. Model Dev.*, vol. 5, no. 6, pp. 1471–1492, 2012.

[123] J.-F. Lamarque, T. C. Bond, V. Eyring, C. Granier, A. Heil, Z. Klimont, D. Lee, C. Liousse, A. Mieville, B. Owen, M. G. Schultz, D. Shindell, S. J. Smith, E. Stehfest, J. Van Aardenne, O. R. Cooper, M. Kainuma, N. Mahowald, J. R. McConnell, V. Naik, K. Riahi, and D. P. van Vuuren, "Historical (1850-2000) gridded anthropogenic and biomass burning emissions of reactive gases and aerosols: methodology and application," *Atmos. Chem. Phys.*, vol. 10, no. 15, pp. 7017–7039, 2010.

[124] D. C. Oderbolz, S. Aksoyoglu, J. Keller, I. Barmpadimos, R. Steinbrecher, C. A. Skjøth, C. Plaß-Dülmer, and A. S. H. Prévôt, "A comprehensive emission inventory of biogenic volatile organic compounds in Europe: improved seasonality and land-cover," *Atmos. Chem. Phys.*, vol. 13, no. 4, pp. 1689–1712, Feb. 2013.

[125] S. N. Pandis, S. E. Paulson, J. H. Seinfeld, and R. C. Flagan, "Aerosol formation of isoprene and β-pinene," *Atmos. Environ.*, vol. 25A, pp. 997–1008, 1991.

[126] A. G. Carlton, C. Wiedinmyer, and J. H. Kroll, "A review of Secondary Organic Aerosol (SOA) formation from isoprene," *Atmos. Chem. Phys.*, vol. 9, no. 14, pp. 4987–5005, 2009.

[127] L. Brégonzio-Rozier, F. Siekmann, C. Giorio, E. Pangui, S. B. Morales, B. Temime-Roussel, A. Gratien, V. Michoud, S. Ravier, M. Cazaunau, A. Tapparo, A. Monod, and J.-F. Doussin, "Gaseous products and secondary organic aerosol formation during long term oxidation of isoprene and methacrolein," *Atmos. Chem. Phys.*, vol. 15, no. 6, pp. 2953–2968, Mar. 2015.

[128] A. Lee, A. H. Goldstein, J. H. Kroll, N. L. Ng, V. Varutbangkul, R. C. Flagan, and J. H. Seinfeld, "Gas-phase products and secondary aerosol yields from the photooxidation of 16 different terpenes," *J. Geophys. Res.*, vol. 111, no. D17, D17305, 2006.

[129] M. Jaoui, T. E. Kleindienst, K. S. Docherty, M. Lewandowski, and J. H. Offenberg, "Secondary organic aerosol formation from the oxidation of a series of sesquiterpenes: α-cedrene, β-caryophyllene, α-humulene and α-farnesene with O_3, OH and NO_3 radicals," *Environ. Chem.*, vol. 10, pp. 178–193, 2013.

[130] T. R. Duhl, D. Helmig, and A. Guenther, "Sesquiterpene emissions from vegetation: a review," *Biogeosciences*, vol. 5, no. 3, pp. 761–777, 2008.

[131] E. Kleist, T. F. Mentel, S. Andres, A. Bohne, A. Folkers, A. Kiendler-Scharr, Y. Rudich, M. Springer, R. Tillmann, and J. Wildt, "Irreversible impacts of heat on the emissions of monoterpenes, sesquiterpenes, phenolic BVOC and green leaf volatiles from several tree species," *Biogeosciences*, vol. 9, no. 12, pp. 5111–5123, 2012.

[132] T. F. Mentel, E. Kleist, S. Andres, M. Dal Maso, T. Hohaus, A. Kiendler-Scharr, Y. Rudich, M. Springer, R. Tillmann, R. Uerlings, A. Wahner, and J. Wildt, "Secondary aerosol formation from stress-induced biogenic emissions and possible climate feedbacks," *Atmos. Chem. Phys.*, vol. 13, no. 17, pp. 8755–8770, 2013.

[133] S. Szidat, T. M. Jenk, H. W. Gäggeler, H.-A. Synal, R. Fisseha, U. Baltensperger, M. Kalberer, V. Samburova, S. Reimann, A. Kasper-Giebl, and I. Hajdas, "Radiocarbon (14C)-deduced biogenic and anthropogenic contributions to organic carbon (OC) of urban aerosols from Zürich, Switzerland," *Atmos. Environ.*, vol. 38, no. 24, pp. 4035–4044, Aug. 2004.

[134] S. Szidat, M. Ruff, N. Perron, L. Wacker, H.-A. Synal, M. Hallquist, A. S. Shannigrahi, K. E. Yttri, C. Dye, and D. Simpson, "Fossil and non-fossil sources of organic carbon (OC) and elemental carbon (EC) in Göteborg, Sweden," *Atmos. Chem. Phys.*, vol. 9, no. 5, pp. 1521–1535, Mar. 2009.

[135] R. Atkinson, "Kinetics of the gas-phase reactions of OH radicals with alkanes and cycloalkanes," *Atmos. Chem. Phys.*, vol. 3, no. 6, pp. 2233–2307, Dec. 2003.

[136] A. P. Grieshop, J. M. Logue, N. M. Donahue, and A. L. Robinson, "Laboratory investigation of photochemical oxidation of organic aerosol from wood fires 1: measurement and simulation of organic aerosol evolution," *Atmos. Chem. Phys.*, vol. 9, no. 4, pp. 1263–1277, 2009.

[137] T. E. Lane, N. M. Donahue, and S. N. Pandis, "Effect of NOx on secondary organic aerosol concentrations," *Environ. Sci. Technol.*, vol. 42, no. 16, pp. 6022–6027, Aug. 2008.

[138] N. L. Ng, A. J. Kwan, J. D. Surratt, A. W. H. Chan, P. S. Chhabra, A. Sorooshian, H. O. T. Pye, J. D. Crounse, P. O. Wennberg, R. C. Flagan, and J. H. Seinfeld, "Secondary organic aerosol (SOA) formation from reaction of isoprene with nitrate radicals (NO3)," *Atmos. Chem. Phys.*, vol. 8, no. 14, pp. 4117–4140, Aug. 2008.

[139] A. P. Tsimpidi, V. A. Karydis, M. Zavala, W. Lei, L. Molina, I. M. Ulbrich, J. L. Jimenez, and S. N. Pandis, "Evaluation of the volatility basis-set approach for the simulation of organic aerosol formation in the Mexico City metropolitan area," *Atmos. Chem. Phys.*, vol. 10, pp. 525–546, 2010.

[140] J. H. Kroll, N. M. Donahue, J. L. Jimenez, S. H. Kessler, M. R. Canagaratna, K. R. Wilson, K. E. Altieri, L. R. Mazzoleni, A. S. Wozniak, H. Bluhm, E. R. Mysak, J. D. Smith, C. E. Kolb, and D. R. Worsnop, "Carbon oxidation state as a metric for describing the chemistry of atmospheric organic aerosol," *Nat. Chem.*, vol. 3, no. 2, pp. 133–139, Feb. 2011.

[141] N. M. Donahue, K. M. Henry, T. F. Mentel, A. Kiendler-Scharr, C. Spindler, B. Bohn, T. Brauers, H. P. Dorn, H. Fuchs, R. Tillmann, A. Wahner, H. Saathoff, K.-H. Naumann, O. Moehler, T. Leisner, L. Mueller, M.-C. Reinnig, T. Hoffmann, K. Salo, M. Hallquist, M. Frosch, M. Bilde, T. Tritscher, P. Barmet, A. P. Praplan, P. F. DeCarlo, J. Dommen, A. S. H. Prevot, and U. Baltensperger, "Aging of biogenic secondary organic aerosol via gas-phase OH radical reactions," *P. Natl. Acad. Sci. USA*, vol. 109, no. 34, pp. 13503–13508, Aug. 2012.

[142] K. M. Henry and N. M. Donahue, "Photochemical Aging of α-Pinene Secondary Organic Aerosol: Effects of OH Radical Sources and Photolysis," *J. Phys. Chem. A*, vol. 116, pp. 5932–5940, 2012.

[143] J. P. S. Wong, S. Zhou, and J. P. D. Abbatt, "Changes in Secondary Organic Aerosol Composition and Mass due to Photolysis: Relative Humidity Dependence," *J. Phys. Chem. A*, vol. 119, no. 19, pp. 4309–4316, May 2015.

[144] T. E. Lane, N. M. Donahue, and S. N. Pandis, "Simulating secondary organic aerosol formation using the volatility basis-set approach in a chemical transport model," *Atmos. Environ.*, vol. 42, no. 32, pp. 7439–7451, 2008.

[145] B. N. Murphy and S. N. Pandis, "Simulating the Formation of Semivolatile Primary and Secondary Organic Aerosol in a Regional Chemical Transport Model," *Environ. Sci. Technol.*, vol. 43, no. 13, pp. 4722–4728, Jul. 2009.

[146] B. Bessagnet, C. Seigneur, and L. Menut, "Impact of dry deposition of semi-volatile organic compounds on secondary organic aerosols," *Atmos. Environ.*, vol. 44, pp. 1781–1787, 2010.

[147] A. Hodzic, S. Madronich, B. Aumont, J. Lee-Taylor, T. Karl, M. Camredon, and C. Mouchel-Vallon, "Limited influence of dry deposition of semivolatile organic vapors on secondary organic aerosol formation in the urban plume," *Geophys. Res. Lett.*, vol. 40, no. 12, pp. 3302–3307, 2013.

[148] A. Hodzic, B. Aumont, C. Knote, J. Lee-Taylor, S. Madronich, and G. Tyndall, "Volatility dependence of Henry's law constants of condensable organics: Application to estimate depositional loss of secondary organic aerosols," *Geophys. Res. Lett.*, vol. 41, no. 13, pp. 4795–4804, 2014.

[149] C. Knote, A. Hodzic, and J. L. Jimenez, "The effect of dry and wet deposition of condensable vapors on secondary organic aerosols concentrations over the continental US," *Atmos. Chem. Phys.*, vol. 15, no. 1, pp. 1–18, 2015.

[150] V. A. Lanz, A. S. H. Prevot, M. R. Alfarra, S. Weimer, C. Mohr, P. F. DeCarlo, M. F. D. Gianini, C. Hueglin, J. Schneider, O. Favez, B. D'Anna, C. George, and U. Baltensperger, "Characterization of aerosol chemical composition with aerosol mass spectrometry in Central Europe: an overview," *Atmos. Chem. Phys.*, vol. 10, no. 21, pp. 10453–10471, 2010.

[151] D. Simpson, K. E. Yttri, Z. Klimont, K. Kupiainen, A. Caseiro, A. Gelencsér, C. Pio, H. Puxbaum, and M. Legrand, "Modeling carbonaceous aerosol over Europe: Analysis of the CARBOSOL and EMEP EC/OC campaigns," *J. Geophys. Res. Atmos.*, vol. 112, no. 23, D23S14, 2007.

[152] C. Fountoukis, P. N. Racherla, H. A. C. Denier van der Gon, P. Polymeneas, P. E. Charalampidis, C. Pilinis, A. Wiedensohler, M. Dall'Osto, C. O'Dowd, and S. N. Pandis, "Evaluation of a three-dimensional chemical transport model (PMCAMx) in the European domain during the EUCAARI May 2008 campaign," *Atmos. Chem. Phys.*, vol. 11, no. 20, pp. 10331–10347, 2011.

[153] T. Nussbaumer, C. Czasch, N. Klippel, L. Johansson, and C. Tullin, "Particulate Emissions from Biomass Combustion in IEA Countries - Survey on Measurements and Emission Factors," International Energy Agency (IEA) Bioenergy Task 32, Zürich, 2008.

[154] Norsk Standard, "Norwegian Standard for Enclosed wood heaters - Smoke emission - Part 2: Determination of particulate emission; NS 3058-2," 1994.

[155] A. J. H. Visschedijk, H. A. C. Denier van der Gon, R. Dröge, and H. der Brugh, "A European high resolution and size-differentiated emission inventory for elemental and organic carbon for the year 2005," *TNO-034-UT-2009-00688_PT-ML, TNO, Utrecht, Netherlands*, 2009.

[156] J. K. Holopainen, "Multiple functions of inducible plant volatiles," *Trends Plant Sci.*, vol. 9, no. 11, pp. 529–533, 2004.

[157] A. Arneth and Ü. Niinemets, "Induced BVOCs: how to bug our models?," *Trends Plant Sci.*, vol. 15, no. 3, pp. 118–125, 2010.

[158] F. Loreto and J.-P. Schnitzler, "Abiotic stresses and induced BVOCs," *Trends Plant Sci.*, vol. 15, no. 3, pp. 154–166, 2010.

[159] F. Spinelli, A. Cellini, L. Marchetti, K. M. Nagesh, and C. Piovene, "Emission and Function of Volatile Organic Compounds in Response to Abiotic Stress," in *Abiotic Stress in Plants - Mechanisms and Adaptions*, A. Shanker and B. Venkateswarlu, Eds. InTech, 2011, pp. 367–394.

[160] J. K. Holopainen and J. Gershenzon, "Multiple stress factors and the emission of plant VOCs," *Trends Plant Sci.*, vol. 15, no. 3, pp. 176–184, 2010.

[161] M. E. Maffei, "Sites of synthesis, biochemistry and functional role of plant volatiles," *South African J. Bot.*, vol. 76, no. 4, pp. 612–631, 2010.

[162] Ü. Niinemets, "Mild versus severe stress and BVOCs: thresholds, priming and consequences," *Trends Plant Sci.*, vol. 15, no. 3, pp. 145–153, 2010.

[163] A. R. Berg, C. L. Heald, K. E. H. Hartz, A. G. Hallar, A. J. H. Meddens, J. A. Hicke, J.-F. Lamarque, and S. Tilmes, "The impact of bark beetle infestations on monoterpene emissions and secondary organic aerosol formation in western North America," *Atmos. Chem. Phys.*, vol. 13, no. 6, pp. 3149–3161, 2013.

[164] ICP Forests, "The Condition of Forests in Europe. 2011 Executive Report," *ICP Forests Report ISSN 1020-587X, ICP Forests, Hamburg, http://www.icp-forests.org/RepEx.htm*, 2011.

[165] R. Fischer, P. Waldner, J. Carnicer, M. Coll, M. Dobbertin, M. Ferretti, K. Hansen, G. Kindermann, P. Lasch-Born, M. Lorenz, A. Marchetto, S. Meining, T. Nieminen, J. Peñuelas, P. Rautio, C. Reyer, P. Roskams, and G. Sánchez, "The Condition of Forests in Europe. 2012 Executive Report," *ICP Forests Report ISSN 1020-587X, ICP Forests, Hamburg, http://www.icp-forests.org/RepEx.htm*, 2012.

[166] P. Merilä, T. Kilponen, and J. Derome (eds.), "Forest Condition Monitoring in Finland - National Report 2002–2005," *Working Papers of the Finnish Forest Research Institute 45, Finnish Forest Research Institute, http://www.metla.fi/julkaisut/workingpapers/*, 2007.

[167] M. E. Jenkin, K. P. Wyche, C. J. Evans, T. Carr, P. S. Monks, M. R. Alfarra, M. H. Barley, G. B. McFiggans, J. C. Young, and A. R. Rickard, "Development and chamber evaluation of the MCM v3.2 degradation scheme for β-caryophyllene," *Atmos. Chem. Phys.*, vol. 12, no. 11, pp. 5275–5308, 2012.

[168] C. E. Canosa-Mas, J. M. Duffy, M. D. King, K. C. Thompson, and R. P. Wayne, "The atmospheric chemistry of methyl salicylate - reactions with atomic chlorine and with ozone," *Atmos. Environ.*, vol. 36, no. 13, pp. 2201–2205, 2002.

[169] T. Karl, A. Guenther, A. Turnipseed, E. G. Patton, and K. Jardine, "Chemical sensing of plant stress at the ecosystem scale," *Biogeosciences*, vol. 5, no. 5, pp. 1287–1294, 2008.

11 Errata

Paper I, page 8505 Table 2. Notes for Illmitz: (j 2006) should be (i 2006)

Paper I, page 8527 One author (H. Puxbaum) missing in the reference:

Simpson, D., Yttri, K., Klimont, Z., Kupiainen, K., Caseiro, A.,Gelencsér, A., Pio, C., Puxbaum, H., and Legrand, M.: Modeling Carbonaceous Aerosol over Europe. Analysis of the CARBOSOL and EMEP EC/OC campaigns, J. Geophys. Res., 112, D23S14, doi:10.1029/2006JD008158, 2007.

Paper III, page 13655, Sec 3.4, third sentence should read:

For BW, the modelled regional background $PM_{2.5}$ concentration is about 50–70% higher than that in the reference case without SIE, as shown in Fig. 8.

Paper IV, page 8724, second column, sentence on lines 9–13 should read**:**

Emissions from the open burning of vegetation (from FINNv1) were treated differently; they were distributed over the nine lowest model layers (up to ~2.6 km height), loosely based on data from Sofiev et al. (2009).

Paper IV, page 8729, Fig. 8.

The emission fractions of “Residential wood combustion” and “Other residential combustion” are switched. The correct fractions should be:

18 % Residential wood combustion and 12 % Other residential combustion.